Available online at www.sciencedirect.com

ScienceDirect

Nuclear Physics B 996 (2023) 116373

NUCLEAR PHYSICS B

www.elsevier.com/locate/nuclphysb

High Energy Physics – Phenomenology

The $Zb\bar{b}$ vertex in a left–right model

Duarte Fontes [a], Darius Jurčiukonis [b,*], Luís Lavoura [c]

[a] *Department of Physics, Brookhaven National Laboratory, Upton, NY 11973, USA*
[b] *Vilnius University, Institute of Theoretical Physics and Astronomy, Saulėtekio ave. 3, Vilnius 10257, Lithuania*
[c] *Universidade de Lisboa, Instituto Superior Técnico, CFTP, Av. Rovisco Pais 1, 1049-001 Lisboa, Portugal*

Received 11 September 2023; received in revised form 9 October 2023; accepted 10 October 2023
Available online 16 October 2023
Editor: Tommy Ohlsson

Abstract

We consider the one-loop corrections to the $Zb\bar{b}$ vertex in a CP-conserving left–right model (LRM), *viz.* a model with gauge group $SU(2)_L \times SU(2)_R \times U(1)$. We allow the gauge coupling constants of $SU(2)_L$ and $SU(2)_R$ to be different. The spontaneous symmetry breaking is accomplished only by doublets and/or singlets of $SU(2)_L$ and $SU(2)_R$. The lightest massive neutral gauge boson of our LRM is assumed to have the same Yukawa couplings to bottom-quark pairs as the Z of the Standard Model (SM); this assumption has the advantage that, then, the infrared divergences automatically cancel down in the subtraction of the $Zb\bar{b}$ vertex in the SM from the same vertex in the LRM. We effect a proper renormalization of the $Zb\bar{b}$ vertex and check explicitly both its gauge invariance and the cancellation of all the ultraviolet divergences. We find out that a LRM with the above assumptions cannot achieve a better fit to the $Zb\bar{b}$ vertex than a multi-Higgs extension of the SM, *viz.* both models can only achieve a decent fit when one admits scalar particles with very low masses $\lesssim 50$ GeV. This is true even when we allow for markedly different gauge coupling constants of $SU(2)_L$ and $SU(2)_R$.

* Corresponding author.
E-mail addresses: dfontes@bnl.gov (D. Fontes), darius.jurciukonis@tfai.vu.lt (D. Jurčiukonis), balio@cftp.tecnico.ulisboa.pt (L. Lavoura).

https://doi.org/10.1016/j.nuclphysb.2023.116373

1. Introduction

In the Standard Model (SM), the $Zb\bar{b}$ interaction is written

$$\mathcal{L}_{Zb\bar{b}} = \frac{g}{c_w} Z_\mu \, \bar{b} \, \gamma^\mu \left(g_L P_L + g_R P_R \right) b, \tag{1}$$

where c_w is the cosine of the weak mixing angle, P_L and P_R are the projection operators of chirality, and g_L and g_R are the $Zb\bar{b}$ couplings. At tree level g_L and g_R have the values

$$g_L^{\text{tree,SM}} = \frac{s_w^2}{3} - \frac{1}{2}, \qquad g_R^{\text{tree,SM}} = \frac{s_w^2}{3}, \tag{2}$$

respectively, where s_w is the sine of the weak mixing angle. With $s_w^2 = 0.22339$ [1], Eq. (2) gives $g_L^{\text{tree,SM}} = -0.42554$ and $g_R^{\text{tree,SM}} = 0.07446$. After inclusion of radiative corrections, the SM prediction for the couplings is [2]

$$g_L^{\text{SM}} = -0.420875, \qquad g_R^{\text{SM}} = 0.077362. \tag{3}$$

In the presence of New Physics (NP), we define δg_L and δg_R through

$$\delta g_L = g_L - g_L^{\text{SM}}, \quad \delta g_R = g_R - g_R^{\text{SM}}. \tag{4}$$

Experimentally, g_L and g_R are obtained from the observable quantities A_b and R_b; their precise experimental definitions may be found in Refs. [2–4] and in appendix A of Ref. [5]. One has

$$A_b = \frac{2 r_b \sqrt{1 - 4\mu_b}}{1 - 4\mu_b + (1 + 2\mu_b) r_b^2}, \tag{5}$$

where $r_b = (g_L + g_R)/(g_L - g_R)$ and $\mu_b = m_b^2\left(m_Z^2\right)/m_Z^2$. We use the numerical values $m_b\left(m_Z^2\right) = 3$ GeV and $m_Z = 91.1876$ GeV [1]. Furthermore,

$$R_b = \frac{s_b \, c^{\text{QCD}} \, c^{\text{QED}}}{s_b \, c^{\text{QCD}} \, c^{\text{QED}} + s_c + s_u + s_s + s_d}, \tag{6}$$

where $c^{\text{QCD}} = 0.9953$ and $c^{\text{QED}} = 0.99975$ are QCD and QED corrections, respectively,

$$s_b = (1 - 6\mu_b) \left(g_L - g_R\right)^2 + \left(g_L + g_R\right)^2, \tag{7}$$

and $s_c + s_u + s_s + s_d = 1.3184$. A recent overall fit of many electroweak observables gives [4]

$$R_b^{\text{fit}} = 0.21629 \pm 0.00066, \tag{8a}$$

$$A_b^{\text{fit}} = 0.923 \pm 0.020. \tag{8b}$$

On the other hand, A_b has been extracted by measuring the Z-pole forward–backward asymmetry $A_{FB}^{0,b}$ at LEP1 and by measuring the left–right forward–backward asymmetry A_{LR}^{FB} at SLAC—for details see Ref. [4] and appendix A of Ref. [5]. The averaged result of those measurements is

$$A_b^{\text{average}} = 0.901 \pm 0.013. \tag{9}$$

While the A_b^{fit} of Eq. (8b) deviates from the SM prediction $A_b^{\text{SM}} = 0.9347$ by just 0.6σ, the A_b^{average} of Eq. (9) displays a much larger disagreement 2.6σ. The R_b^{fit} of Eq. (8a) is 0.7σ above the SM value $R_b^{\text{SM}} = 0.21582 \pm 0.00002$.

Table 1
The results of Eqs. (5) and (6) for g_L and g_R and the corresponding values of δg_L and δg_R, extracted through Eqs. (3) and (4). The superscript 'fit' corresponds to the input values (8) while the superscript 'average' corresponds to the input values (8a) and (9).

Solution	g_L	g_R	δg_L	δg_R
1^{fit}	−0.420206	0.084172	0.000669	0.006810
2^{fit}	−0.419934	−0.082806	0.000941	−0.160168
1^{average}	−0.417814	0.095496	0.003061	0.018134
2^{average}	−0.417504	−0.094139	0.003371	−0.171501

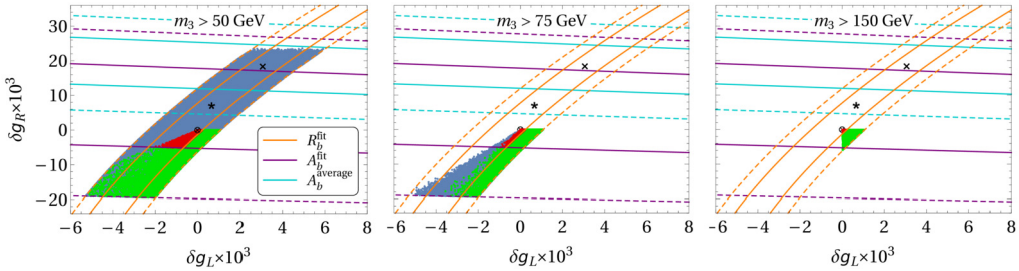

Fig. 1. Scatter plot of the values of δg_L and δg_R in the aligned 2HDM. See Ref. [5] for details.

In this work we consider both the set of values (8), which we denote through the superscript 'fit', and the set formed by values (8a) and (9), which we denote through the superscript 'average'. Plugging the central values of those two sets into Eqs. (5) and (6), we obtain four different solutions for g_L and g_R—for details see Ref. [5]. Two of those solutions may be discarded by both theoretical and experimental arguments [6], while the other two solutions are reasonable; they are given in Table 1. Notice that δg_R seems to be much larger than δg_L.

The two solutions have been studied in the context of the two-Higgs-doublet model (2HDM) and three-Higgs-doublet model (3HDM) [5,7]; it has been found that those extensions of the SM do not improve significantly the fit of the $Zb\bar{b}$ vertex relative to the SM—see Fig. 1.

Two decades ago, research has been carried out on the $Z \to b\bar{b}$ decay asymmetry in simplified left–right models [8–10]. A model with an additional neutral gauge boson including two Higgs doublets, a scalar singlet, and one charged and one neutral vector-like singlets has been studied in Ref. [11]. The SM extended by an additional vector boson Z' has been claimed to provide a good fit to $A_{FB}^{0,b}$ near the Z pole and to R_b measured at energies above that pole [12,13]. In Refs. [14,15] it is shown that some natural composite Higgs models with a subgroup of the custodial symmetry $O(3)$ are able to solve the $A_{FB}^{0,b}$ anomaly while reproducing the observed R_b. There are also studies of contributions from models with extra dimensions to the process $Z \to b\bar{b}$ [16–18], an analysis of Z-pole observables in an effective theory [19], revised QCD effects on the $Zb\bar{b}$ forward–backward asymmetry [20], and a recent explanation [21] of the $Zb\bar{b}$ forward–backward asymmetry by adding to the SM new heavy-quark multiplets—an $SU(2)_L$ doublet with hypercharge $-5/6$ and an $SU(2)_L$ singlet with hypercharge $-1/3$.

The discrepancies in A_b may be evidence for NP, but they may also be due to a statistical fluctuation or to another experimental effect on one of asymmetries; more precise experiments are needed. Hadron colliders may cover the experimental regions of the $Zb\bar{b}$ couplings of LEP1,

but with large uncertainties [22]. Lepton colliders of the next generation offer better opportunities for further studies of the $Zb\bar{b}$ vertex, since they could collect a large amount of data around the Z pole [23]. Some recent papers [24–27] propose novel methods to probe the $Zb\bar{b}$ couplings at both existing and future colliders.

In this paper we seek to reproduce solution 1 in Table 1 by invoking a version of the left–right model (LRM) [28–32], *i.e.* a model with gauge group $SU(2)_L \times SU(2)_R \times U(1)$, at the one-loop level. (We also comment on the possibility of reproducing that solution at the tree level.) We are inspired in this endeavour by the observation that, since δg_R appears to be much larger than δg_L, then maybe a model with right-handed gauge interactions provides a better fit to the $Zb\bar{b}$ vertex; the same rationale was used before in Ref. [10]. The version of the LRM that we use here is characterized by the following four features:

- The gauge coupling constants of $SU(2)_L$ and $SU(2)_R$ are allowed to differ.[1,2] This is done in order to allow greater flexibility of the LRM in fitting the $Zb\bar{b}$ vertex.
- The spontaneous symmetry breaking of $SU(2)_L$ and $SU(2)_R$ is achieved exclusively by scalar doublets of those groups, avoiding the triplets that exist in other versions of the LRM.
- We assume CP conservation, both at the Lagrangian level and in the vacuum state.
- The lightest neutral gauge boson couples to the left- and right-handed fermions with exactly the same strength as the Z gauge boson of the SM.

While the first feature above complicates our LRM, the other three features simplify it considerably. The fourth feature is very helpful to our computation, because it makes the infrared divergences in the $Z_l b\bar{b}$ vertex of the LRM exactly identical to the same divergences in the $Zb\bar{b}$ vertex of the SM; those divergences then disappear when comparing the vertices in the two models. That feature should not constitute an unreasonable restriction, because—as discussed below—previous studies of (different versions of) the LRM suggest that the mixing of the two neutral massive gauge bosons of the LRM should be extremely small anyway.

Another feature of our model is that we only include in it the top and bottom quarks—we neglect both all the other quarks and the leptons; we do this because they are inessential for the $Zb\bar{b}$ vertex.

In this paper we carefully work out the renormalization of the vertex, which is non-trivial because of the enlarged gauge group. This forces us to be painstaking in the definition of the model and, in particular, of all its symmetries. The paper is organized as follows. In Sec. 2 we describe the gauge structure of the model. Section 3 deals with the fit of the $Zb\bar{b}$ vertex in the LRM at tree level. Section 4 proceeds with the description of the scalar structure of the model. In Sec. 5 we collect all the parameters of the model and outline our procedure for fitting the $Zb\bar{b}$ vertex. Section 6 deals with the one-loop calculation and the renormalization procedure. In Sec. 7 we give the practical results of our work. Thereafter, many appendices deal in detail with technical issues.

[1] This is fully compatible with left–right symmetry at very high energies. Namely, that *discrete* symmetry, which has been called P in Ref. [33] or D in some other papers, may be broken at a very high energy while keeping the $SU(2)_L \times SU(2)_R \times U(1)$ gauge group intact [33].

[2] We do not take into account in this paper the constraints on the LRM derived in Refs. [34,35], since those papers assume left–right symmetry, at least in the scalar potential.

2. Description of the model: gauge interactions and quarks

2.1. Gauge coupling constants and covariant derivative

Gauge coupling constants, θ_w, and α We consider a *CP-conserving* left–right model (LRM), *i.e.* a model with gauge group $SU(2)_L \times SU(2)_R \times U(1)_X$. The gauge coupling constant of $SU(2)_L$ is g; the gauge coupling constant of $SU(2)_R$ is l[3]; the gauge coupling constant of $U(1)_X$ is h. We define

$$G \equiv g^2, \qquad L \equiv l^2, \qquad H \equiv h^2, \tag{10a}$$

$$\varrho_1 \equiv \sqrt{GL + GH + LH}, \qquad \varrho_2 \equiv g\sqrt{L + H}, \tag{10b}$$

$$c_w \equiv \frac{\varrho_2}{\varrho_1}, \quad s_w \equiv \frac{-lh}{\varrho_1}, \qquad c_\alpha \equiv \frac{gl}{\varrho_2}, \quad s_\alpha \equiv \frac{-gh}{\varrho_2}, \tag{10c}$$

where $c_w \equiv \cos\theta_w$, $s_w \equiv \sin\theta_w$, $c_\alpha \equiv \cos\alpha$, and $s_\alpha \equiv \sin\alpha$. The electromagnetic coupling constant e is given by

$$e = \frac{-glh}{\varrho_1}, \qquad E \equiv e^2. \tag{11}$$

Notice that

$$Lc_w^2 - Gs_w^2 = \frac{GL^2}{\varrho_1^2} > 0. \tag{12}$$

Using the measured value of s_w, Eq. (12) produces the lower bound

$$\left|\frac{l}{g}\right| > \left|\frac{s_w}{c_w}\right| \approx 0.53. \tag{13}$$

Covariant derivative The covariant derivative is

$$\begin{aligned} D^\mu = {} & \partial^\mu - ig\left(T_L^+ W^{+\mu} + T_L^- W^{-\mu}\right) - il\left(T_R^+ V^{+\mu} + T_R^- V^{-\mu}\right) \\ & + ieA^\mu Q - i\,\frac{g}{c_w}\,Z^\mu\left(T_{L3} - Qs_w^2\right) - i\,\frac{l}{c_\alpha}\,X^\mu\left(T_{R3} - Ys_\alpha^2\right), \end{aligned} \tag{14}$$

where

- $T_L^\pm$ and $T_R^\pm$ are the raising and lowering operators of $SU(2)_L$ and $SU(2)_R$, respectively;
- T_{L3} and T_{R3} are the third generators of $SU(2)_L$ and $SU(2)_R$, respectively;
- $Y = T_{R3} + X$ is the weak hypercharge and $Q = T_{L3} + Y$ is the electric charge[4];
- A^μ is the photon field, which is the only massless gauge field.

Signs It is clear in Eq. (14) that

- The sign of the field $W^{\pm\mu}$ may be chosen so that g is positive.

[3] The left–right-symmetric model assumes $l = g$. *We allow l to be different from g* for the sake of generality.

[4] X is the quantum number that generates $U(1)_X$. It should not be confused with the gauge field X^μ.

- The sign of the field $V^{\pm\mu}$ may be chosen so that l is positive.
- The sign of the field A^μ may be chosen so that e is negative.
- The sign of the field Z^μ may be chosen so that g/c_w is positive.
- The sign of the field X^μ may be chosen so that l/c_α is positive.

Accordingly, from now on we shall assume that g, l, $-e$, c_w, and c_α are positive. Equation (10c) then informs us that ϱ_2 and ϱ_1 are positive too. Equation (11) tells us that h is positive too. Hence, θ_w and α are both angles of the fourth quadrant in our sign convention.

2.2. Gauge-boson mixing

The fields Z_μ and X_μ mix, just as the fields W_μ^+ and V_μ^+. We write

$$\begin{pmatrix} Z_\mu \\ X_\mu \end{pmatrix} = \begin{pmatrix} c_\psi & -s_\psi \\ s_\psi & c_\psi \end{pmatrix} \begin{pmatrix} Z_{l\mu} \\ Z_{h\mu} \end{pmatrix}, \qquad \begin{pmatrix} W_\mu^+ \\ V_\mu^+ \end{pmatrix} = \begin{pmatrix} c_\xi & s_\xi \\ -s_\xi & c_\xi \end{pmatrix} \begin{pmatrix} W_{l\mu}^+ \\ W_{h\mu}^+ \end{pmatrix}, \tag{15}$$

where $Z_{l\mu}$ and $Z_{h\mu}$ are neutral eigenstates of mass with squared masses M_l and M_h, respectively, and $W_{l\mu}^+$ and $W_{h\mu}^+$ are charged eigenstates of mass with squared masses $\bar{M}_l$ and $\bar{M}_h$, respectively. By definition, $M_l < M_h$ and $\bar{M}_l < \bar{M}_h$. We identify Z_l as the observed neutral gauge boson with mass $m_Z = \sqrt{M_l} = 91.1876$ GeV and $W_l^\pm$ as the observed charged gauge bosons with mass $m_W = \sqrt{\bar{M}_L} = 80.378$ GeV. In Eqs. (15) $c_\psi \equiv \cos\psi$, $s_\psi \equiv \sin\psi$, $c_\xi \equiv \cos\xi$, and $s_\xi \equiv \sin\xi$, where ψ and ξ are mixing angles. Note that, if our LRS model had not been assumed to be CP-invariant, then the second Eq. (15) would have contained a phase in the mixing matrix. Without loss of generality, one may choose the overall sign of $\left(Z_{l\mu},\ Z_{h\mu}\right)^T$ in such a way that c_ψ is non-negative[5]; similarly, we also assume $c_\xi \geq 0$. Equations (15) come about because in the Lagrangian there are mass terms

$$\mathcal{L} = \cdots + \frac{1}{2} \begin{pmatrix} Z_\mu & X_\mu \end{pmatrix} M_n \begin{pmatrix} Z^\mu \\ X^\mu \end{pmatrix} + \begin{pmatrix} W_\mu^- & V_\mu^- \end{pmatrix} M_c \begin{pmatrix} W^{+\mu} \\ V^{+\mu} \end{pmatrix} \tag{16a}$$

$$= \frac{1}{2} \left(M_l\, Z_{l\mu} Z_l^\mu + M_h\, Z_{h\mu} Z_h^\mu \right) + \bar{M}_l\, W_{l\mu}^- W_l^{\mu+} + \bar{M}_h\, W_{h\mu}^- W_h^{\mu+}. \tag{16b}$$

In Eq. (16a) the 2×2 matrices M_n and M_c are real and symmetric.

2.3. Quarks

Multiplets In our simplified LRM we only consider the third-generation quarks, *viz.* the left-handed t_L and b_L and the right-handed t_R and b_R[6]; we disconsider both the lepton sector and the other two quark generations. Under $SU(2)_L \times SU(2)_R \times U(1)_X$,

$$\begin{pmatrix} t_L \\ b_L \end{pmatrix} \to \mathcal{U}_\mathcal{L} \begin{pmatrix} t_L \\ b_L \end{pmatrix} e^{i\gamma/6}, \qquad \begin{pmatrix} t_R \\ b_R \end{pmatrix} \to \mathcal{U}_\mathcal{R} \begin{pmatrix} t_R \\ b_R \end{pmatrix} e^{i\gamma/6}. \tag{17}$$

The quantum numbers of the quark fields are in Table 2.

[5] The *relative* sign of $Z_{l\mu}$ and $Z_{h\mu}$ is fixed by the requirement that the mixing matrix $\begin{pmatrix} c_\psi & -s_\psi \\ s_\psi & c_\psi \end{pmatrix}$ has *positive* determinant.

[6] There should be no confusion between the left-handed and right-handed bottom-quark fields—b_L and b_R, respectively—and the scalar field b.

Table 2
The $U(1)$ quantum numbers of the quark fields.

Fields	T_{L3}	T_{R3}	X	$Y = T_{R3} + X$	$Q = T_{L3} + Y$
t_L	$1/2$	0	$1/6$	$1/6$	$2/3$
b_L	$-1/2$	0	$1/6$	$1/6$	$-1/3$
t_R	0	$1/2$	$1/6$	$2/3$	$2/3$
b_R	0	$-1/2$	$1/6$	$-1/3$	$-1/3$

3. Fitting the $Zb\bar{b}$ coupling at tree level in the LRM

With the covariant derivative in Eq. (14) and since the bottom quark has the quantum numbers in Table 2, one has

$$\begin{aligned}\mathcal{L} = \cdots &+ \bar{b}_L \gamma_\mu \left[\frac{g}{c_w} Z^\mu \left(\frac{s_w^2}{3} - \frac{1}{2} \right) - \frac{l s_\alpha^2}{6 c_\alpha} X^\mu \right] b_L \\ &+ \bar{b}_R \gamma_\mu \left[\frac{g s_w^2}{3 c_w} Z^\mu + \frac{l}{c_\alpha} X^\mu \left(\frac{s_\alpha^2}{3} - \frac{1}{2} \right) \right] b_R . \end{aligned} \tag{18a}$$

Using both Eq. (10c) and the first Eq. (15), we find the coupling of the b quark to the light neutral gauge boson—which we identify as the observed one—written in the form of Eq. (1) as

$$\mathcal{L}_{Z_l b\bar{b}} = \frac{g}{c_w} Z_l^\mu \, \bar{b} \, \gamma_\mu \left(g_L^{\text{tree,LRM}} P_L + g_R^{\text{tree,LRM}} P_R \right) b, \tag{19}$$

with

$$g_L^{\text{tree,LRM}} = c_\psi \left(\frac{s_w^2}{3} - \frac{1}{2} \right) - s_\psi \, \frac{g s_w^2}{6 \sqrt{L c_w^2 - G s_w^2}}, \tag{20a}$$

$$g_R^{\text{tree,LRM}} = c_\psi \, \frac{s_w^2}{3} + s_\psi \, \frac{g}{\sqrt{L c_w^2 - G s_w^2}} \left(\frac{s_w^2}{3} - \frac{L c_w^2}{2G} \right). \tag{20b}$$

One sees that, besides the Weinberg angle θ_w, the two quantities $g_L^{\text{tree,LRM}}$ and $g_R^{\text{tree,LRM}}$ depend on two parameters of the LRM, *viz.* l/g and ψ. It should be possible to adjust the latter in order to reproduce the observed δg_L and δg_R in either the 'average' or 'fit' solutions:

$$\delta g_L = \left(\frac{s_w^2}{3} - \frac{1}{2} \right) (\cos\psi - 1) - \frac{s_w^2}{6} \left(\frac{l^2}{g^2} c_w^2 - s_w^2 \right)^{-1/2} \sin\psi, \tag{21a}$$

$$\delta g_R = \frac{s_w^2}{3} (\cos\psi - 1) + \left(\frac{s_w^2}{3} - \frac{l^2}{g^2} \frac{c_w^2}{2} \right) \left(\frac{l^2}{g^2} c_w^2 - s_w^2 \right)^{-1/2} \sin\psi. \tag{21b}$$

The solution to Eqs. (21) is depicted in Fig. 2. In particular, one sees that

$$\frac{l}{g} = 1.112, \quad \psi = -0.0144 \quad \text{for the 'fit' solution} \tag{22}$$

and

$$\frac{l}{g} = 0.929, \quad \psi = -0.0467 \quad \text{for the 'average' solution.} \tag{23}$$

Thus, in order to fit the $Zb\bar{b}$ vertex in the LRM at tree level one needs a mixing angle $\psi \lesssim -10^{-2}$; moreover, one should not be very far from the left–right-symmetric case $l = g$.

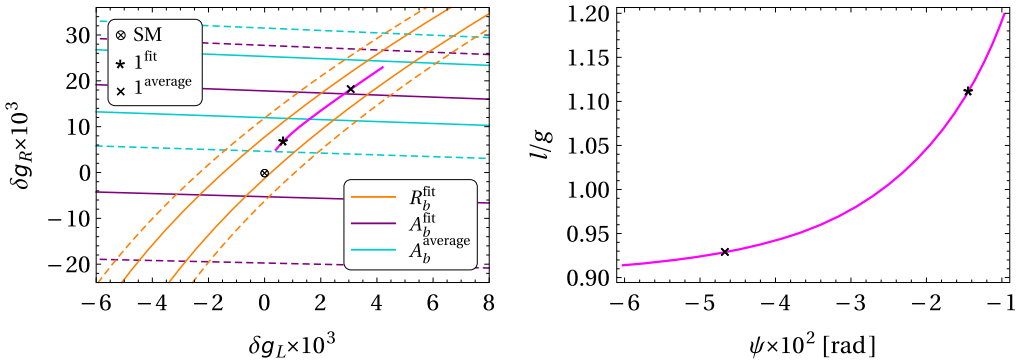

Fig. 2. Left panel: a smooth trajectory in the δg_R *vs.* δg_L plane connecting the $1^{\rm fit}$ and $1^{\rm average}$ points of Table 1. Right panel: the same trajectory translated into the l/g *vs.* ψ plane through solving Eqs. (21). We have used $c_w^2 = m_W^2 \big/ m_Z^2$.

It remains to be seen whether values of l/g and ψ like those in the right panel of Fig. 2 are compatible with phenomenology. This matter goes beyond the scope of the present work. We just refer to the rather old Ref. [36] and the more recent Refs. [37–39]; their authors have investigated how large ψ is allowed to be in a left–right-symmetric model (*viz.* a model with $l = g$). They all conclude that $|\psi| \lesssim 10^{-3}$. It is conceivable that allowing for $l/g \neq 1$ may give $|\psi|$ some room for being larger; but $\psi \sim -0.01$ seems far-fetched. One thus concludes that using the LRM at tree level for fitting the $Zb\bar{b}$ vertex does not work. It remains to be seen whether the LRM at one-loop level can do a better job; that is the aim of this work. Unfortunately, in order to do that job properly one must carefully renormalize the LRM; that forces us to define the model completely, including its scalar sector. That is what we do in the next section.

4. Description of the model: scalars

4.1. Multiplets

The scalar multiplets of our LRM consist of an $SU(2)_L$ doublet H_L, an $SU(2)_R$ doublet H_R,[7] and a 'bi-doublet'—*i.e.*, a doublet both of $SU(2)_L$ and of $SU(2)_R$—Φ. Thus,

$$H_L = \begin{pmatrix} m \\ n \end{pmatrix}, \quad H_R = \begin{pmatrix} p \\ q \end{pmatrix}, \quad \Phi = \begin{pmatrix} b^* & c \\ -a^* & d \end{pmatrix}, \quad \tilde{\Phi} \equiv \tau_2 \Phi^* \tau_2 = \begin{pmatrix} d^* & a \\ -c^* & b \end{pmatrix}, \tag{24}$$

where m, n, p, q, a, b, c, and d are complex Klein–Gordon fields. The multiplets (24) transform under $SU(2)_L \times SU(2)_R \times U(1)_X$ as

$$H_L \to \mathcal{U}_\mathcal{L}\, H_L\, e^{i\gamma/2}, \quad H_R \to \mathcal{U}_\mathcal{R}\, H_R\, e^{i\gamma/2}, \quad \Phi \to \mathcal{U}_\mathcal{L}\, \Phi\, \mathcal{U}_\mathcal{R}^\dagger, \quad \tilde{\Phi} \to \mathcal{U}_\mathcal{L}\, \tilde{\Phi}\, \mathcal{U}_\mathcal{R}^\dagger, \tag{25}$$

where $\mathcal{U}_\mathcal{L}$ and $\mathcal{U}_\mathcal{R}$ are the 2×2 unitary matrices with determinant 1 representing the $SU(2)_L$ and $SU(2)_R$ transformations, respectively, in the doublet representation. The phase γ is the parameter of the $U(1)_X$ transformation: both H_L and H_R have $X = 1/2$ while Φ has $X = 0$. The $U(1)$ quantum numbers of the scalar fields are given in Table 3.

[7] Other left–right models use triplets of $SU(2)_L$ and $SU(2)_R$ instead of H_L and H_R.

Table 3
The $U(1)$ quantum numbers of the scalar fields.

Fields	T_{L3}	T_{R3}	X	$Y = T_{R3} + X$	$Q = T_{L3} + Y$
m	1/2	0	1/2	1/2	1
n	−1/2	0	1/2	1/2	0
p	0	1/2	1/2	1	1
q	0	−1/2	1/2	0	0
$a,\ c$	1/2	1/2	0	1/2	1
$b,\ d$	−1/2	1/2	0	1/2	0

4.2. VEVs

The electromagnetism-conserving[8] vacuum expectation values (VEVs) are

$$\langle 0|m|0\rangle = \langle 0|p|0\rangle = \langle 0|a|0\rangle = \langle 0|c|0\rangle = 0, \tag{26a}$$

$$\langle 0|n|0\rangle = u_L, \quad \langle 0|q|0\rangle = u_R, \quad \langle 0|b|0\rangle = v_1, \quad \langle 0|d|0\rangle = v_2. \tag{26b}$$

Since we assume our model to be CP-conserving, u_L, u_R, v_1, and v_2 are taken to be *real*. Without loss of generality, one may choose the signs of the scalar multiplets to set u_L, u_R, and v_2 non-negative; only the sign of v_1 remains free. We define

$$U_L \equiv u_L^2, \quad U_R \equiv u_R^2, \quad V_1 \equiv v_1^2, \quad V_2 \equiv v_2^2. \tag{27}$$

One may interchange Φ and $\tilde{\Phi}$, *i.e.* one may make $a \leftrightarrow c$ and $b \leftrightarrow d$. Thus, from now on we shall assume V_2 to be larger than V_1.

4.3. Mixing of the scalars

Definition of the mixing matrices We expand the neutral-scalar fields about their VEVs as

$$n = u_L + \frac{\rho_L + i\eta_L}{\sqrt{2}}, \quad q = u_R + \frac{\rho_R + i\eta_R}{\sqrt{2}}, \quad b = v_1 + \frac{\rho_1 + i\eta_1}{\sqrt{2}}, \quad d = v_2 + \frac{\rho_2 + i\eta_2}{\sqrt{2}}, \tag{28}$$

where $\rho_{L,R,1,2}$ and $\eta_{L,R,1,2}$ are *real* Klein–Gordon fields. Because of the assumed CP invariance, the fields $\rho_{L,R,1,2}$ (*viz.* the scalars) mix among themselves, but they do not mix with the fields $\eta_{L,R,1,2}$ (*viz.* the pseudoscalars). Thus,

$$\begin{pmatrix} \rho_1 \\ \rho_2 \\ \rho_L \\ \rho_R \end{pmatrix} = V_\rho \begin{pmatrix} S_5^0 \\ S_6^0 \\ S_7^0 \\ S_8^0 \end{pmatrix}, \tag{29}$$

where $S^0_{5,6,7,8}$ are real eigenstates of mass with masses $\mu_{5,6,7,8}$, respectively. The 4×4 matrix V_ρ is real and orthogonal. Analogously to Eq. (29),

[8] We *assume* conservation of electromagnetism by the vacuum state.

$$\begin{pmatrix} \eta_1 \\ \eta_2 \\ \eta_L \\ \eta_R \end{pmatrix} = V_\eta \begin{pmatrix} G_l^0 \\ G_h^0 \\ S_3^0 \\ S_4^0 \end{pmatrix}, \tag{30}$$

where G_l^0 and G_h^0 are the Goldstone bosons that are 'eaten' by $Z_{l\mu}$ and $Z_{h\mu}$, respectively, while S_3^0 and S_4^0 are physical pseudoscalars with squared masses $M_{\eta 1}$ and $M_{\eta 2}$, respectively. The matrix V_η is real and orthogonal. Also,

$$\begin{pmatrix} a \\ c \\ m \\ p \end{pmatrix} = V_\varphi \begin{pmatrix} G_l^+ \\ G_h^+ \\ H_3^+ \\ H_4^+ \end{pmatrix}, \tag{31}$$

where G_l^+ and G_h^+ are Goldstone bosons that are 'eaten' by $W_{l\mu}^+$ and $W_{h\mu}^+$, respectively, while H_3^+ and H_4^+ are physical charged scalars with squared masses $M_{\varphi 1}$ and $M_{\varphi 2}$, respectively. The matrix V_φ is real and orthogonal because of the assumed CP conservation.

Parameterization of V_ρ The parameterization that we use for the matrix V_ρ in Eq. (29) is the following:

$$\begin{aligned} V_\rho = {} & \begin{pmatrix} 1 & 0 & 0 & 0 \\ 0 & 1 & 0 & 0 \\ 0 & 0 & c_3 & -s_3 \\ 0 & 0 & s_3 & c_3 \end{pmatrix} \times \begin{pmatrix} 1 & 0 & 0 & 0 \\ 0 & c_2 & -s_2 & 0 \\ 0 & s_2 & c_2 & 0 \\ 0 & 0 & 0 & 1 \end{pmatrix} \times \begin{pmatrix} 1 & 0 & 0 & 0 \\ 0 & 1 & 0 & 0 \\ 0 & 0 & c_6 & s_6 \\ 0 & 0 & s_6 & -c_6 \end{pmatrix} \\ & \times \begin{pmatrix} c_1 & s_1 & 0 & 0 \\ s_1 & -c_1 & 0 & 0 \\ 0 & 0 & 1 & 0 \\ 0 & 0 & 0 & 1 \end{pmatrix} \times \begin{pmatrix} 1 & 0 & 0 & 0 \\ 0 & s_4 & 0 & c_4 \\ 0 & 0 & 1 & 0 \\ 0 & c_4 & 0 & -s_4 \end{pmatrix} \times \begin{pmatrix} 1 & 0 & 0 & 0 \\ 0 & 0 & c_5 & s_5 \\ 0 & 0 & s_5 & -c_5 \\ 0 & 1 & 0 & 0 \end{pmatrix}, \end{aligned} \tag{32}$$

where $c_i \equiv \cos\theta_i$ and $s_i \equiv \sin\theta_i$ for $i = 1, \ldots, 6$. In this way one obtains a matrix V_ρ with a simple first row and a simple first column:

$$V_\rho = \begin{pmatrix} c_1 & s_1 c_4 & s_1 s_4 c_5 & s_1 s_4 s_5 \\ s_1 c_2 & (V_\rho)_{22} & (V_\rho)_{23} & (V_\rho)_{24} \\ s_1 s_2 c_3 & (V_\rho)_{32} & (V_\rho)_{33} & (V_\rho)_{34} \\ s_1 s_2 s_3 & (V_\rho)_{42} & (V_\rho)_{43} & (V_\rho)_{44} \end{pmatrix}. \tag{33}$$

The sign of S_5^0 is chosen in such a way that $\det V_\rho = +1$ is positive. We choose the signs of S_6^0, S_7^0, and S_8^0 in such a way that c_4, c_5, and s_5 are non-negative.

Goldstone bosons Since the scalar doublets of $SU(2)_L$ are

$$\begin{pmatrix} m \\ n \end{pmatrix}, \quad \begin{pmatrix} a \\ b \end{pmatrix}, \quad \text{and} \quad \begin{pmatrix} c \\ d \end{pmatrix}, \tag{34}$$

and the scalar doublets of $SU(2)_R$ are

$$\begin{pmatrix} p \\ q \end{pmatrix}, \quad \begin{pmatrix} -a \\ d^* \end{pmatrix}, \quad \text{and} \quad \begin{pmatrix} -c \\ b^* \end{pmatrix}, \tag{35}$$

the neutral fields

$$u_L\eta_L + v_1\eta_1 + v_2\eta_2 \quad \text{and} \quad u_R\eta_R - v_1\eta_1 - v_2\eta_2 \tag{36}$$

are Goldstone bosons. The charged fields

$$u_L m + v_1 a + v_2 c \quad \text{and} \quad u_R p - v_2 a - v_1 c \tag{37}$$

are Goldstone bosons too. Thus, there are two neutral Goldstone bosons and two charged Goldstone bosons, and it is a non-trivial problem to find out how they mix to form the states that are 'swallowed' by the neutral gauge bosons $Z_{l\mu}$ and $Z_{h\mu}$ and by the charged gauge bosons $W^+_{l\mu}$ and $W^+_{h\mu}$, respectively. This problem is addressed in Appendix A. The results of that appendix may be summarized as follows:

$$\begin{aligned}
(V_\eta)_{11} &= \frac{v_1\left(c_\psi\varrho_1 - s_\psi L\right)}{\sqrt{2M_l}\sqrt{L+H}}, & (V_\eta)_{12} &= \frac{v_1\left(-s_\psi\varrho_1 - c_\psi L\right)}{\sqrt{2M_h}\sqrt{L+H}},\\
(V_\eta)_{21} &= \frac{v_2\left(c_\psi\varrho_1 - s_\psi L\right)}{\sqrt{2M_l}\sqrt{L+H}}, & (V_\eta)_{22} &= \frac{v_2\left(-s_\psi\varrho_1 - c_\psi L\right)}{\sqrt{2M_h}\sqrt{L+H}},\\
(V_\eta)_{31} &= \frac{u_L\left(c_\psi\varrho_1 + s_\psi H\right)}{\sqrt{2M_l}\sqrt{L+H}}, & (V_\eta)_{32} &= \frac{u_L\left(-s_\psi\varrho_1 + c_\psi H\right)}{\sqrt{2M_h}\sqrt{L+H}},\\
(V_\eta)_{41} &= s_\psi\,\frac{u_R\sqrt{L+H}}{\sqrt{2M_l}}, & (V_\eta)_{42} &= c_\psi\,\frac{u_R\sqrt{L+H}}{\sqrt{2M_h}},
\end{aligned} \tag{38}$$

and

$$\begin{aligned}
(V_\varphi)_{11} &= \frac{c_\xi g v_1 + s_\xi l v_2}{\sqrt{2\bar{M}_l}}, & (V_\varphi)_{12} &= \frac{s_\xi g v_1 - c_\xi l v_2}{\sqrt{2\bar{M}_h}},\\
(V_\varphi)_{21} &= \frac{c_\xi g v_2 + s_\xi l v_1}{\sqrt{2\bar{M}_l}}, & (V_\varphi)_{22} &= \frac{s_\xi g v_2 - c_\xi l v_1}{\sqrt{2\bar{M}_h}},\\
(V_\varphi)_{31} &= \frac{c_\xi g u_L}{\sqrt{2\bar{M}_l}}, & (V_\varphi)_{32} &= \frac{s_\xi g u_L}{\sqrt{2\bar{M}_h}},\\
(V_\varphi)_{41} &= \frac{-s_\xi l u_R}{\sqrt{2\bar{M}_l}}, & (V_\varphi)_{42} &= \frac{c_\xi l u_R}{\sqrt{2\bar{M}_h}}.
\end{aligned} \tag{39}$$

The physical pseudoscalars Two orthonormalized linear combinations of the η fields that are orthogonal to the Goldstone bosons (36) are

$$\eta_a \equiv \frac{v_2\eta_1 - v_1\eta_2}{\sqrt{T_1}}, \qquad \eta_b \equiv \frac{T_1\left(u_L\eta_R + u_R\eta_L\right) + u_L u_R\left(v_1\eta_1 + v_2\eta_2\right)}{\sqrt{T_1}\sqrt{T_2}}, \tag{40}$$

where

$$T_1 \equiv V_1 + V_2, \qquad T_2 \equiv U_L U_R + T_1\left(U_L + U_R\right). \tag{41}$$

Note that $\sqrt{T_1}$ and $\sqrt{T_2}$ are positive—this corresponds to the definition of the signs of η_a and η_b. The Lagrangian contains mass terms for the pseudoscalar fields as

$$\mathcal{L} = \cdots - \frac{1}{2}\begin{pmatrix}\eta_a, & \eta_b\end{pmatrix} M_\eta \begin{pmatrix}\eta_a\\ \eta_b\end{pmatrix}, \tag{42}$$

where M_η is a real 2×2 symmetric matrix. This matrix is diagonalized as

$$\begin{pmatrix} c_\eta & -s_\eta\\ s_\eta & c_\eta\end{pmatrix} M_\eta \begin{pmatrix} c_\eta & s_\eta\\ -s_\eta & c_\eta\end{pmatrix} = \begin{pmatrix} M_{\eta 1} & 0\\ 0 & M_{\eta 2}\end{pmatrix}, \tag{43}$$

where $c_\eta \equiv \cos\eta$, $s_\eta \equiv \sin\eta$, and $M_{\eta 1} < M_{\eta 2}$. From Eq. (43),

$$\left(M_\eta\right)_{11} = M_{\eta 1} c_\eta^2 + M_{\eta 2} s_\eta^2, \tag{44a}$$

$$\left(M_\eta\right)_{22} = M_{\eta 1} s_\eta^2 + M_{\eta 2} c_\eta^2, \tag{44b}$$

$$\left(M_\eta\right)_{12} = \left(M_{\eta 2} - M_{\eta 1}\right) c_\eta s_\eta. \tag{44c}$$

Since

$$\begin{pmatrix} \eta_a \\ \eta_b \end{pmatrix} = \begin{pmatrix} c_\eta & s_\eta \\ -s_\eta & c_\eta \end{pmatrix} \begin{pmatrix} S_3^0 \\ S_4^0 \end{pmatrix}, \tag{45}$$

one has

$$\begin{aligned}
\left(V_\eta\right)_{13} &= c_\eta \frac{v_2}{\sqrt{T_1}} - s_\eta \frac{v_1 u_L u_R}{\sqrt{T_1 T_2}}, & \left(V_\eta\right)_{14} &= s_\eta \frac{v_2}{\sqrt{T_1}} + c_\eta \frac{v_1 u_L u_R}{\sqrt{T_1 T_2}}, \\
\left(V_\eta\right)_{23} &= c_\eta \frac{-v_1}{\sqrt{T_1}} - s_\eta \frac{v_2 u_L u_R}{\sqrt{T_1 T_2}}, & \left(V_\eta\right)_{24} &= s_\eta \frac{-v_1}{\sqrt{T_1}} + c_\eta \frac{v_2 u_L u_R}{\sqrt{T_1 T_2}}, \\
\left(V_\eta\right)_{33} &= s_\eta u_R \sqrt{\frac{T_1}{T_2}}, & \left(V_\eta\right)_{34} &= -c_\eta u_R \sqrt{\frac{T_1}{T_2}}, \\
\left(V_\eta\right)_{43} &= -s_\eta u_L \sqrt{\frac{T_1}{T_2}}, & \left(V_\eta\right)_{44} &= c_\eta u_L \sqrt{\frac{T_1}{T_2}}.
\end{aligned} \tag{46}$$

In Eq. (45), we choose the sign of $\left(S_3^0,\ S_4^0\right)^T$ in such a way that c_η is non-negative.[9]

The physical charged scalars Two orthonormalized fields that are orthogonal to the charged Goldstone bosons (37) are

$$\varphi_a^+ \equiv \frac{\left(V_1 - V_2\right) m - v_1 u_L a + v_2 u_L c}{\sqrt{K_1}}, \tag{47a}$$

$$\varphi_b^+ \equiv \frac{2 v_1 v_2 u_L u_R m - K_1 p + v_2 u_R \left(V_1 - V_2 - U_L\right) a + v_1 u_R \left(V_2 - V_1 - U_L\right) c}{\sqrt{K_1}\sqrt{K_2}}, \tag{47b}$$

where

$$K_1 \equiv \left(V_1 - V_2\right)^2 + \left(V_1 + V_2\right) U_L, \qquad K_2 \equiv U_L U_R + K_1 + \left(V_1 + V_2\right) U_R. \tag{48}$$

In Eqs. (47), the normalization factors $\sqrt{K_1}$ and $\sqrt{K_2}$ are positive—this corresponds to a convention for the signs of φ_a^+ and φ_b^+. The Lagrangian contains mass terms for the charged-scalar fields as

$$\mathcal{L} = \cdots - \begin{pmatrix} \varphi_a^- , & \varphi_b^- \end{pmatrix} M_\varphi \begin{pmatrix} \varphi_a^+ \\ \varphi_b^+ \end{pmatrix}, \tag{49}$$

where M_φ is a real (because our model is CP-conserving) 2×2 symmetric matrix. That matrix is diagonalized as

$$\begin{pmatrix} c_\varphi & -s_\varphi \\ s_\varphi & c_\varphi \end{pmatrix} M_\varphi \begin{pmatrix} c_\varphi & s_\varphi \\ -s_\varphi & c_\varphi \end{pmatrix} = \begin{pmatrix} M_{\varphi 1} & 0 \\ 0 & M_{\varphi 2} \end{pmatrix}, \tag{50}$$

[9] The relative sign of S_3^0 and S_4^0 is fixed by the condition that the determinant of the mixing matrix $\begin{pmatrix} c_\eta & s_\eta \\ -s_\eta & c_\eta \end{pmatrix}$ is positive.

where $c_\varphi \equiv \cos\varphi$, $s_\varphi \equiv \sin\varphi$, and $M_{\varphi 1} < M_{\varphi 2}$. It follows from Eqs. (50) that

$$\left(M_\varphi\right)_{11} = M_{\varphi 1} c_\varphi^2 + M_{\varphi 2} s_\varphi^2, \tag{51a}$$
$$\left(M_\varphi\right)_{22} = M_{\varphi 1} s_\varphi^2 + M_{\varphi 2} c_\varphi^2, \tag{51b}$$
$$\left(M_\varphi\right)_{12} = \left(M_{\varphi 2} - M_{\varphi 1}\right) c_\varphi s_\varphi. \tag{51c}$$

Since

$$\begin{pmatrix} \varphi_a^+ \\ \varphi_b^+ \end{pmatrix} = \begin{pmatrix} c_\varphi & s_\varphi \\ -s_\varphi & c_\varphi \end{pmatrix} \begin{pmatrix} H_3^+ \\ H_4^+ \end{pmatrix}, \tag{52}$$

one has

$$\left(V_\varphi\right)_{13} = \frac{-c_\varphi v_1 u_L}{\sqrt{K_1}} + \frac{s_\varphi v_2 u_R \left(V_2 - V_1 + U_L\right)}{\sqrt{K_1 K_2}}, \tag{53a}$$
$$\left(V_\varphi\right)_{23} = \frac{c_\varphi v_2 u_L}{\sqrt{K_1}} + \frac{s_\varphi v_1 u_R \left(V_1 - V_2 + U_L\right)}{\sqrt{K_1 K_2}}, \tag{53b}$$
$$\left(V_\varphi\right)_{33} = \frac{c_\varphi \left(V_1 - V_2\right)}{\sqrt{K_1}} - \frac{2 s_\varphi v_1 v_2 u_L u_R}{\sqrt{K_1 K_2}}, \tag{53c}$$
$$\left(V_\varphi\right)_{43} = s_\varphi \sqrt{\frac{K_1}{K_2}}, \tag{53d}$$
$$\left(V_\varphi\right)_{14} = \frac{-s_\varphi v_1 u_L}{\sqrt{K_1}} + \frac{c_\varphi v_2 u_R \left(V_1 - V_2 - U_L\right)}{\sqrt{K_1 K_2}}, \tag{54a}$$
$$\left(V_\varphi\right)_{24} = \frac{s_\varphi v_2 u_L}{\sqrt{K_1}} + \frac{c_\varphi v_1 u_R \left(V_2 - V_1 - U_L\right)}{\sqrt{K_1 K_2}}, \tag{54b}$$
$$\left(V_\varphi\right)_{34} = \frac{s_\varphi \left(V_1 - V_2\right)}{\sqrt{K_1}} + \frac{2 c_\varphi v_1 v_2 u_L u_R}{\sqrt{K_1 K_2}}, \tag{54c}$$
$$\left(V_\varphi\right)_{44} = -c_\varphi \sqrt{\frac{K_1}{K_2}}. \tag{54d}$$

In Eq. (52), we choose the sign of $\left(H_3^+,\ H_4^+\right)$ such that $c_\varphi \geq 0$.[10]

4.4. Gauge-fixing terms

The terms in the Lagrangian that are bi-linear in either the gauge-boson fields or the scalar fields are

$$\begin{aligned}\mathcal{L} = \cdots &+ \frac{1}{2}\left(\partial_\mu G_l^0\ \partial^\mu G_l^0 + \partial_\mu G_h^0\ \partial^\mu G_h^0 + \partial_\mu S_3^0\ \partial^\mu S_3^0 + \partial_\mu S_4^0\ \partial^\mu S_4^0\right) \\ &- \frac{1}{4}\left(\partial_\mu Z_{lv} - \partial_v Z_{l\mu}\right)\left(\partial^\mu Z_l^v - \partial^v Z_l^\mu\right) \\ &- \frac{1}{4}\left(\partial_\mu Z_{hv} - \partial_v Z_{h\mu}\right)\left(\partial^\mu Z_h^v - \partial^v Z_h^\mu\right)\end{aligned}$$

[10] The relative sign of H_3^+ and H_4^+ is not free, since altering it would change the sign of the determinant of the mixing matrix $\begin{pmatrix} c_\varphi & s_\varphi \\ -s_\varphi & c_\varphi \end{pmatrix}$.

$$
\begin{aligned}
&-\frac{1}{4}\left(\partial_\mu A_\nu - \partial_\nu A_\mu\right)\left(\partial^\mu A^\nu - \partial^\nu A^\mu\right)\\
&-\frac{M_{\eta_1}}{2}\left(S_3^0\right)^2 - \frac{M_{\eta_2}}{2}\left(S_4^0\right)^2 + \frac{M_l}{2}\,Z_{l\mu}\,Z_l^\mu + \frac{M_h}{2}\,Z_{h\mu}\,Z_h^\mu\\
&+\sqrt{M_l}\,Z_{l\mu}\,\partial^\mu G_l^0 + \sqrt{M_h}\,Z_{h\mu}\,\partial^\mu G_h^0,
\end{aligned}
\tag{55}
$$

and

$$
\begin{aligned}
\mathcal{L} = \cdots &+ \partial_\mu G_l^-\;\partial^\mu G_l^+ + \partial_\mu G_h^-\;\partial^\mu G_h^+ + \partial_\mu H_3^-\;\partial^\mu H_3^+ + \partial_\mu H_4^-\;\partial^\mu H_4^+\\
&-\left(\partial^\mu W_l^{+\nu}\right)\left(\partial_\mu W_{l\nu}^-\right) + \left(\partial^\mu W_l^{+\nu}\right)\left(\partial_\nu W_{l\mu}^-\right)\\
&-\left(\partial^\mu W_h^{+\nu}\right)\left(\partial_\mu W_{h\nu}^-\right) + \left(\partial^\mu W_h^{+\nu}\right)\left(\partial_\nu W_{h\mu}^-\right),\\
&-M_{\varphi_1} H_3^- H_3^+ - M_{\varphi_2} H_4^- H_4^+ + \bar{M}_l\,W_{l\mu}^- W_l^{\mu+} + \bar{M}_h\,W_{h\mu}^- W_h^{\mu+}\\
&+i\left(\sqrt{\bar{M}_l}\;W_{l\mu}^-\,\partial^\mu G_l^+ + \sqrt{\bar{M}_h}\;W_{h\mu}^-\,\partial^\mu G_h^+ - \text{H.c.}\right)
\end{aligned}
\tag{56}
$$

cf. Eq. (A.13). We add to them the gauge-fixing terms[11]

$$
\mathcal{L}_{\text{gf},0} = -\frac{\left(\partial_\mu Z_l^\mu - \xi_l\sqrt{M_l}\,G_l^0\right)^2}{2\xi_l} - \frac{\left(\partial_\mu Z_h^\mu - \xi_h\sqrt{M_h}\,G_h^0\right)^2}{2\xi_h} - \frac{\left(\partial_\mu A^\mu\right)^2}{2\xi_A},
\tag{57a}
$$

$$
\begin{aligned}
\mathcal{L}_{\text{gf},\pm} = &-\frac{\left(\partial_\mu W_l^{+\mu} - i\bar{\xi}_l\sqrt{\bar{M}_l}\,G_l^+\right)\left(\partial_\nu W_l^{-\nu} + i\bar{\xi}_l\sqrt{\bar{M}_l}\,G_l^-\right)}{\bar{\xi}_l}\\
&-\frac{\left(\partial_\mu W_h^{+\mu} - i\bar{\xi}_h\sqrt{\bar{M}_h}\,G_h^+\right)\left(\partial_\nu W_h^{+\nu} + i\bar{\xi}_h\sqrt{\bar{M}_h}\,G_h^-\right)}{\bar{\xi}_h}.
\end{aligned}
\tag{57b}
$$

4.5. Scalar potential

The scalar potential appears in the Lagrangian as $\mathcal{L} = \cdots - V$ and is in our model of the form $V = V_H + V_\Phi + V_{H\Phi}$, where

$$
\begin{aligned}
V_H = &\,\mu_L\,H_L^\dagger H_L + \mu_R\,H_R^\dagger H_R\\
&+\lambda_L\,H_L^\dagger H_L\,H_L^\dagger H_L + \lambda_R\,H_R^\dagger H_R\,H_R^\dagger H_R + \lambda_{LR}\,H_L^\dagger H_L\,H_R^\dagger H_R,
\end{aligned}
\tag{58a}
$$

$$
\begin{aligned}
V_\Phi = &\,\mu_1\,\text{tr}\left(\Phi^\dagger\Phi\right) + \mu_2\,\text{tr}\left(\tilde{\Phi}^\dagger\Phi + \Phi^\dagger\tilde{\Phi}\right)\\
&+\lambda_1\left[\text{tr}\left(\Phi^\dagger\Phi\right)\right]^2 + \lambda_2\left\{\left[\text{tr}\left(\Phi^\dagger\tilde{\Phi}\right)\right]^2 + \text{H.c.}\right\} + \lambda_3\left|\text{tr}\left(\Phi^\dagger\tilde{\Phi}\right)\right|^2\\
&+\lambda_4\,\text{tr}\left(\Phi^\dagger\Phi\right)\text{tr}\left(\tilde{\Phi}^\dagger\Phi + \Phi^\dagger\tilde{\Phi}\right),
\end{aligned}
\tag{58b}
$$

$$
\begin{aligned}
V_{H\Phi} = &\,m_1\left(H_L^\dagger\Phi H_R + H_R^\dagger\Phi^\dagger H_L\right) + m_2\left(H_L^\dagger\tilde{\Phi}H_R + H_R^\dagger\tilde{\Phi}^\dagger H_L\right)\\
&+\lambda_{3L}\,H_L^\dagger\Phi\Phi^\dagger H_L + \lambda_{3R}\,H_R^\dagger\Phi^\dagger\Phi H_R + \lambda_{4L}\,H_L^\dagger\tilde{\Phi}\tilde{\Phi}^\dagger H_L + \lambda_{4R}\,H_R^\dagger\tilde{\Phi}^\dagger\tilde{\Phi}H_R\\
&+\lambda_{5L}\,H_L^\dagger\left(\Phi\tilde{\Phi}^\dagger + \tilde{\Phi}\Phi^\dagger\right)H_L + \lambda_{5R}\,H_R^\dagger\left(\Phi^\dagger\tilde{\Phi} + \tilde{\Phi}^\dagger\Phi\right)H_R.
\end{aligned}
\tag{58c}
$$

[11] We restrict ourselves to R_ξ gauges.

The parameters λ_L, λ_R, λ_{LR}, λ_1, λ_2, λ_3, λ_4, λ_{3L}, λ_{3R}, λ_{4L}, λ_{4R}, λ_{5L}, and λ_{5R} are dimensionless; the parameters m_1 and m_2 have mass dimension; the parameters μ_L, μ_R, μ_1, and μ_2 have mass-squared dimension. All these parameters are real because of the assumed CP conservation. Notice that we have *not* imposed the parity symmetry $H_L \leftrightarrow H_R$, $\Phi \to \Phi^\dagger$, $\tilde{\Phi} \to \tilde{\Phi}^\dagger$ on V. In component fields, $V = V_{(2)} + V_{(3)} + V_{(4)}$, where

$$V_{(2)} = \mu_L \left(|m|^2 + |n|^2\right) + \mu_R \left(|p|^2 + |q|^2\right) + \mu_1 \left(|a|^2 + |b|^2 + |c|^2 + |d|^2\right) + 2\mu_2 \left(a^* c + a c^* + b^* d + b d^*\right), \tag{59a}$$

$$V_{(3)} = m_1 \left(-a^* n^* p - a n p^* + b^* m^* p + b m p^* + c m^* q + c^* m q^* + d n^* q + d^* n q^*\right) + m_2 \left(-c^* n^* p - c n p^* + d^* m^* p + d m p^* + a m^* q + a^* m q^* + b n^* q + b^* n q^*\right), \tag{59b}$$

$$\begin{aligned} V_{(4)} = {} & \lambda_L \left(|m|^2 + |n|^2\right)^2 + \lambda_R \left(|p|^2 + |q|^2\right)^2 + \lambda_{LR} \left(|m|^2 + |n|^2\right)\left(|p|^2 + |q|^2\right) \\ & + \lambda_1 \left(|a|^2 + |b|^2 + |c|^2 + |d|^2\right)^2 \\ & + 4\lambda_2 \left(a^2 c^{*2} + b^2 d^{*2} + 2abc^*d^* + \text{H.c.}\right) \\ & + 4\lambda_3 \left(|ac|^2 + |bd|^2 + adb^*c^* + a^*d^*bc\right) \\ & + 2\lambda_4 \left(|a|^2 + |b|^2 + |c|^2 + |d|^2\right)\left(a^*c + b^*d + ac^* + bd^*\right) \\ & + \lambda_{3L} \left\{\left(|b|^2 + |c|^2\right)|m|^2 + \left(|a|^2 + |d|^2\right)|n|^2 + 2\,\text{Re}\left[\left(cd^* - ab^*\right)m^*n\right]\right\} \\ & + \lambda_{4L} \left\{\left(|b|^2 + |c|^2\right)|n|^2 + \left(|a|^2 + |d|^2\right)|m|^2 - 2\,\text{Re}\left[\left(cd^* - ab^*\right)m^*n\right]\right\} \\ & + \lambda_{5L} \left(|m|^2 + |n|^2\right)\left(ac^* + a^*c + bd^* + b^*d\right) \\ & + \lambda_{3R} \left\{\left(|a|^2 + |b|^2\right)|p|^2 + \left(|c|^2 + |d|^2\right)|q|^2 + 2\,\text{Re}\left[(bc - ad)\,p^*q\right]\right\} \\ & + \lambda_{4R} \left\{\left(|a|^2 + |b|^2\right)|q|^2 + \left(|c|^2 + |d|^2\right)|p|^2 - 2\,\text{Re}\left[(bc - ad)\,p^*q\right]\right\} \\ & + \lambda_{5R} \left(|p|^2 + |q|^2\right)\left(ac^* + a^*c + bd^* + b^*d\right). \end{aligned} \tag{59c}$$

The parameters in $V_{(4)}$ are constrained by the unitarity and bounded-from-below conditions; these are worked out in Appendices B and C, respectively. Additional constraints derive from the condition that the assumed minimum of the potential is a global, not just local, minimum; they are partially given in Appendix D. Still other constraints have to do with the observed couplings of the scalar of mass 125 GeV, which we assume to be S_5^0,[12] to pairs of gauge bosons or to quark pairs; they are worked out in Appendix E.

[12] We do not in general assume, though, S_5^0 to be *the lightest* scalar.

4.6. Yukawa couplings and quark masses

Yukawa couplings The Yukawa couplings are given by

$$\mathcal{L}_{\text{Yukawa}} = -\left(\bar{t}_L, \quad \bar{b}_L\right)\left(y_1\Phi + y_2\tilde{\Phi}\right)\begin{pmatrix} t_R \\ b_R \end{pmatrix} + \text{H.c.} \tag{60a}$$

$$\begin{aligned} &= -\left(y_1 b^* + y_2 d^*\right)\bar{t}_L t_R - \left(y_1 c + y_2 a\right)\bar{t}_L b_R \\ &\quad + \left(y_1 a^* + y_2 c^*\right)\bar{b}_L t_R - \left(y_1 d + y_2 b\right)\bar{b}_L b_R + \text{H.c.}, \end{aligned} \tag{60b}$$

where the Yukawa coupling constants y_1 and y_2 are real because of the assumed CP invariance of the model.

Quark masses When b and d acquire real VEVs v_1 and v_2, respectively, Eq. (60b) gives rise to quark masses

$$m_t = y_1 v_1 + y_2 v_2, \qquad m_b = y_1 v_2 + y_2 v_1. \tag{61}$$

From Eqs. (61),

$$y_1 = \frac{-v_1 m_t + v_2 m_b}{V_2 - V_1}, \qquad y_2 = \frac{v_2 m_t - v_1 m_b}{V_2 - V_1}. \tag{62}$$

Without loss of generality, we fix the relative sign of $(t_L,\ b_L)^T$ and $(t_R,\ b_R)^T$ in such a way that $y_2 \geq 0$. Since we have already fixed $V_2 \geq V_1$, this means that we always use $m_t \geq 0$. The sign of m_b—just as the sign of v_1—remains free.

5. Parameter counting and procedure

Counting of parameters Our left–right model has in its Lagrangian the following parameters:

- The gauge coupling constants g, l, and h.
- The parameters of the potential μ_L, μ_R, μ_1, μ_2, m_1, m_2, λ_L, λ_R, λ_{LR}, λ_1, λ_2, λ_3, λ_4, λ_{3L}, λ_{3R}, λ_{4L}, λ_{4R}, λ_{5L}, and λ_{5R}.
- The Yukawa couplings y_1 and y_2.

This makes 24 real parameters. (There are other parameters in the model, but they are dependent on these 24. For instance, θ_w and α depend on the gauge coupling constants; the VEVs $u_{L,R}$ and $v_{1,2}$ depend on the parameters of the potential.)

Counting of observables We use observable quantities as input of the renormalization procedure. We choose these observables to be exclusively masses, mixing angles, and the electromagnetic coupling constant. The quantities at our disposal are:

- The squared electromagnetic coupling constant, *viz.* E.
- The squared masses of the neutral gauge bosons, *viz.* M_l and M_h.
- The squared masses of the charged gauge bosons, *viz.* $\bar{M}_l$ and $\bar{M}_h$.
- The mixing angle ψ between the two neutral gauge bosons.
- The mixing angle ξ between the two charged gauge bosons.
- The masses μ_5, μ_6, μ_7, and μ_8 of the four scalars.

- The six mixing angles θ_i ($i = 1, \ldots, 6$) that parameterize the mixing matrix V_ρ.
- The squared masses of the two pseudoscalars, *viz.* $M_{\eta 1}$ and $M_{\eta 2}$.
- The mixing angle η between the two pseudoscalars.
- The squared masses of the two charged scalars, *viz.* $M_{\varphi 1}$ and $M_{\varphi 2}$.
- The mixing angle φ between the two charged scalars.
- The masses m_t and m_b of the top and bottom quarks.

This makes 25 real observables. There is, thus, one more observable than there are parameters in the model. This means that there must be one constraint among the 25 observables; that constraint is derived in Appendix G, *viz.* it is in Eq. (G.11).

Procedure Our practical procedure is the following.

1. We input the following 24 quantities:
   - The squared electromagnetic coupling constant, *viz.* $E = 4\pi \,/\, 137.035\,999\,084$.
   - The squared masses of the neutral gauge bosons, *viz.* M_l and M_h. We choose $\sqrt{M_l} = 91.1876$ GeV and $\sqrt{M_h} \in [0.75,\ 4]$ TeV.[13]
   - The squared masses of the charged gauge bosons, *viz.* $\bar{M}_l$ and $\bar{M}_h$. We choose $\sqrt{\bar{M}_l} = 80.377$ GeV and $\sqrt{\bar{M}_h} \in \left[0.75\text{ TeV},\ \sqrt{M_h}\right]$.[14]
   - The mixing angle between the two neutral gauge bosons is chosen $\psi = 0$. In this way the neutral gauge boson Z_l of the LRM has the same interactions, at the tree level, as the observed boson of mass $\sqrt{M_l} = 91.1876$ GeV. As a consequence, the infrared divergences—due to the zero masses of the photon and of the gluons—in the one-loop diagrams for the vertex $Z_l b\bar{b}$ in the LRM cancel out when one subtracts from those diagrams the analogous diagrams for the vertex $Zb\bar{b}$ in the SM, *viz.* when one compares the LRM to the SM in order to compute δg_L and δg_R.
   - The mixing angle between the two charged gauge bosons, *viz.* $\xi \in [-0.01,\ +0.01]$. In practice, this angle cannot be larger than 0.005, because of the lower bound 0.75 TeV that we impose on $\sqrt{\bar{M}_h}$—see Appendix H.
   - The masses $m_t = 172.69$ GeV and $m_b = \pm 4.18$ GeV of the top and bottom quarks, respectively. We choose m_t positive; the sign of m_b may be either positive or negative.
   - The masses of the four physical scalars, *viz.* $\mu_5 = 125.25$ GeV and $\mu_6 < \mu_7 < \mu_8 < 1$ TeV.[15]
   - The mass of the lightest pseudoscalar, *viz.* $\sqrt{M_{\eta 1}} < 1$ TeV.
   - The masses of the two physical charged scalars, *viz.* $\sqrt{M_{\varphi 1}} < \sqrt{M_{\varphi 2}} < 1$ TeV.
   - The mixing angle between the two pseudoscalars, *viz.* $\eta \in [-\pi/2,\ +\pi/2]$.
   - The mixing angle between the two charged scalars, *viz.* $\varphi \in [-\pi/2,\ +\pi/2]$.
   - The six mixing angles that parameterize the mixing matrix of the scalars V_ρ, *viz.* the θ_i ($i = 1, 2, \ldots, 6$). We choose $\theta_4 \in [-\pi/2,\ +\pi/2]$ and $\theta_5 \in [0,\ +\pi/2]$; the other four

[13] Actually, a more realistic lower bound on the masses of the new gauge bosons of the LRM would be 2 TeV or 3 TeV [39–50]. (The precise bound depends on the ratio g/l between the gauge coupling constants of $SU(2)_L$ and $SU(2)_R$.) We opt for the lax lower bound 750 GeV in order to explore all the possibilities to fit the $Zb\bar{b}$ vertex.

[14] In our LRM $\bar{M}_h$ must always smaller than M_h, see Appendix F.

[15] We allow for very light scalars of mass as low as 10 GeV, although these are in practice most likely excluded by experiment. We do this in order to explore whether this radical possibility might allow us to fit g_L and g_R adequately.

mixing angles are in principle free, but in practice $\theta_{1,2,3}$ are strongly constrained by the experimental constraints of Appendix E.

2. Following the procedure outlined in Appendix F for the case $\psi = 0$, we determine G, L, H, V_1, V_2, U_L, and U_R. In order for the procedure to run smoothly, the inequalities (F.20) must hold, and $(a_s)^2 - 4xyD^2$ in Eqs. (F.22) must be positive; furthermore, all seven final quantities must turn out positive. If any of these does not happen, then the input values are inadequate and must be discarded. This requirement alone forces ξ to be very small.
3. We fix $v_2 = \sqrt{V_2}$, $u_L = \sqrt{U_L}$, and $u_R = \sqrt{U_R}$. We also fix $v_1 = \pm\sqrt{V_1}$; its sign is opposite to the one of ξ, *cf.* Eq. (A.11). The gauge coupling constants $g = \sqrt{G}$, $l = \sqrt{L}$, and $h = \sqrt{H}$ are positive.
4. We compute the Yukawa coupling constants by means of Eqs. (62). We check that they are not much too large, *viz.* that $|y_1| \lesssim M$ and $|y_2| \lesssim M$ with $M \approx 4\pi$.
5. We compute T_1, T_2, K_1, and K_2 by means of Eqs. (41) and (48).
6. We compute the matrix elements of M_φ by using Eqs. (51).
7. We compute $M_{\eta 2}$ by using Eq. (G.11). If we obtain $M_{\eta 2} < M_{\eta 1}$, then we make $M_{\eta 2} \leftrightarrow M_{\eta 1}$ together with $\eta \to \eta - \pi/2$.
8. We compute the matrix elements of M_η by using Eqs. (44).
9. We compute the matrix elements of M_ρ by using Eq. (G.2).
10. We compute the parameters of $V_{(3)}$ and $V_{(4)}$ in Eqs. (59) by following the steps in the last paragraph of Appendix G.
11. We check the unitarity conditions on the parameters of $V_{(4)}$.
12. We check the bounded-from-below conditions on the parameters of $V_{(4)}$.
13. We compute μ_L, μ_R, μ_1, μ_2, and V_0 by using Eqs. (D.3) and (D.4).
14. We check the extra conditions in Appendix D.
15. We compute the experimental parameters κ of Appendix E. We enforce the conditions [51, 52] $\kappa_W \in [0.59,\ 1.46]$, $\kappa_Z \in [0.63,\ 1.32]$, $\kappa_t \in [0.81,\ 1.47]$, and $|\kappa_b| \in [0.11,\ 1.79]$. Note that:

    We allow κ_b to be either positive or negative, since experiment is as yet unable to fix its sign.

    We require the parameters κ to be in their 3σ ranges, because we do not want to miss out any possibility that the LRM might offer to fit g_L and g_R.

    In our model κ_W and κ_Z always turn out to be smaller than 1 and almost equal to each other, for reasons explained in Appendix E, *cf.* Appendix H.

6. Calculation and renormalization

We now describe the calculation of the renormalized one-loop process $Z_l \to b\bar{b}$. We do it by using FeynMaster [53,54], which resorts to FeynRules [55,56], QGRAF [57], and FeynCalc [58–60]. More specifically, we use FeynMaster to generate the Feynman rules of the model (both for the renormalized interactions and for the counterterms), to generate the Feynman diagrams, and to calculate the one-loop amplitudes and the counterterms.

The ultraviolet (UV) renormalized one-loop process (denoted $i\,\hat{\Gamma}_\mu^{Z_l b\bar{b}}$) is the sum of the non-renormalized one-loop process (denoted $i\,\Gamma_\mu^{Z_l b\bar{b}}$) and the counterterms of the process (denoted $i\,\Gamma_\mu^{Z_l b\bar{b}}\Big|_{\rm CT}$); that is,

$$i\,\hat{\Gamma}_\mu^{Z_l b\bar{b}} = i\,\Gamma_\mu^{Z_l b\bar{b}} + i\,\Gamma_\mu^{Z_l b\bar{b}}\Big|_{\rm CT}. \tag{63}$$

The terms in the right-hand side of Eq. (63) are determined when considering the theory up to the one-loop level; more specifically, one must take the original Lagrangian of the theory, identify each parameter and each field as a bare quantity, and then split it into a renormalized quantity and a counterterm[16]; thus, for a generic bare parameter $p_{(0)}$ and a generic bare field $\phi_{(0)}$, we write

$$p_{(0)} = p + \delta p, \qquad \phi_{(0)} = \phi + \frac{1}{2}\,\delta Z_\phi\,\phi, \tag{64}$$

where p is the renormalized parameter, δp is the corresponding counterterm, ϕ is the renormalized field, and δZ_ϕ is its counterterm.

The Feynman rules for the renormalized parameters are obtained by expanding the Lagrangian and keeping only the terms with power zero in the counterterms. They are used to calculate the interactions of the theory; in particular, it is this set of rules that is used to calculate the (non-renormalized, one-loop) diagrams contributing to $i\,\Gamma_\mu^{Z_l b\bar{b}}$.

The Feynman rules for the counterterms are obtained by expanding the Lagrangian and keeping only the terms with power one in the counterterms. The set of all those terms that contribute to $Z_l \to b\bar{b}$ constitutes $i\,\Gamma_\mu^{Z_l b\bar{b}}\Big|_{\rm CT}$. By using FeynMaster it is straightforward to conclude that

$$i\,\Gamma_\mu^{Zb\bar{b}}\Big|_{\rm CT} = i\gamma_\mu\left(F_L P_L + F_R P_R\right), \tag{65}$$

where, with $\psi = 0$,

$$\begin{aligned} F_L = {} & \frac{s_w\,h\,\delta c_\alpha + c_\alpha\,h\,\delta s_w + c_\alpha\,s_w\,\delta h}{6} - \frac{g\,\delta c_w + c_w\,\delta g}{2} \\ & + \frac{s_\alpha\,h}{6}\,\delta s_\psi + \left(\frac{\delta Z_{Z_l Z_l}}{2} + \frac{\delta Z_{33}^{dq,\mathrm{L}*}}{2} + \frac{\delta Z_{33}^{dq,\mathrm{L}}}{2}\right) i\,\Gamma_{\mu,\mathrm{L}}^{Z_l b\bar{b}}\Big|_{\rm tree} \\ & + \frac{\delta Z_{AZ_l}}{2}\,i\,\Gamma_{\mu,\mathrm{L}}^{Ab\bar{b}}\Big|_{\rm tree} + \frac{\delta Z_{Z_h Z_l}}{2}\,i\,\Gamma_{\mu,\mathrm{L}}^{Z_h b\bar{b}}\Big|_{\rm tree}, \end{aligned} \tag{66a}$$

$$\begin{aligned} F_R = {} & \frac{s_w\,h\,\delta c_\alpha + c_\alpha\,h\,\delta s_w + c_\alpha\,s_w\,\delta h}{6} + \frac{s_w\,l\,\delta s_\alpha + s_\alpha\,l\,\delta s_w + s_\alpha\,s_w\,\delta l}{2} \\ & + \left(\frac{s_\alpha\,h}{6} - \frac{c_\alpha\,l}{2}\right)\delta s_\psi + \left(\frac{\delta Z_{Z_l Z_l}}{2} + \frac{\delta Z_{33}^{dq,\mathrm{R}*}}{2} + \frac{\delta Z_{33}^{dq,\mathrm{R}}}{2}\right) i\,\Gamma_{\mu,\mathrm{R}}^{Z_l b\bar{b}}\Big|_{\rm tree} \\ & + \frac{\delta Z_{AZ_l}}{2}\,i\,\Gamma_{\mu,\mathrm{R}}^{Ab\bar{b}}\Big|_{\rm tree} + \frac{\delta Z_{Z_h Z_l}}{2}\,i\,\Gamma_{\mu,\mathrm{R}}^{Z_h b\bar{b}}\Big|_{\rm tree}. \end{aligned} \tag{66b}$$

Notice that, when $\psi = 0$,

$$i\,\Gamma_{\mu,\mathrm{L}}^{Z_l b\bar{b}}\Big|_{\rm tree} = \frac{c_\alpha\,s_w\,h}{6} - \frac{c_w\,g}{2}, \tag{67a}$$

$$i\,\Gamma_{\mu,\mathrm{L}}^{Ab\bar{b}}\Big|_{\rm tree} = \frac{c_\alpha\,c_w\,h}{6} + \frac{s_w\,g}{2}, \tag{67b}$$

$$i\,\Gamma_{\mu,\mathrm{L}}^{Z_h b\bar{b}}\Big|_{\rm tree} = \frac{s_\alpha\,h}{6}, \tag{67c}$$

[16] For details see e.g. Ref. [61].

$$i\,\Gamma^{Z_l b\bar{b}}_{\mu,\mathrm{R}}\Big|_{\mathrm{tree}} = \frac{c_\alpha\, s_w\, h}{6} + \frac{s_\alpha\, s_w\, l}{2}, \tag{67d}$$

$$i\,\Gamma^{A b\bar{b}}_{\mu,\mathrm{R}}\Big|_{\mathrm{tree}} = \frac{c_\alpha\, c_w\, h}{6} + \frac{s_\alpha\, c_w\, l}{2}, \tag{67e}$$

$$i\,\Gamma^{Z_h b\bar{b}}_{\mu,\mathrm{R}}\Big|_{\mathrm{tree}} = \frac{s_\alpha\, h}{6} - \frac{c_\alpha\, l}{2}. \tag{67f}$$

It is important to understand the role of the neutral-gauge-boson mixing angle ψ in these equations. As mentioned in the previous section, since we identify the LRM gauge boson Z_l with the observed neutral boson of mass 91.1876 GeV, we set the renormalized ψ to zero. However, there is no symmetry of the theory that implies $\psi = 0$; the choice $\psi = 0$ is just a particular solution of a model where ψ is in general nonzero. Therefore, when renormalizing that model a nonzero bare parameter $\psi_{(0)}$ must be allowed and renormalized; the circumstance that we consider a particular solution of the model where the renormalized ψ vanishes does not change the fact that the bare $\psi_{(0)}$ is in general nonzero and has a nonzero counterterm $\delta\psi$.[17]

We need to compute the counterterms that appear in Eqs. (66b). We perform that computation by using on-shell subtraction (OSS), except for the independent mixing angles; the latter are fixed through a symmetry relation [54].[18]

Let us start with the field counterterms. Through a trivial generalization of the field counterterms calculated through OSS in the SM, we find:

$$\delta Z_{V_i V_i} = \widetilde{\mathrm{Re}}\,\frac{\partial\,\Sigma_{\mathrm{T}}^{V_i V_i}\left(k^2\right)}{\partial k^2}\bigg|_{k^2=m_{V_i}^2}, \tag{68a}$$

$$\delta Z_{V_i V_j} = 2\,\widetilde{\mathrm{Re}}\,\frac{\Sigma_{\mathrm{T}}^{V_i V_j}\left(m_{V_j}^2\right)}{m_{V_j}^2 - m_{V_i}^2} \quad \Leftarrow i \neq j, \tag{68b}$$

$$\begin{aligned}\delta Z_{33}^{dq,\mathrm{L}} = {} & -\widetilde{\mathrm{Re}}\,\Sigma_{\mathrm{L}}^{b\bar{b}}\left(m_b^2\right) \\ & - m_b\,\frac{\partial}{\partial p^2}\,\widetilde{\mathrm{Re}}\left\{m_b\left[\Sigma_{\mathrm{L}}^{b\bar{b}}\left(p^2\right) + \Sigma_{\mathrm{R}}^{b\bar{b}}\left(p^2\right)\right] + \Sigma_{\mathrm{l}}^{b\bar{b}}\left(p^2\right) + \Sigma_{\mathrm{r}}^{b\bar{b}}\left(p^2\right)\right\}\Big|_{p^2=m_b^2},\end{aligned} \tag{68c}$$

$$\begin{aligned}\delta Z_{33}^{dq,\mathrm{R}} = {} & -\widetilde{\mathrm{Re}}\,\Sigma_{\mathrm{R}}^{b\bar{b}}\left(m_b^2\right) \\ & - m_b\,\frac{\partial}{\partial p^2}\,\widetilde{\mathrm{Re}}\left\{m_b\left[\Sigma_{\mathrm{L}}^{b\bar{b}}\left(p^2\right) + \Sigma_{\mathrm{R}}^{b\bar{b}}\left(p^2\right)\right] + \Sigma_{\mathrm{l}}^{b\bar{b}}\left(p^2\right) + \Sigma_{\mathrm{r}}^{b\bar{b}}\left(p^2\right)\right\}\Big|_{p^2=m_b^2}.\end{aligned} \tag{68d}$$

[17] Actually, $\delta\psi$ is crucial to absorb the divergences of the process $Z_l \to b\bar{b}$. The non-inclusion of that counterterm would lead to the same kind of inconsistency as the one pointed out in Ref. [62].

[18] For details see Ref. [61]. Note that in this paper we use $\eta_g = \eta_f = 1$, while Refs. [63,64] have used $\eta_g = -\eta_f = -1$ instead. (The purely conventional parameters η_g and η_f are defined in Eqs. (F.23) of Ref. [61].)

Here, $\Sigma_k^{xy}\left(p^2\right)$ represents the k^{th} component of the non-renormalized one-loop two-point function for the fields x, y with 4-momentum p.[19] The operator $\widetilde{\text{Re}}$ discards the absorptive parts of the loop integrals but keeps the imaginary parts of complex parameters.[20]

We now turn to the parameter counterterms. The first thing to notice is that not all the parameters which intervene in Eqs. (66b) are independent, *i.e.* not all of them are counterterms of the independent parameters. Indeed, we choose as independent parameters the squared masses of Z_l, Z_h, W_l, and W_h together with e, ψ, and ξ. One may use the relations of the model to rewrite Eqs. (66b) in terms of the counterterms of the independent parameters (we omit this here as the rewritten expressions are extremely long). Those counterterms are defined, as usual, by the splitting of the bare version of the independent parameters:

$$M_{l(0)} = M_l + \delta M_l, \tag{69a}$$
$$M_{h(0)} = M_h + \delta M_h, \tag{69b}$$
$$\bar{M}_{l(0)} = \bar{M}_l + \delta \bar{M}_l, \tag{69c}$$
$$\bar{M}_{h(0)} = \bar{M}_h + \delta \bar{M}_h, \tag{69d}$$
$$e_{(0)} = (1 + \delta Z_e)\, e, \tag{69e}$$
$$\psi_{(0)} = \delta\psi, \tag{69f}$$
$$\xi_{(0)} = \xi + \delta\xi. \tag{69g}$$

The mass counterterms in the OSS scheme are

$$\delta m_{V_i}^2 = -\widetilde{\text{Re}}\, \Sigma_{\text{T}}^{V_i V_i}\left(m_{V_i}^2\right). \tag{70}$$

The counterterm δZ_e, which *a priori* has a very complicated expression, may be significantly simplified by using a Ward identity. That identity was derived in detail, for the case of the SM, in appendix F of Ref. [61]. By generalizing it to the LRM, we obtain:

$$\delta Z_e = -\frac{1}{2}\delta Z_{AA} - \frac{1}{2c_w}\delta Z_{Z_l A}\left(s_w\, c_\psi + \frac{s_\alpha}{c_\alpha}\, s_\psi\right) - \frac{1}{2c_w}\delta Z_{Z_h A}\left(\frac{s_\alpha}{c_\alpha}\, c_\psi - s_w\, s_\psi\right), \tag{71}$$

which we use after setting $\psi = 0$. Note that Eq. (71) reduces to its SM version, *viz.* to equation (F.60) of Ref. [61], when $\alpha = \psi = 0$ and $Z_l = Z$.

In order to fix the counterterms $\delta\psi$ and $\delta\xi$ we apply a method similar to the one described in Ref. [54] to obtain[21]:

[19] For details see section 5.4.1 of Ref. [61]. We are assuming the tadpole scheme dubbed PRTS in Ref. [61]. This implies that the Green's functions considered here do not include the one-loop tadpoles.

[20] This detail is actually irrelevant in this paper, since in our LRM there are no complex parameters. Hence, in this case we might have used Re instead of $\widetilde{\text{Re}}$.

[21] Whereas the counterterms of the mixing parameters in Ref. [54] were fixed in Feynman gauge, the counterterms $\delta\psi$ and $\delta\xi$ in this paper are not fixed in any specific gauge. This has to do with the tadpole scheme. Namely, Ref. [54] used the tadpole scheme dubbed FJTS, wherein the parameter counterterms are required to behave as gauge-independent (*i.e.* not to change when the gauge is changed) in order for the observables to be gauge-independent; and while that naturally happens for the parameter counterterms fixed through on-shell or minimal subtraction, one needs to enforce it in the case of parameter counterterms fixed by symmetry relations. In the present paper, by contrast, the tadpole scheme at stake is PRTS, wherein the parameter counterterms are in general gauge dependent; that gauge dependence ends up cancelling in the renormalized functions, as long as the whole set of parameter counterterms is renormalized by using a momentum-subtraction scheme. Since the latter condition is satisfied in this paper, the renormalized functions of this paper are gauge-independent, as we have explicitly checked (numerically). For details see Ref. [61].

$$\delta\psi = \frac{1}{4}\left[\delta Z_{Z_l Z_h} - \delta Z_{Z_h Z_l} + \frac{s_w}{c_w}\left(\delta Z_{Z_h A} - \delta Z_{A Z_h}\right)\right], \tag{72a}$$

$$\delta\xi = \frac{1}{4}\left(\delta Z_{W_h W_l} - \delta Z_{W_l W_h}\right). \tag{72b}$$

Using Eqs. (66b) to (72) we calculate $i\,\Gamma_\mu^{Z_l b\bar{b}}\Big|_{\rm CT}$ and hence Eq. (63).

Using FeynMaster we have numerically checked both the UV-finiteness and the gauge-independence of $i\,\hat{\Gamma}_\mu^{Z_l b\bar{b}}$.

7. Discussion

In this section we discuss the results obtained by using the procedure in section 5. In our numerical analysis the scalar masses were assumed to be lower than 1 TeV; this bound is mostly irrelevant, because the contributions of the new scalars to δg_L and δg_R tend to zero when the scalars become very heavy. On the other hand, the lower bound on the masses of the scalars is important, because scalars with very low masses allow one to fit the $Zb\bar{b}$ vertex, as has already been found out in the context of the 2HDM and 3HDM [5]. For this reason, in this section we display four different fits:

In the first fit (for which we have used green points in our scatter plots) we have assumed a lower bound 10 GeV on the masses of all the scalars.[22]
In the second fit (displayed through blue points in the scatter plots), the lower bound on the scalar masses is 125 GeV.
In the third fit (red points) the lower bound is 500 GeV.
In the fourth fit (displayed exclusively in the right panel of Fig. 3), the lower bound on all the scalar masses is 125 GeV, *except* only the lightest scalar and the lightest pseudoscalar, which are allowed to have mass as low as 10 GeV.

We emphasize that we have attempted to explore whether very small masses allow one to fit g_L and g_R adequately, irrespective of whether such low masses are realistic or not; we do *not* claim that our very-low-mass scalars may ever be compatible with the experimental data.

We depict in Fig. 3 the confrontation between experiment and the values of g_L and g_R attainable in our LR model. In the left panel one sees that, when one forces the scalar masses to be larger than 125 GeV, the LRM is unable to achieve a better agreement with experiment than the SM—it even does not attain the 2σ interval on the value of A_b (9). Only when one allows very low scalar masses $\gtrsim 10$ GeV are the central values of both solutions $1^{\rm fit}$ and $1^{\rm average}$ attainable. In the right panel of Fig. 3 one sees that, if both the masses of the lightest pseudoscalar, *viz.* $m_{\eta 1}$, and lightest neutral scalar, *viz.* m_6, are $\gtrsim 10$ GeV, while all the other charged and neutral scalars are above 125 GeV, then the central values of both solutions $1^{\rm fit}$ and $1^{\rm average}$ are attainable too. This shows that only one light scalar and one light pseudoscalar are needed in order to correct g_R. However, the other scalars are important too; when the lower bound on their masses is increased to 200 GeV we are already unable to reach solution $1^{\rm fit}$ (points for that fit are not shown).

[22] This is avowedly a lax lower bound. In particular, there is a recent experimental lower bound of 150 GeV on the masses of charged scalars [65,66]; but it is also true that low-mass charged scalars are *not* very useful to adequately fit the $Zb\bar{b}$ vertex. We have used this lower bound to illustrate that neutral scalars with *very* low masses are really *needed* to fit the $Zb\bar{b}$ vertex in our LRM.

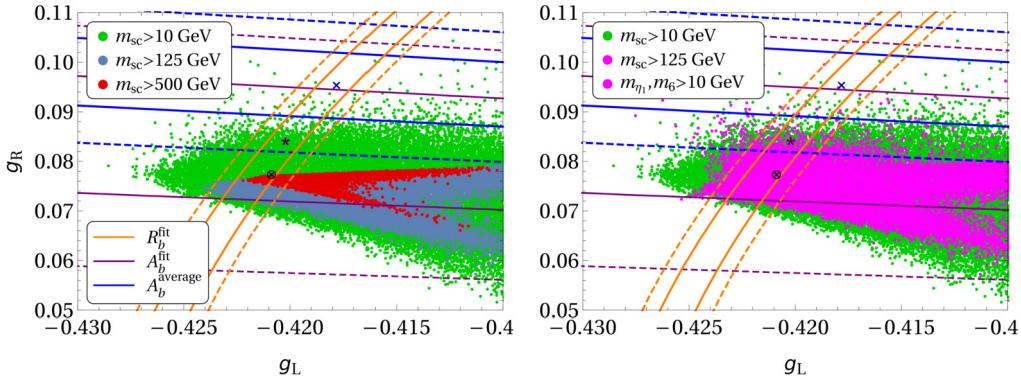

Fig. 3. Scatter plot of the values of g_L and g_R in our model. The crossed circle marks the SM prediction (3); the star marks the best-fit point of solution 1^{fit} and the cross the best-fit point of solution 1^{average}, *cf.* Table 1. The orange lines mark the 1σ (full lines) and 2σ (dashed lines) boundaries of the region determined by the experimental value (8a); similarly, the violet lines correspond to the value (8b) and the blue lines to the value (9). Left panel: the three cases where the lower bound on the masses of the scalars are 10 GeV (green points), 125 GeV (blue points), and 500 GeV (red points). Right panel: the green points are the same as in the left panel; the magenta points have only the masses $m_{\eta 1}$ of the lightest pseudoscalar and m_6 of the lightest neutral scalar above 10 GeV, while all the other scalars have masses above 125 GeV. (For interpretation of the colours in the figure(s), the reader is referred to the web version of this article.)

The unexpected conclusion of this paper is thus that, in spite of its many parameters—most of them in the scalar sector—and in spite of the existence of right-handed currents, our LRM with $\psi = 0$ is basically unable to fit the experimental values of g_L and—mainly—g_R, unless one resorts to scalars with extremely low masses. In particular, our LRM does not do a better job in fitting the $Zb\bar{b}$ vertex than the much simpler 2HDM or 3HDM.

We should emphasize once again that we have assumed the renormalized mixing angle ψ to be zero. This assumption has a crucial technical advantage: instead of having to deal with the effect of soft photons and gluons on the $Zb\bar{b}$ vertex, and on the way they operate to cancel the infrared divergences in the loops—both in the SM and in the LRM—we could simply subtract g_L and g_R in both models to eliminate those divergences. On the one hand, this assumption is certainly a weakness of our computation. On the other hand, taking into account the soft photons and gluons would certainly entail various technical difficulties; moreover, since recent analyses [37–39] suggest that $|\psi|$ cannot be much larger than 10^{-3} anyway, while at the tree level one needs $\psi \sim 10^{-2}$ to fit the $Zb\bar{b}$ vertex—see Section 3—we believe that allowing $\psi \neq 0$ would not change our final conclusions substantially.

We may also comment on the ratio l/g between the gauge coupling constants of $SU(2)_L$ and $SU(2)_R$. The right panel of Fig. 2 suggests that l/g should not be very far from 1 in a fit of the $Zb\bar{b}$ vertex at tree level. At loop level we see, in Fig. 6, that l/g is much freer; we have found points (not depicted in that figure) with l/g as high as 6. We emphasize, however, that in making Fig. 6 we just require the points to adequately fit R_b, while in Fig. 2 what is at stake is fitting both R_b *and* A_b.

In Appendix H we give more information on the ranges of the parameters of the LRM.

CRediT authorship contribution statement

Duarte Fontes: Conceptualization, Investigation, Software, Writing – review & editing. **Darius Jurčiukonis:** Conceptualization, Investigation, Software, Visualization, Writing – review &

editing. **Luís Lavoura:** Conceptualization, Investigation, Methodology, Writing – original draft, Writing – review & editing.

Declaration of competing interest

The authors declare that they have no known competing financial interests or personal relationships that could have appeared to influence the work reported in this paper.

Data availability

Data will be made available on request.

Acknowledgements

We thank Kristjan Kannike and Per Osland for explanations about Refs. [67] and [37–39], respectively. The work of D.F. is supported by the United States Department of Energy under Grant Contract DE-SC0012704. The work of D.J. is supported by the Lithuanian Academy of Sciences through project DaFi2021 and by a COST STSM grant through action CA1620. The work of L.L. is supported by the Portuguese Foundation for Science and Technology through projects UIDB/00777/2020, UIDP/00777/2020, CERN/FIS-PAR/0008/2019, CERN/FIS-PAR/0002/2021, CERN/FIS-PAR/0004/2019, and CERN/FIS-PAR/0019/2021.

Appendix A. The Goldstone bosons

Gauge-boson mass matrices From Eq. (14) and Table 3, the covariant derivatives of the scalar fields are

$$D^\mu m = \partial^\mu m - \frac{ig}{\sqrt{2}} W^{+\mu} n + ieA^\mu m + \frac{ig\left(s_w^2 - c_w^2\right)}{2c_w} Z^\mu m + \frac{ils_\alpha^2}{2c_\alpha} X^\mu m, \tag{A.1a}$$

$$D^\mu n = \partial^\mu n - \frac{ig}{\sqrt{2}} W^{-\mu} m + \frac{ig}{2c_w} Z^\mu n + \frac{ils_\alpha^2}{2c_\alpha} X^\mu n, \tag{A.1b}$$

$$D^\mu p = \partial^\mu p - \frac{il}{\sqrt{2}} V^{+\mu} q + ieA^\mu p + \frac{igs_w^2}{c_w} Z^\mu p + \frac{il\left(s_\alpha^2 - c_\alpha^2\right)}{2c_\alpha} X^\mu p, \tag{A.1c}$$

$$D^\mu q = \partial^\mu q - \frac{il}{\sqrt{2}} V^{-\mu} p + \frac{il}{2c_\alpha} X^\mu q, \tag{A.1d}$$

$$D^\mu a = \partial^\mu a - \frac{ig}{\sqrt{2}} W^{+\mu} b + \frac{il}{\sqrt{2}} V^{+\mu} d^* + ieA^\mu a + \frac{ig\left(s_w^2 - c_w^2\right)}{2c_w} Z^\mu a - \frac{ilc_\alpha}{2} X^\mu a, \tag{A.1e}$$

$$D^\mu b = \partial^\mu b - \frac{ig}{\sqrt{2}} W^{-\mu} a - \frac{il}{\sqrt{2}} V^{+\mu} c^* + \frac{ig}{2c_w} Z^\mu b - \frac{ilc_\alpha}{2} X^\mu b, \tag{A.1f}$$

$$D^\mu c = D^\mu a\left(a \to c,\, b \to d,\, d^* \to b^*\right), \tag{A.1g}$$

$$D^\mu d = D^\mu b\left(b \to d,\, a \to c,\, c^* \to a^*\right). \tag{A.1h}$$

When the scalar fields in Eqs. (A.1) get substituted by their VEVs (26), one obtains

$$D^\mu m \to -\frac{igu_L}{\sqrt{2}}\, W^{+\mu}, \tag{A.2a}$$

$$D^\mu n \to \frac{iu_L}{2}\left(\frac{g}{c_w}\, Z^\mu + \frac{ls_\alpha^2}{c_\alpha}\, X^\mu\right), \tag{A.2b}$$

$$D^\mu p \to -\frac{ilu_R}{\sqrt{2}}\, V^{+\mu}, \tag{A.2c}$$

$$D^\mu q \to \frac{ilu_R}{2c_\alpha}\, X^\mu, \tag{A.2d}$$

$$D^\mu a \to \frac{i}{\sqrt{2}}\left(-gW^{+\mu}v_1 + lV^{+\mu}v_2\right), \tag{A.2e}$$

$$D^\mu b \to \frac{iv_1}{2}\left(\frac{g}{c_w}\, Z^\mu - lc_\alpha X^\mu\right), \tag{A.2f}$$

$$D^\mu c \to \frac{i}{\sqrt{2}}\left(-gW^{+\mu}v_2 + lV^{+\mu}v_1\right), \tag{A.2g}$$

$$D^\mu d \to \frac{iv_2}{2}\left(\frac{g}{c_w}\, Z^\mu - lc_\alpha X^\mu\right). \tag{A.2h}$$

From Eqs. (A.2a), (A.2c), (A.2e), and (A.2g) one gets the charged-gauge-boson mass matrix M_c, given by

$$A \equiv (M_c)_{11} = \frac{GV_L^2}{2}, \qquad B \equiv (M_c)_{22} = \frac{LV_R^2}{2}, \qquad D \equiv (M_c)_{12} = -glv_1v_2, \tag{A.3}$$

where

$$V_L \equiv \sqrt{V_1 + V_2 + U_L}, \qquad V_R \equiv \sqrt{V_1 + V_2 + U_R} \tag{A.4}$$

are positive by definition. From Eqs. (A.2b), (A.2d), (A.2f), and (A.2h) one has, for the neutral-gauge-boson mass matrix M_n, the formulas

$$R \equiv (M_n)_{11} = \frac{GL + GH + LH}{2\,(L+H)}\, V_L^2, \tag{A.5a}$$

$$S \equiv (M_n)_{22} = \frac{L^2\,(V_1+V_2) + H^2 U_L + (L+H)^2\, U_R}{2\,(L+H)}, \tag{A.5b}$$

$$T \equiv (M_n)_{12} = \frac{\varrho_1}{2\,(L+H)}\left[HU_L - L\,(V_1+V_2)\right]. \tag{A.5c}$$

Note that $(M_n)_{12}$ cannot be made zero in any natural (*i.e.* enforceable through a symmetry) way. This means that the mixing angle ψ cannot be made zero through any symmetry.

$G_W^\pm$ and $G_V^\pm$ We define the normalized states

$$G_W^- \equiv \frac{u_L m^* + v_1 a^* + v_2 c^*}{V_L}, \qquad G_V^- \equiv \frac{u_R p^* - v_2 a^* - v_1 c^*}{V_R}. \tag{A.6}$$

Then, from Eqs. (A.1a), (A.1c), (A.1e), and (A.1g),

$$\mathcal{L} = \cdots - i\left(\sqrt{A}\; W_\mu^+\, \partial^\mu G_W^- + \sqrt{B}\; V_\mu^+\, \partial^\mu G_V^-\right) + \text{H.c.}, \tag{A.7}$$

where

$$\sqrt{A} = \frac{g V_L}{\sqrt{2}}, \qquad \sqrt{B} = \frac{l V_R}{\sqrt{2}} \tag{A.8}$$

are positive by definition.

Diagonalization of M_c From Eqs. (15) and (16),

$$\begin{pmatrix} c_\xi & -s_\xi \\ s_\xi & c_\xi \end{pmatrix} \begin{pmatrix} A & D \\ D & B \end{pmatrix} \begin{pmatrix} c_\xi & s_\xi \\ -s_\xi & c_\xi \end{pmatrix} = \begin{pmatrix} \bar{M}_l & 0 \\ 0 & \bar{M}_h \end{pmatrix}. \tag{A.9}$$

Therefore,

$$2 c_\xi s_\xi = \frac{2D}{\bar{M}_h - \bar{M}_l}, \tag{A.10a}$$

$$c_\xi^2 - s_\xi^2 = \frac{B - A}{\bar{M}_h - \bar{M}_l}, \tag{A.10b}$$

$$\bar{M}_h - \bar{M}_l = \sqrt{(A-B)^2 + 4D^2}, \tag{A.10c}$$

$$\bar{M}_l = \frac{A + B - \left(\bar{M}_h - \bar{M}_l\right)}{2}, \tag{A.10d}$$

$$\bar{M}_h = \frac{A + B + \left(\bar{M}_h - \bar{M}_l\right)}{2}. \tag{A.10e}$$

From Eqs. (A.3) and (A.10a),

$$c_\xi s_\xi \left(\bar{M}_h - \bar{M}_l\right) = -g l v_1 v_2. \tag{A.11}$$

Since c_ξ, $\bar{M}_h - \bar{M}_l$, g, l, and v_2 are positive (without lack of generality), Eq. (A.11) means that the sign of s_ξ must be chosen opposite to the sign of v_1.

$G_l^\pm$ and $G_h^\pm$ We now define

$$G_l^- \equiv \frac{c_\xi \sqrt{A}\, G_W^- - s_\xi \sqrt{B}\, G_V^-}{\sqrt{\bar{M}_l}}, \tag{A.12a}$$

$$G_h^- \equiv \frac{s_\xi \sqrt{A}\, G_W^- + c_\xi \sqrt{B}\, G_V^-}{\sqrt{\bar{M}_h}}, \tag{A.12b}$$

where $\sqrt{\bar{M}_l}$ and $\sqrt{\bar{M}_h}$ are positive by definition. Then Eq. (A.7) is rewritten as

$$\mathcal{L} = \cdots - i \left(\sqrt{\bar{M}_l}\, W_{l\mu}^+ \, \partial^\mu G_l^- + \sqrt{\bar{M}_h}\, W_{h\mu}^+ \, \partial^\mu G_h^- \right) + \text{H.c.}, \tag{A.13}$$

which goes into the last line of Eq. (56). Equations (A.12) are the definition of $G_l^\pm$ and $G_h^\pm$. Note that these states are orthogonal:

$$\sqrt{\bar{M}_l \bar{M}_h}\; G_l^- \cdot G_h^- = c_\xi s_\xi \,(A - B) + \left(c_\xi^2 - s_\xi^2\right) \sqrt{AB}\; G_W^- \cdot G_V^- \tag{A.14a}$$

$$= \frac{D}{\bar{M}_h - \bar{M}_l}\,(A - B) + \frac{B - A}{\bar{M}_h - \bar{M}_l}\,\sqrt{AB}\,\frac{-2 v_1 v_2}{V_L V_R} \tag{A.14b}$$

$$= \frac{D}{\bar{M}_h - \bar{M}_l}(A-B) + \frac{B-A}{\bar{M}_h - \bar{M}_l}\sqrt{AB}\,\frac{2D}{glV_LV_R} \tag{A.14c}$$
$$= \frac{D}{\bar{M}_h - \bar{M}_l}(A-B) + \frac{B-A}{\bar{M}_h - \bar{M}_l}D \tag{A.14d}$$
$$= 0. \tag{A.14e}$$

They are also correctly normalized:

$$\bar{M}_l\, G_l^- \cdot G_l^- = c_\xi^2 A + s_\xi^2 B - 2c_\xi s_\xi \sqrt{AB}\, G_W^- \cdot G_V^- \tag{A.15a}$$
$$= \frac{1+c_\xi^2 - s_\xi^2}{2}A + \frac{1-c_\xi^2+s_\xi^2}{2}B - 2c_\xi s_\xi\sqrt{AB}\,\frac{-2v_1v_2}{V_LV_R} \tag{A.15b}$$
$$= \frac{A+B}{2} + \frac{B-A}{2\left(\bar{M}_h - \bar{M}_l\right)}(A-B) - \frac{2D}{\bar{M}_h - \bar{M}_l}\sqrt{AB}\,\frac{D}{\sqrt{AB}} \tag{A.15c}$$
$$= \frac{A+B}{2} - \frac{(A-B)^2}{2\left(\bar{M}_h - \bar{M}_l\right)} - \frac{2D^2}{\bar{M}_h - \bar{M}_l} \tag{A.15d}$$
$$= \bar{M}_l, \tag{A.15e}$$
$$\bar{M}_h\, G_h^- \cdot G_h^- = s_\xi^2 A + c_\xi^2 B + 2c_\xi s_\xi \sqrt{AB}\, G_W^- \cdot G_V^- \tag{A.16a}$$
$$= \frac{1-c_\xi^2 + s_\xi^2}{2}A + \frac{1+c_\xi^2-s_\xi^2}{2}B + 2c_\xi s_\xi\sqrt{AB}\,\frac{-2v_1v_2}{V_LV_R} \tag{A.16b}$$
$$= \frac{A+B}{2} - \frac{B-A}{2\left(\bar{M}_h - \bar{M}_l\right)}(A-B) + \frac{2D}{\bar{M}_h - \bar{M}_l}\sqrt{AB}\,\frac{D}{\sqrt{AB}} \tag{A.16c}$$
$$= \frac{A+B}{2} + \frac{(A-B)^2}{2\left(\bar{M}_h - \bar{M}_l\right)} + \frac{2D^2}{\bar{M}_h - \bar{M}_l} \tag{A.16d}$$
$$= \bar{M}_h. \tag{A.16e}$$

G_Z and G_X We define

$$G_Z \equiv \frac{u_L\eta_L + v_1\eta_1 + v_2\eta_2}{V_L}, \qquad G'_X \equiv \frac{u_R\eta_R - v_1\eta_1 - v_2\eta_2}{V_R}. \tag{A.17}$$

These states are normalized, but they are not orthogonal to each other:

$$G_Z \cdot G_Z = G'_X \cdot G'_X = 1, \qquad G_Z \cdot G'_X = \frac{-V_1 - V_2}{V_LV_R}. \tag{A.18}$$

From Eqs. (A.1b), (A.1d), (A.1f), and (A.1h),

$$\mathcal{L} = \cdots + \left(\frac{g}{\sqrt{2}c_w}Z^\mu + \frac{ls_\alpha^2}{\sqrt{2}c_\alpha}X^\mu\right)V_L\,\partial_\mu G_Z + \frac{l}{\sqrt{2}c_\alpha}X^\mu\,V_R\,\partial_\mu G'_X. \tag{A.19}$$

Using the quantities R and S in Eqs. (A.5), one may rewrite Eq. (A.19) as

$$\mathcal{L} = \cdots + \sqrt{R}\,Z^\mu\,\partial_\mu G_Z + \sqrt{S}\,X^\mu\,\partial_\mu G_X, \tag{A.20}$$

where

$$\sqrt{R} = \frac{gV_L}{\sqrt{2}c_w} \tag{A.21}$$

and

$$G_X \equiv \frac{1}{\sqrt{S}}\,\frac{l}{\sqrt{2}c_\alpha}\left(s_\alpha^2 V_L G_Z + V_R G'_X\right). \tag{A.22}$$

Notice that both $\sqrt{R}$ and $\sqrt{S}$ are, by definition, positive. One easily ascertains that

$$G_X \cdot G_X = 1, \qquad G_Z \cdot G_X = \frac{T}{\sqrt{RS}}, \tag{A.23}$$

where T is in Eq. (A.5c).

G_l^0 and G_h^0 We define

$$G_l^0 \equiv \frac{c_\psi\sqrt{R}\,G_Z + s_\psi\sqrt{S}\,G_X}{\sqrt{M_l}}, \qquad G_h^0 \equiv \frac{-s_\psi\sqrt{R}\,G_Z + c_\psi\sqrt{S}\,G_X}{\sqrt{M_h}}. \tag{A.24}$$

Applying the first Eq. (15) to Eq. (A.20), we obtain

$$\mathcal{L} = \cdots + \sqrt{M_l}\,Z_l^\mu\,\partial_\mu G_l^0 + \sqrt{M_h}\,Z_h^\mu\,\partial_\mu G_h^0, \tag{A.25}$$

as in the last line of Eq. (55). The diagonalization of the neutral-gauge-boson mass matrix proceeds as

$$\begin{pmatrix} R & T \\ T & S \end{pmatrix} = \begin{pmatrix} c_\psi & -s_\psi \\ s_\psi & c_\psi \end{pmatrix}\begin{pmatrix} M_l & 0 \\ 0 & M_h \end{pmatrix}\begin{pmatrix} c_\psi & s_\psi \\ -s_\psi & c_\psi \end{pmatrix}, \tag{A.26}$$

i.e.

$$R = M_l\,c_\psi^2 + M_h\,s_\psi^2, \tag{A.27a}$$
$$S = M_l\,s_\psi^2 + M_h\,c_\psi^2, \tag{A.27b}$$
$$T = (M_l - M_h)\,c_\psi s_\psi. \tag{A.27c}$$

Hence,

$$G_l^0 \cdot G_l^0 = G_h^0 \cdot G_h^0 = 1, \qquad G_l^0 \cdot G_h^0 = 0, \tag{A.28}$$

viz. the states G_l^0 and G_h^0 are orthonormal as they should. Equations (A.24) lead to Eqs. (38); for instance, defining $v_\eta \equiv v_1\eta_1 + v_2\eta_2$,

$$G_l^0 = \frac{1}{\sqrt{M_l}}\left\{c_\psi\sqrt{R}\,\frac{v_\eta + u_L\eta_L}{V_L} + s_\psi\,\frac{l}{\sqrt{2}c_\alpha}\left[s_\alpha^2\left(v_\eta + u_L\eta_L\right) + u_R\eta_R - v_\eta\right]\right\} \tag{A.29a}$$
$$= \frac{1}{\sqrt{2M_l}}\left[c_\psi\,\frac{g}{c_w}\left(v_\eta + u_L\eta_L\right) + s_\psi\left(\frac{l}{c_\alpha}\,u_R\eta_R - l c_\alpha v_\eta\right)\right] \tag{A.29b}$$
$$= \frac{1}{\sqrt{2M_l}}\left[c_\psi\,\frac{\varrho_1}{\sqrt{L+H}}\left(v_\eta + u_L\eta_L\right) + s_\psi\left(\sqrt{L+H}\,u_R\eta_R - \frac{L}{\sqrt{L+H}}\,v_\eta\right)\right]. \tag{A.29c}$$

Appendix B. Unitarity conditions

The unitarity conditions constrain the quartic part of the scalar potential in Eq. (59c).

The states with $T_{L3} = T_{R3} = X = 0$ Let us consider the scattering among themselves of the twelve two-scalar states with quantum numbers $T_{L3} = T_{R3} = X = 0$. Those states are

$$aa^*,\ cc^*,\ bb^*,\ dd^*,\ ac^*,\ ca^*,\ bd^*,\ db^*,\ mm^*,\ nn^*,\ pp^*,\ \text{and}\ qq^* \tag{B.1}$$

in this fixed, conventional order. The coefficients for their scattering among themselves are given by the 12×12 symmetric matrix

$$M_{12\times12} = \begin{pmatrix} A_{2\times2} & B_{2\times2} & C_{2\times2} & D_{2\times2} & E_{2\times2} & F_{2\times2} \\ B_{2\times2} & A_{2\times2} & D_{2\times2} & C_{2\times2} & G_{2\times2} & F_{2\times2} \\ C_{2\times2} & D_{2\times2} & H_{2\times2} & I_{2\times2} & J_{2\times2} & K_{2\times2} \\ D_{2\times2} & C_{2\times2} & I_{2\times2} & H_{2\times2} & J_{2\times2} & K_{2\times2} \\ E_{2\times2} & G_{2\times2} & J_{2\times2} & J_{2\times2} & L_{2\times2} & M_{2\times2} \\ F_{2\times2} & F_{2\times2} & K_{2\times2} & K_{2\times2} & M_{2\times2} & N_{2\times2} \end{pmatrix}, \tag{B.2}$$

where

$$A_{2\times2} = \begin{pmatrix} 4\lambda_1 & 2\lambda_1 + 4\lambda_3 \\ 2\lambda_1 + 4\lambda_3 & 4\lambda_1 \end{pmatrix},\ B_{2\times2} = \begin{pmatrix} 2\lambda_1 & 2\lambda_1 \\ 2\lambda_1 & 2\lambda_1 \end{pmatrix}, \tag{B.3a}$$

$$C_{2\times2} = \begin{pmatrix} 4\lambda_4 & 4\lambda_4 \\ 4\lambda_4 & 4\lambda_4 \end{pmatrix},\ D_{2\times2} = \begin{pmatrix} 2\lambda_4 & 2\lambda_4 \\ 2\lambda_4 & 2\lambda_4 \end{pmatrix}, \tag{B.3b}$$

$$E_{2\times2} = \begin{pmatrix} \lambda_{4L} & \lambda_{3L} \\ \lambda_{3L} & \lambda_{4L} \end{pmatrix},\ F_{2\times2} = \begin{pmatrix} \lambda_{3R} & \lambda_{4R} \\ \lambda_{4R} & \lambda_{3R} \end{pmatrix}, \tag{B.3c}$$

$$G_{2\times2} = \begin{pmatrix} \lambda_{3L} & \lambda_{4L} \\ \lambda_{4L} & \lambda_{3L} \end{pmatrix},\ H_{2\times2} = \begin{pmatrix} 2\lambda_1 + 4\lambda_3 & 16\lambda_2 \\ 16\lambda_2 & 2\lambda_1 + 4\lambda_3 \end{pmatrix}, \tag{B.3d}$$

$$I_{2\times2} = \begin{pmatrix} 4\lambda_3 & 8\lambda_2 \\ 8\lambda_2 & 4\lambda_3 \end{pmatrix},\ J_{2\times2} = \begin{pmatrix} \lambda_{5L} & \lambda_{5L} \\ \lambda_{5L} & \lambda_{5L} \end{pmatrix}, \tag{B.3e}$$

$$K_{2\times2} = \begin{pmatrix} \lambda_{5R} & \lambda_{5R} \\ \lambda_{5R} & \lambda_{5R} \end{pmatrix},\ L_{2\times2} = \begin{pmatrix} 4\lambda_L & 2\lambda_L \\ 2\lambda_L & 4\lambda_L \end{pmatrix}, \tag{B.3f}$$

$$M_{2\times2} = \begin{pmatrix} \lambda_{LR} & \lambda_{LR} \\ \lambda_{LR} & \lambda_{LR} \end{pmatrix},\ N_{2\times2} = \begin{pmatrix} 4\lambda_R & 2\lambda_R \\ 2\lambda_R & 4\lambda_R \end{pmatrix}. \tag{B.3g}$$

It is readily found that $M_{12\times12}$ is equivalent to the direct sum of the six matrices

$$\left(2\lambda_1 - 8\lambda_2\right),\qquad \left(2\lambda_1 - 24\lambda_2 + 8\lambda_3\right),\qquad \begin{pmatrix} 2\lambda_1 + 4\lambda_3 & 4\lambda_4 \\ 4\lambda_4 & 2\lambda_1 + 8\lambda_2 \end{pmatrix}, \tag{B.4a}$$

$$\begin{pmatrix} 2\lambda_1 - 4\lambda_3 & \sqrt{2}\,(\lambda_{3L} - \lambda_{4L}) \\ \sqrt{2}\,(\lambda_{3L} - \lambda_{4L}) & 2\lambda_L \end{pmatrix},\qquad \begin{pmatrix} 2\lambda_1 - 4\lambda_3 & \sqrt{2}\,(\lambda_{3R} - \lambda_{4R}) \\ \sqrt{2}\,(\lambda_{3R} - \lambda_{4R}) & 2\lambda_R \end{pmatrix}, \tag{B.4b}$$

$$\begin{pmatrix} 2\lambda_1 + 24\lambda_2 + 8\lambda_3 & 12\lambda_4 & 2\sqrt{2}\lambda_{5L} & 2\sqrt{2}\lambda_{5R} \\ 12\lambda_4 & 10\lambda_1 + 4\lambda_3 & \sqrt{2}\,(\lambda_{3L} + \lambda_{4L}) & \sqrt{2}\,(\lambda_{3R} + \lambda_{4R}) \\ 2\sqrt{2}\lambda_{5L} & \sqrt{2}\,(\lambda_{3L} + \lambda_{4L}) & 6\lambda_L & 2\lambda_{LR} \\ 2\sqrt{2}\lambda_{5R} & \sqrt{2}\,(\lambda_{3R} + \lambda_{4R}) & 2\lambda_{LR} & 6\lambda_R \end{pmatrix}. \tag{B.4c}$$

Other states Besides the 12 states (B.1), there are other sets (with quantum numbers other than $T_{L3} = T_{R3} = X = 0$) of two-scalar states that scatter among themselves. Most of them yield

matrices of scattering coefficients that are equivalent to one or more of the matrices (B.4). But there are a few extra scattering matrices, *viz.*

- the four states with $T_{L3} = 0$ and $T_{R3} = X = 1/2$, *i.e.* an, cn, bm, and dm produce a 4×4 matrix that is equivalent to the direct sum of the two 2×2 matrices

$$\begin{pmatrix} \lambda_{3L} & \lambda_{5L} \\ \lambda_{5L} & \lambda_{4L} \end{pmatrix}, \qquad \begin{pmatrix} 2\lambda_{3L} - \lambda_{4L} & \lambda_{5L} \\ \lambda_{5L} & 2\lambda_{4L} - \lambda_{3L} \end{pmatrix}; \tag{B.5}$$

- the four states with $T_{R3} = 0$ and $T_{L3} = X = 1/2$ produce the same scattering matrices as in Eq. (B.5) but with all the sub-indices $L \to R$;
- the scattering of the single state mn produces the matrix $\begin{pmatrix} 2\lambda_L \end{pmatrix}$;
- the scattering of the single state pq produces the matrix $\begin{pmatrix} 2\lambda_R \end{pmatrix}$;
- the scattering of the single state mp produces the matrix $\begin{pmatrix} \lambda_{LR} \end{pmatrix}$.

All the other scatterings just reproduce one or more of the matrices above.

Summary of the unitarity conditions Unitarity means that no scattering has too large an amplitude. This implies that the eigenvalues of all the scattering matrices in the previous two paragraphs are no larger, in modulus, than a certain number M; we use $M = 8\pi$. Thus, the unitarity constraints on V_4 are[23]

$$2\,|\lambda_L| < M; \tag{B.6a}$$
$$2\,|\lambda_R| < M; \tag{B.6b}$$
$$|\lambda_{LR}| < M; \tag{B.6c}$$
$$|\lambda_{3L} + \lambda_{4L}| + \sqrt{(\lambda_{3L} - \lambda_{4L})^2 + 4\,(\lambda_{5L})^2} < 2M; \tag{B.6d}$$
$$|\lambda_{3L} + \lambda_{4L}| + \sqrt{9\,(\lambda_{3L} - \lambda_{4L})^2 + 4\,(\lambda_{5L})^2} < 2M; \tag{B.6e}$$
$$|\lambda_{3R} + \lambda_{4R}| + \sqrt{(\lambda_{3R} - \lambda_{4R})^2 + 4\,(\lambda_{5R})^2} < 2M; \tag{B.6f}$$
$$|\lambda_{3R} + \lambda_{4R}| + \sqrt{9\,(\lambda_{3R} - \lambda_{4R})^2 + 4\,(\lambda_{5R})^2} < 2M; \tag{B.6g}$$
$$2\,|\lambda_1 - 4\lambda_2| < M; \tag{B.6h}$$
$$2\,|\lambda_1 - 12\lambda_2 + 4\lambda_3| < M; \tag{B.6i}$$
$$|2\lambda_1 + 4\lambda_2 + 2\lambda_3| + \sqrt{(4\lambda_2 - 2\lambda_3)^2 + 16\,(\lambda_4)^2} < M; \tag{B.6j}$$
$$|2\lambda_1 - 4\lambda_3 + 2\lambda_L| + \sqrt{(2\lambda_1 - 4\lambda_3 - 2\lambda_L)^2 + 8\,(\lambda_{3L} - \lambda_{4L})^2} < 2M; \tag{B.6k}$$
$$|2\lambda_1 - 4\lambda_3 + 2\lambda_R| + \sqrt{(2\lambda_1 - 4\lambda_3 - 2\lambda_R)^2 + 8\,(\lambda_{3R} - \lambda_{4R})^2} < 2M. \tag{B.6l}$$

Moreover, the moduli of the four (potentially complex) eigenvalues of the 4×4 matrix (B.4c) must be smaller than M.

[23] Clearly, some of the conditions (B.6) are redundant—for instance, inequality (B.6e) is stronger than inequality (B.6d)—but we do not have to care much about that.

Appendix C. Bounded-from-below conditions

The bounded-from-below (BFB) conditions state that the quartic part of the scalar potential, *viz.* Eq. (59c), must be positive for any values of the fields. In order to derive the BFB conditions on $V_{(4)}$ we follow Ref. [67].

Auxiliary quantities We define the quantities:

$$r_L \equiv |m|^2 + |n|^2 \,, \tag{C.1a}$$
$$r_R \equiv |p|^2 + |q|^2 \,, \tag{C.1b}$$
$$r_0 \equiv |a|^2 + |b|^2 + |c|^2 + |d|^2 \,, \tag{C.1c}$$
$$r_1 \equiv a^* c + a c^* + b^* d + b d^* , \tag{C.1d}$$
$$r_2 \equiv -i \left(a^* c - a c^* + b^* d - b d^* \right) , \tag{C.1e}$$
$$k \equiv \frac{r_1}{r_0} , \tag{C.1f}$$
$$\rho_L \equiv \frac{\left(|b|^2 + |c|^2\right) |m|^2 + \left(|a|^2 + |d|^2\right) |n|^2 + 2\,\mathrm{Re}\left[(cd^* - ab^*)\, m^* n\right]}{r_0 r_L} , \tag{C.1g}$$
$$\rho_R \equiv \frac{\left(|a|^2 + |b|^2\right) |p|^2 + \left(|c|^2 + |d|^2\right) |q|^2 + 2\,\mathrm{Re}\left[(bc - ad)\, p^* q\right]}{r_0 r_R} . \tag{C.1h}$$

Equation (59c) is then rewritten

$$\begin{aligned} V_{(4)} = {} & \lambda_L \left(r_L\right)^2 + \lambda_R \left(r_R\right)^2 + \lambda_{LR} r_L r_R \\ & + \lambda_1 \left(r_0\right)^2 + \left(\lambda_3 + 2\lambda_2\right) \left(r_1\right)^2 + \left(\lambda_3 - 2\lambda_2\right) \left(r_2\right)^2 + 2\lambda_4\, r_0\, r_1 \\ & + \lambda_{3L} \rho_L r_0 r_L + \lambda_{4L} \left(1 - \rho_L\right) r_0 r_L + \lambda_{5L} r_1 r_L \\ & + \lambda_{3R} \rho_R r_0 r_R + \lambda_{4R} \left(1 - \rho_R\right) r_0 r_R + \lambda_{5R} r_1 r_R . \end{aligned} \tag{C.2}$$

Elimination of r_2 We note that

$$\begin{aligned} \left(r_0\right)^2 - \left(r_1\right)^2 - \left(r_2\right)^2 &= \left(|a|^2 + |b|^2 + |c|^2 + |d|^2\right)^2 - 4 \left|a^* c + b^* d\right|^2 \\ &= \left(|a|^2 - |c|^2\right)^2 + \left(|b|^2 - |d|^2\right)^2 + 2 \left(\left|ab^* - cd^*\right|^2 + |ad - bc|^2\right) \\ &\geq 0 . \end{aligned} \tag{C.3}$$

Therefore, $\left(r_2\right)^2 \leq \left(r_0\right)^2 - \left(r_1\right)^2$. This implies that

$$\min\left[\left(\lambda_3 - 2\lambda_2\right) \left(r_2\right)^2\right] = \left(\lambda_3 - 2\lambda_2\right) \Theta\left(2\lambda_2 - \lambda_3\right) \left[\left(r_0\right)^2 - \left(r_1\right)^2\right] , \tag{C.4}$$

where Θ is Heaviside's theta function. Therefore,

$$\begin{aligned} \min\left[V_{(4)}\right] = {} & \lambda_L \left(r_L\right)^2 + \lambda_R \left(r_R\right)^2 + \lambda_{LR} r_L r_R \\ & + \left[\lambda_1 + \left(\lambda_3 + 2\lambda_2\right) k^2 + \left(\lambda_3 - 2\lambda_2\right) \Theta\left(2\lambda_2 - \lambda_3\right) \left(1 - k^2\right) + 2\lambda_4 k\right] \left(r_0\right)^2 \\ & + \left[\lambda_{3L} \rho_L + \lambda_{4L} \left(1 - \rho_L\right) + \lambda_{5L} k\right] r_0 r_L \\ & + \left[\lambda_{3R} \rho_R + \lambda_{4R} \left(1 - \rho_R\right) + \lambda_{5R} k\right] r_0 r_R . \end{aligned} \tag{C.5}$$

This must be positive for any realistic values of ρ_L, ρ_R, k, r_L, r_R, and r_0. We define the matrix

$$\Lambda = \begin{pmatrix} 2\lambda_{00} & \lambda_{L0} & \lambda_{R0} \\ \lambda_{L0} & 2\lambda_L & \lambda_{LR} \\ \lambda_{R0} & \lambda_{LR} & 2\lambda_R \end{pmatrix}, \tag{C.6}$$

where

$$\lambda_{00} \equiv \lambda_1 + (\lambda_3 + 2\lambda_2)\, k^2 + (\lambda_3 - 2\lambda_2)\, \Theta(2\lambda_2 - \lambda_3) \left(1 - k^2\right) + 2\lambda_4 k, \tag{C.7a}$$

$$\lambda_{L0} \equiv \lambda_{3L}\rho_L + \lambda_{4L}\,(1 - \rho_L) + \lambda_{5L} k, \tag{C.7b}$$

$$\lambda_{R0} \equiv \lambda_{3R}\rho_R + \lambda_{4R}\,(1 - \rho_R) + \lambda_{5R} k \tag{C.7c}$$

are functions of ρ_L, ρ_R, and k. Equation (C.5) then reads

$$\min\left[V_{(4)}\right] = \frac{1}{2}\begin{pmatrix} r_0, & r_L, & r_R \end{pmatrix} \Lambda \begin{pmatrix} r_0 \\ r_L \\ r_R \end{pmatrix}. \tag{C.8}$$

Since r_0, r_L, and r_R are non-negative, the BFB condition is equivalent to the requirement that the matrix Λ be co-positive [68], *viz.* that

$$\lambda_{00} > 0, \tag{C.9a}$$

$$\lambda_L > 0, \tag{C.9b}$$

$$\lambda_R > 0, \tag{C.9c}$$

$$\bar{\lambda}_{L0} > 0, \tag{C.9d}$$

$$\bar{\lambda}_{R0} > 0, \tag{C.9e}$$

$$\bar{\lambda}_{LR} > 0, \tag{C.9f}$$

$$\sqrt{\lambda_{00}\lambda_L\lambda_R} + \frac{\lambda_{L0}}{2}\sqrt{\lambda_R} + \frac{\lambda_{R0}}{2}\sqrt{\lambda_L} + \frac{\lambda_{LR}}{2}\sqrt{\lambda_{00}} + \sqrt{2\bar{\lambda}_{L0}\bar{\lambda}_{R0}\bar{\lambda}_{LR}} > 0, \tag{C.9g}$$

where

$$\bar{\lambda}_{L0} \equiv \frac{\lambda_{L0}}{2} + \sqrt{\lambda_L\lambda_{00}}, \tag{C.10a}$$

$$\bar{\lambda}_{R0} \equiv \frac{\lambda_{R0}}{2} + \sqrt{\lambda_R\lambda_{00}}, \tag{C.10b}$$

$$\bar{\lambda}_{LR} \equiv \frac{\lambda_{LR}}{2} + \sqrt{\lambda_L\lambda_R}. \tag{C.10c}$$

The inequalities (C.9) must hold for all realistic values of ρ_L, ρ_R, and k. The inequalities (C.9b), (C.9c), and (C.9f) do not depend on those parameters; the same does not apply to the other four inequalities.

The inequality (C.9a) The quantity λ_{00} does not depend on ρ_L and ρ_R, it only depends on k. Clearly,

$$(r_0)^2 - (r_1)^2 - (r_2)^2 \geq 0 \;\Rightarrow\; |r_1| \leq |r_0| \;\Leftrightarrow\; k \in [-1, +1]. \tag{C.11}$$

Thus, the inequality (C.9a) means that λ_{00} must be positive for any value of $k \in [-1, +1]$. Since λ_{00} is a quadratic polynomial in k, it is easy to derive the conditions for this to happen. Kannike [67] proposed

$$\lambda_1 > 0, \tag{C.12a}$$
$$\lambda_1 - 2|\lambda_2| + \lambda_3 > 0, \tag{C.12b}$$
$$\lambda_1 + 2\lambda_2 + \lambda_3 - 2|\lambda_4| > 0, \tag{C.12c}$$
$$\lambda_1 - 2\lambda_2 - \lambda_3 + \sqrt{(\lambda_1 + 2\lambda_2 + \lambda_3)^2 - 4(\lambda_4)^2} > 0, \tag{C.12d}$$
$$\lambda_1 - 6\lambda_2 + \lambda_3 + \sqrt{(\lambda_1 + 2\lambda_2 + \lambda_3)^2 - 4(\lambda_4)^2} > 0. \tag{C.12e}$$

Alternatively, Chauhan [69] gave

$$\lambda_1 > 0, \tag{C.13a}$$
$$\lambda_1 + 2\lambda_2 + \lambda_3 - 2|\lambda_4| > 0, \tag{C.13b}$$
$$\lambda_1 - \frac{(\lambda_4)^2}{2\lambda_2 + \lambda_3} > 0 \quad \Leftarrow \quad 2\lambda_2 + \lambda_3 > |\lambda_4|, \tag{C.13c}$$
$$\lambda_1 - 2\lambda_2 + \lambda_3 - \frac{(\lambda_4)^2}{4\lambda_2} > 0 \quad \Leftarrow \quad 4\lambda_2 > |\lambda_4|. \tag{C.13d}$$

We instead suggest

$$\lambda_1 + 2\lambda_2 + \lambda_3 - 2|\lambda_4| > 0, \tag{C.14a}$$
$$\lambda_1 - 2\lambda_2 + \lambda_3 - \frac{(\lambda_4)^2}{4\lambda_2} > 0 \quad \Leftarrow \quad (4\lambda_2 > |\lambda_4| \text{ and } 2\lambda_2 > \lambda_3), \tag{C.14b}$$
$$\lambda_1 - \frac{(\lambda_4)^2}{2\lambda_2 + \lambda_3} > 0 \quad \Leftarrow \quad (2\lambda_2 + \lambda_3 > |\lambda_4| \text{ and } 2\lambda_2 < \lambda_3). \tag{C.14c}$$

The sets of inequalities (C.12), (C.13), and (C.14) are equivalent to each other and they are equivalent to $\lambda_{00} > 0,\ \forall k \in [-1, +1]$.

The inequalities (C.9d), (C.9e), *and* (C.9g) For any values of the scalar fields, one may use an $SU(2)_L$ transformation to make $m = 0$ and then perform an $SU(2)_R$ transformation to render $a = 0$. In the gauge $a = m = 0$ one has

$$r_L = |n|^2, \tag{C.15a}$$
$$r_0 = |b|^2 + |c|^2 + |d|^2, \tag{C.15b}$$
$$r_1 = b^* d + b d^*, \tag{C.15c}$$
$$\rho_L = \frac{|d|^2}{|b|^2 + |c|^2 + |d|^2}. \tag{C.15d}$$

Then,

$$\begin{aligned}(r_0)^2\left[k^2 + (2\rho_L - 1)^2 - 1\right] &= (r_1)^2 + 4(\rho_L r_0)\left[(\rho_L - 1) r_0\right] \\ &= 4\left[\mathrm{Re}\left(b^* d\right)\right]^2 - 4|d|^2\left(|b|^2 + |c|^2\right) \\ &= -4|cd|^2 - 4\left\{|bd|^2 - \left[\mathrm{Re}\left(b^* d\right)\right]^2\right\} \\ &= -4|cd|^2 - 4\left[\mathrm{Im}\left(b^* d\right)\right]^2 \\ &\leq 0. \end{aligned} \tag{C.16}$$

Therefore,

$$k^2 + (2\rho_L - 1)^2 \leq 1. \tag{C.17}$$

Inequality (C.17) tells us that, for any $k \in [-1,\ +1]$,

$$\frac{1-\sqrt{1-k^2}}{2} \leq \rho_L \leq \frac{1+\sqrt{1-k^2}}{2}. \tag{C.18}$$

The quantity $\bar{\lambda}_{L0}$ is, for any fixed value of k, a linear function of ρ_L. Therefore, the inequality (C.9d) holds for every possible ρ_L provided it holds for

$$\rho_L = \frac{1+(-1)^{n_L}\sqrt{1-k^2}}{2}, \tag{C.19}$$

where n_L may be either 0 or 1. Similarly, the inequality (C.9e) holds for every ρ_R provided it holds for

$$\rho_R = \frac{1+(-1)^{n_R}\sqrt{1-k^2}}{2}, \tag{C.20}$$

where n_R may be either 0 or 1. At last, the inequality (C.9g) holds for every ρ_L and ρ_R provided it holds for the ρ_L and ρ_R given by eqs. (C.19) and (C.20), respectively.

Recipe for BFB Our recipe for ascertaining the boundedness-from-below of $V_{(4)}$ consists of the following three steps:

1. Firstly we check that inequalities (C.9b), (C.9c), and (C.9f) hold.
2. Secondly we check that inequalities (C.13) hold.
3. Thirdly we make a scan over k from $k = -1$ to $k = +1$ in steps of 0.001, *i.e.* we make $k = -1 + 0.001 n_s$ for $n_s = 0, 1, \ldots, 2000$. For every such value of k, we consider the two values of ρ_L and the two values of ρ_R given by eqs. (C.19) and (C.20), respectively, depending on whether $n_L = 0$ or $n_L = 1$ and on whether $n_R = 0$ or $n_R = 1$. We check that inequalities (C.9d), (C.9e), and (C.9g) hold for all those four values of the pair $(\rho_L,\ \rho_R)$.

Of course, step 3 is just an approximation for considering every $k \in [-1,\ +1]$, but we have numerically checked that it is an almost perfect approximation because the step 0.001 is sufficiently small. Provided the approximation is perfect, it is clear from our derivation that the three requirements above are *necessary and sufficient conditions* for the boundedness-from-below of V_4.

Appendix D. Other conditions on the scalar potential

Vacuum equations In the potential (59) we substitute the fields by their VEVs (26) to obtain the VEV of the potential

$$\begin{aligned}\langle 0|V|0\rangle \equiv V_0 = {} & \mu_1 (V_1 + V_2) + 4\mu_2 v_1 v_2 + \mu_L U_L + \mu_R U_R \\ & + 2 (m_1 v_2 + m_2 v_1) u_L u_R \\ & + \lambda_L U_L^2 + \lambda_R U_R^2 + \lambda_{LR} U_L U_R \\ & + \lambda_1 (V_1 + V_2)^2 + (8\lambda_2 + 4\lambda_3) V_1 V_2 + 4\lambda_4 (V_1 + V_2) v_1 v_2\end{aligned}$$

$$
\begin{aligned}
&+\lambda_{3L} V_2 U_L + \lambda_{4L} V_1 U_L + 2\lambda_{5L} U_L v_1 v_2 \\
&+\lambda_{3R} V_2 U_R + \lambda_{4R} V_1 U_R + 2\lambda_{5R} U_R v_1 v_2 .
\end{aligned} \tag{D.1}
$$

The equations of vacuum stability are

$$
\begin{aligned}
0 = \frac{1}{2}\frac{\partial V_0}{\partial v_1} &= \mu_1 v_1 + 2\mu_2 v_2 + m_2 u_L u_R \\
&+2\lambda_1 (V_1 + V_2) v_1 + (8\lambda_2 + 4\lambda_3) V_2 v_1 + 2\lambda_4 (3V_1 + V_2) v_2 \\
&+\lambda_{4L} U_L v_1 + \lambda_{5L} U_L v_2 + \lambda_{4R} U_R v_1 + \lambda_{5R} U_R v_2 ,
\end{aligned} \tag{D.2a}
$$

$$
\begin{aligned}
0 = \frac{1}{2}\frac{\partial V_0}{\partial v_2} &= \mu_1 v_2 + 2\mu_2 v_1 + m_1 u_L u_R \\
&+2\lambda_1 (V_1 + V_2) v_2 + (8\lambda_2 + 4\lambda_3) V_1 v_2 + 2\lambda_4 (V_1 + 3V_2) v_1 \\
&+\lambda_{3L} U_L v_2 + \lambda_{5L} U_L v_1 + \lambda_{3R} U_R v_2 + \lambda_{5R} U_R v_1 ,
\end{aligned} \tag{D.2b}
$$

$$
\begin{aligned}
0 = \frac{1}{2}\frac{\partial V_0}{\partial u_L} &= \mu_L u_L + (m_1 v_2 + m_2 v_1) u_R \\
&+2\lambda_L U_L u_L + \lambda_{LR} U_R u_L + \lambda_{3L} V_2 u_L + \lambda_{4L} V_1 u_L + 2\lambda_{5L} v_1 v_2 u_L ,
\end{aligned} \tag{D.2c}
$$

$$
\begin{aligned}
0 = \frac{1}{2}\frac{\partial V_0}{\partial u_R} &= \mu_R u_R + (m_1 v_2 + m_2 v_1) u_L \\
&+2\lambda_R U_R u_R + \lambda_{LR} U_L u_R + \lambda_{3R} V_2 u_R + \lambda_{4R} V_1 u_R + 2\lambda_{5R} v_1 v_2 u_R .
\end{aligned} \tag{D.2d}
$$

Solving Eqs. (D.2) for the μ parameters, one obtains

$$
\begin{aligned}
\mu_1 = &\frac{m_1 v_2 - m_2 v_1}{V_1 - V_2} u_L u_R - 2\lambda_1 (V_1 + V_2) - 4\lambda_4 v_1 v_2 \\
&+\frac{\lambda_{3L} V_2 - \lambda_{4L} V_1}{V_1 - V_2} U_L + \frac{\lambda_{3R} V_2 - \lambda_{4R} V_1}{V_1 - V_2} U_R ,
\end{aligned} \tag{D.3a}
$$

$$
\begin{aligned}
\mu_2 = \frac{1}{2}\Bigg[&\frac{m_1 v_1 - m_2 v_2}{V_2 - V_1} u_L u_R - (8\lambda_2 + 4\lambda_3) v_1 v_2 - 2\lambda_4 (V_1 + V_2) \\
&-\frac{\lambda_{3L} - \lambda_{4L}}{V_1 - V_2} U_L v_1 v_2 - \frac{\lambda_{3R} - \lambda_{4R}}{V_1 - V_2} U_R v_1 v_2 - \lambda_{5L} U_L - \lambda_{5R} U_R \Bigg] ,
\end{aligned} \tag{D.3b}
$$

$$
\begin{aligned}
\mu_L = &-(m_1 v_2 + m_2 v_1)\frac{u_R}{u_L} \\
&-2\lambda_L U_L - \lambda_{LR} U_R - \lambda_{3L} V_2 - \lambda_{4L} V_1 - 2\lambda_{5L} v_1 v_2 ,
\end{aligned} \tag{D.3c}
$$

$$
\begin{aligned}
\mu_R = &-(m_1 v_2 + m_2 v_1)\frac{u_L}{u_R} \\
&-2\lambda_R U_R - \lambda_{LR} U_L - \lambda_{3R} V_2 - \lambda_{4R} V_1 - 2\lambda_{5R} v_1 v_2 .
\end{aligned} \tag{D.3d}
$$

Plugging Eqs. (D.3) back into Eq. (D.1) one obtains

$$
\begin{aligned}
V_0 = &-(m_1 v_2 + m_2 v_1) u_L u_R \\
&-\lambda_L U_L^2 - \lambda_R U_R^2 - \lambda_{LR} U_L U_R \\
&-\lambda_1 (V_1 + V_2)^2 - (8\lambda_2 + 4\lambda_3) V_1 V_2 - 4\lambda_4 (V_1 + V_2) v_1 v_2 \\
&-(\lambda_{3L} V_2 + \lambda_{4L} V_1 + 2\lambda_{5L} v_1 v_2) U_L \\
&-(\lambda_{3R} V_2 + \lambda_{4R} V_1 + 2\lambda_{5R} v_1 v_2) U_R
\end{aligned} \tag{D.4}
$$

Alternative vacua There are terms in the potential (59) that may induce VEVs of fields that *a priori* did not have a VEV. They are the terms that are linear in any field, *viz.*

$$\Big[2\mu_2 + 2\lambda_4\left(|a|^2+|b|^2+|c|^2+|d|^2\right) + \lambda_{5L}\left(|m|^2+|n|^2\right) + \lambda_{5R}\left(|p|^2+|q|^2\right)\Big]\left(a^*c + b^*d + \text{H.c.}\right); \tag{D.5a}$$

$$8\lambda_2\left(abc^*d^* + \text{H.c.}\right); \tag{D.5b}$$

$$4\lambda_3\left(ab^*c^*d + \text{H.c.}\right); \tag{D.5c}$$

$$m_1\left(-anp^* + bmp^* + cqm^* + dqn^* + \text{H.c.}\right); \tag{D.5d}$$

$$m_2\left(-cnp^* + dmp^* + aqm^* + bqn^* + \text{H.c.}\right); \tag{D.5e}$$

$$(\lambda_{3L} - \lambda_{4L})\left[m^*n\left(cd^* - ab^*\right) + \text{H.c.}\right]; \tag{D.5f}$$

$$(\lambda_{3R} - \lambda_{4R})\left[p^*q\left(bc - ad\right) + \text{H.c.}\right]. \tag{D.5g}$$

The presence in the potential of these terms implies that the only possible vacua wherein some of the eight scalar fields are identically equal to zero are the following:

1. All the fields are zero.
2. Only p is nonzero; or, equivalently, only q is nonzero; or, equivalently, only p and q are nonzero. (The three situations are equivalent to each other through gauge transformations.)
3. Only m is nonzero; or, equivalently, only n is nonzero or, equivalently, only m and n are nonzero.
4. Only a and c are nonzero; or, equivalently, only b and d are nonzero.
5. Only a, b, c, and d are nonzero.
6. Only a, c, n, and p are nonzero; or, equivalently, only b, d, m, and p are nonzero; or, equivalently, only a, c, m, and q are nonzero; or, equivalently, only b, d, n, and q are nonzero.

Cases 5 and 6 are impossible to treat analytically. There is yet another case, wherein all eight fields are nonzero in the vacuum, and this is also impossible to treat analytically. So, in the following we just consider cases 1 through 4.

Case 1 In case 1 the minimum of the potential has

$$\langle 0|V|0\rangle = 0 \equiv V^{(1)}. \tag{D.6}$$

Case 2 In case 2 the minimum of the potential has

$$\langle 0|V|0\rangle = -\frac{(\mu_R)^2}{4\lambda_R} \equiv V^{(2)}. \tag{D.7}$$

Case 3 In case 3 the minimum of the potential has

$$\langle 0|V|0\rangle = -\frac{(\mu_L)^2}{4\lambda_L} \equiv V^{(3)}. \tag{D.8}$$

Case 4 Case 4 gives (with b and d nonzero)

$$\begin{aligned} V &= \mu_1 (B+D) + \lambda_1 (B+D)^2 + 4\lambda_3 BD + 8\lambda_2 BD\cos(2\theta) \\ &\quad + 4\left[\mu_2 + \lambda_4 (B+D)\right]\sqrt{BD}\cos\theta \end{aligned} \tag{D.9a}$$

$$\begin{aligned} &= \mu_1 (B+D) + \lambda_1 (B+D)^2 + 4(\lambda_3 - 2\lambda_2) BD \\ &\quad + 16\lambda_2 BD\cos^2\theta + 4\hat{\mu}\sqrt{BD}\cos\theta, \end{aligned} \tag{D.9b}$$

where $B \equiv |b|^2$, $D \equiv |d|^2$, $\theta \equiv \arg(b^* d)$, and $\hat{\mu} \equiv \mu_2 + \lambda_4 (B+D)$. One must find the value of Eq. (D.9b) when

$$\frac{\partial V}{\partial \theta} = \left(4\hat{\mu}\sqrt{BD} + 32\lambda_2 BD\cos\theta\right)(-\sin\theta) = 0, \tag{D.10a}$$

$$\begin{aligned} \frac{\partial V}{\partial B} &= \mu_1 + 2\lambda_1 (B+D) + 4(\lambda_3 - 2\lambda_2) D + 16\lambda_2 D\cos^2\theta \\ &\quad + 2\hat{\mu}\sqrt{\frac{D}{B}}\cos\theta + 4\lambda_4\sqrt{BD}\cos\theta = 0, \end{aligned} \tag{D.10b}$$

$$\begin{aligned} \frac{\partial V}{\partial D} &= \mu_1 + 2\lambda_1 (B+D) + 4(\lambda_3 - 2\lambda_2) B + 16\lambda_2 B\cos^2\theta \\ &\quad + 2\hat{\mu}\sqrt{\frac{B}{D}}\cos\theta + 4\lambda_4\sqrt{BD}\cos\theta = 0. \end{aligned} \tag{D.10c}$$

Equation (D.10a) has three possible solutions:

$$\cos\theta = -\frac{\hat{\mu}}{8\lambda_2\sqrt{BD}}; \tag{D.11a}$$

$$\theta = 0; \tag{D.11b}$$

$$\theta = \pi. \tag{D.11c}$$

Equations (D.10b) and (D.10c) may be subtracted from one another, producing

$$(D-B)\left[4(\lambda_3 - 2\lambda_2) + 16\lambda_2\cos^2\theta + \frac{2\hat{\mu}\cos\theta}{\sqrt{BD}}\right] = 0. \tag{D.12}$$

Therefore, eqs. (D.10b) and (D.10c) have two possible solutions. One of them is

$$B - D = 0, \tag{D.13a}$$

$$\mu_1 + 2\hat{\mu}\cos\theta = -4(\lambda_1 + \lambda_3 - 2\lambda_2) B - 16\lambda_2 B\cos^2\theta - 4\lambda_4 B\cos\theta; \tag{D.13b}$$

and the other one is

$$\mu_1 = -2\lambda_1 (B+D) - 4\lambda_4\sqrt{BD}\cos\theta, \tag{D.14a}$$

$$\hat{\mu}\cos\theta = -8\lambda_2\sqrt{BD}\cos^2\theta - 2(\lambda_3 - 2\lambda_2)\sqrt{BD}. \tag{D.14b}$$

Combining Eqs. (D.11) with either Eqs. (D.13) or Eqs. (D.14), there are altogether six cases:

1. Equations (D.11b) and (D.13) give

$$\theta = 0, \tag{D.15a}$$

$$D = B = -\frac{\mu_1 + 2\mu_2}{4(\lambda_1 + 2\lambda_2 + \lambda_3 + 2\lambda_4)}, \tag{D.15b}$$

$$V = -\frac{(\mu_1 + 2\mu_2)^2}{4\,(\lambda_1 + 2\lambda_2 + \lambda_3 + 2\lambda_4)} \equiv V^{(4)}. \tag{D.15c}$$

2. Equations (D.11c) and (D.13) give

$$\theta = \pi, \tag{D.16a}$$

$$D = B = -\frac{\mu_1 - 2\mu_2}{4\,(\lambda_1 + 2\lambda_2 + \lambda_3 - 2\lambda_4)}, \tag{D.16b}$$

$$V = -\frac{(\mu_1 - 2\mu_2)^2}{4\,(\lambda_1 + 2\lambda_2 + \lambda_3 - 2\lambda_4)} \equiv V^{(5)}. \tag{D.16c}$$

3. Equations (D.11b) and (D.14) give

$$\theta = 0, \tag{D.17a}$$

$$B + D = \frac{-\hat{\lambda}\mu_1 + 4\lambda_4\mu_2}{2\lambda_1\hat{\lambda} - 4\,(\lambda_4)^2}, \tag{D.17b}$$

$$\sqrt{BD} = \frac{\lambda_4\mu_1 - 2\lambda_1\mu_2}{2\lambda_1\hat{\lambda} - 4\,(\lambda_4)^2}, \tag{D.17c}$$

$$V = \frac{-\hat{\lambda}\,(\mu_1)^2 - 8\lambda_1\,(\mu_2)^2 + 8\lambda_4\mu_1\mu_2}{4\left[\lambda_1\hat{\lambda} - 2\,(\lambda_4)^2\right]} \equiv V^{(6)}, \tag{D.17d}$$

with $\hat{\lambda} \equiv 4\lambda_2 + 2\lambda_3$. This solution only exists if

$$2\,|\lambda_4\mu_1 - 2\lambda_1\mu_2| \leq -\hat{\lambda}\mu_1 + 4\lambda_4\mu_2. \tag{D.18}$$

4. Equations (D.11c) and (D.14) give the same result as number 3, except that the sign of $\sqrt{BD}$ gets inverted.
5. Equation (D.11a) and (D.13) give

$$\cos\theta = -\frac{1}{4}\,\frac{2\lambda_4\mu_1 - \bar{\lambda}\mu_2}{2\lambda_2\mu_1 - \lambda_4\mu_2}, \tag{D.19a}$$

$$D = B = \frac{1}{2}\,\frac{2\lambda_2\mu_1 - \lambda_4\mu_2}{(\lambda_4)^2 - \lambda_2\bar{\lambda}}, \tag{D.19b}$$

$$V = \frac{4\lambda_2\,(\mu_1)^2 + \bar{\lambda}\,(\mu_2)^2 - 4\lambda_4\mu_1\mu_2}{4\left[(\lambda_4)^2 - \lambda_2\bar{\lambda}\right]} \equiv V^{(7)}, \tag{D.19c}$$

where $\bar{\lambda} \equiv 4\,(\lambda_1 - 2\lambda_2 + \lambda_3)$.
6. Equations (D.11a) and (D.14) give $(\lambda_3 - 2\lambda_2)\sqrt{BD} = 0$, which is a contradiction because we are assuming that both B and D are nonzero.

The conditions One must require

$$V_0 < V^{(1)}, \qquad V_0 < V^{(2)}, \qquad V_0 < V^{(3)}, \tag{D.20}$$

and also

$$V_0 < V^{(4)} \Leftarrow \frac{\mu_1 + 2\mu_2}{\lambda_1 + 2\lambda_2 + \lambda_3 + 2\lambda_4} < 0, \tag{D.21a}$$

$$V_0 < V^{(5)} \Leftarrow \frac{\mu_1 - 2\mu_2}{\lambda_1 + 2\lambda_2 + \lambda_3 - 2\lambda_4} < 0, \tag{D.21b}$$

$$V_0 < V^{(6)} \Leftarrow 2\left|\lambda_4\mu_1 - 2\lambda_1\mu_2\right| \leq \left|-\hat{\lambda}\mu_1 + 4\lambda_4\mu_2\right| \quad \text{and} \quad \frac{-\hat{\lambda}\mu_1 + 4\lambda_4\mu_2}{\lambda_1\hat{\lambda} - 2\left(\lambda_4\right)^2} \geq 0, \tag{D.21c}$$

$$V_0 < V^{(7)} \Leftarrow \left|2\lambda_4\mu_1 - \bar{\lambda}\mu_2\right| \leq 4\left|2\lambda_2\mu_1 - \lambda_4\mu_2\right| \quad \text{and} \quad \frac{2\lambda_2\mu_1 - \lambda_4\mu_2}{\left(\lambda_4\right)^2 - \lambda_2\bar{\lambda}} \geq 0. \tag{D.21d}$$

In the conditions (D.20) and (D.21), the μ parameters must be substituted by their expressions in terms of the m and λ parameters by using Eqs. (D.3).

Appendix E. Experimental constraints

κ_Z and κ_W From Eq. (A.1),

$$\begin{aligned}
\mathcal{L} = \cdots &+ \left[\frac{g^2}{2}\, W^{+\mu} W^-_\mu + \left(\frac{g}{2c_w}\, Z^\mu + \frac{l s_\alpha^2}{2c_\alpha}\, X^\mu\right)\left(\frac{g}{2c_w}\, Z_\mu + \frac{l s_\alpha^2}{2c_\alpha}\, X_\mu\right)\right]|n|^2 \\
&+ \left(\frac{l^2}{2}\, V^{+\mu} V^-_\mu + \frac{l^2}{4c_\alpha^2}\, X^\mu X_\mu\right)|q|^2 \\
&+ \frac{1}{2}\left(-g W^{+\mu} b + l V^{+\mu} d^*\right)\left(-g W^-_\mu b^* + l V^-_\mu d\right) \\
&+ \frac{1}{2}\left(-g W^{+\mu} d + l V^{+\mu} b^*\right)\left(-g W^-_\mu d^* + l V^-_\mu b\right) \\
&+ \left(\frac{g}{2c_w}\, Z^\mu - \frac{l c_\alpha}{2}\, X^\mu\right)\left(\frac{g}{2c_w}\, Z_\mu - \frac{l c_\alpha}{2}\, X_\mu\right)\left(|b|^2 + |d|^2\right).
\end{aligned} \tag{E.1}$$

Therefore,

$$\begin{aligned}
\mathcal{L} = \cdots &+ Z_l^\mu Z_{l\mu}\left[\left(\frac{g^2}{4c_w^2}\, c_\psi^2 + \frac{l^2 s_\alpha^4}{4c_\alpha^2}\, s_\psi^2 + \frac{g l s_\alpha^2}{2c_w c_\alpha}\, c_\psi s_\psi\right)\sqrt{2} u_L \rho_L + \frac{l^2}{4c_\alpha^2}\, s_\psi^2\, \sqrt{2} u_R \rho_R \right. \\
&\left. + \left(\frac{g^2}{4c_w^2}\, c_\psi^2 + \frac{l^2 c_\alpha^2}{4}\, s_\psi^2 - \frac{g l c_\alpha}{2c_w}\, c_\psi s_\psi\right)\left(\sqrt{2} v_1 \rho_1 + \sqrt{2} v_2 \rho_2\right)\right] \\
&+ \frac{W_l^{+\mu} W^-_{l\mu}}{2}\left[g^2 c_\xi^2 \sqrt{2} u_L \rho_L + l^2 s_\xi^2 \sqrt{2} u_R \rho_R \right. \\
&\left. + \left(g^2 c_\xi^2 + l^2 s_\xi^2\right)\left(\sqrt{2} v_1 \rho_1 + \sqrt{2} v_2 \rho_2\right) + 2 g l c_\xi s_\xi \left(\sqrt{2} v_1 \rho_2 + \sqrt{2} v_2 \rho_1\right)\right].
\end{aligned} \tag{E.2}$$

Hence, the interactions of the scalar S_5^0 with pairs of light massive gauge bosons are given by

$$\begin{aligned}
\mathcal{L} = \cdots &+ \frac{Z_l^\mu Z_{l\mu} S_5^0}{2\sqrt{2}}\left\{\left(\frac{g^2}{c_w^2}\, c_\psi^2 + \frac{l^2 s_\alpha^4}{c_\alpha^2}\, s_\psi^2 + \frac{2 g l s_\alpha^2}{c_w c_\alpha}\, c_\psi s_\psi\right) u_L \left(V_\rho\right)_{31} + \frac{l^2}{c_\alpha^2}\, s_\psi^2\, u_R \left(V_\rho\right)_{41} \right. \\
&\left. + \left(\frac{g^2}{c_w^2}\, c_\psi^2 + l^2 c_\alpha^2 s_\psi^2 - \frac{2 g l c_\alpha}{c_w}\, c_\psi s_\psi\right)\left[v_1 \left(V_\rho\right)_{11} + v_2 \left(V_\rho\right)_{21}\right]\right\} \\
&+ \frac{W_l^{+\mu} W^-_{l\mu} S_5^0}{\sqrt{2}}\left\{g^2 c_\xi^2 u_L \left(V_\rho\right)_{31} + l^2 s_\xi^2 u_R \left(V_\rho\right)_{41} \right. \\
&\left. + \left(g^2 c_\xi^2 + l^2 s_\xi^2\right)\left[v_1 \left(V_\rho\right)_{11} + v_2 \left(V_\rho\right)_{21}\right] + 2 g l c_\xi s_\xi \left[v_1 \left(V_\rho\right)_{21} + v_2 \left(V_\rho\right)_{11}\right]\right\}.
\end{aligned} \tag{E.3}$$

In our fits, we identify S_5^0 as the observed scalar particle of mass 125 GeV. Equation (E.3) should therefore be compared to the corresponding interactions of the Higgs scalar H of the SM, which are given by

$$\mathcal{L}_{\text{SM}} = \cdots + H\,\frac{e m_Z m_W}{\sqrt{m_Z^2 - m_W^2}}\left(W^{+\mu}W^-_\mu + \frac{m_Z^2}{2m_W^2}\,Z^\mu Z_\mu\right). \tag{E.4}$$

We rewrite Eq. (E.3) as

$$\mathcal{L} = \cdots + S_5^0\,\frac{e m_Z m_W}{\sqrt{m_Z^2 - m_W^2}}\left(\kappa_W W^{+\mu}W^-_\mu + \kappa_Z\,\frac{m_Z^2}{2m_W^2}\,Z^\mu Z_\mu\right), \tag{E.5}$$

with

$$\begin{aligned}\kappa_Z = \frac{m_W^2}{m_Z^2}\sqrt{\frac{m_Z^2 - m_W^2}{2Em_Z^2m_W^2}}\Bigg\{&\frac{(GL+GH+LH)\,c_\psi^2 + H^2 s_\psi^2 + 2H\varrho_1\,c_\psi s_\psi}{L+H}\,u_L\left(V_\rho\right)_{31}\\ &+(L+H)\,s_\psi^2\,u_R\left(V_\rho\right)_{41}\\ &+\frac{(GL+GH+LH)\,c_\psi^2 + L^2 s_\psi^2 - 2L\varrho_1\,c_\psi s_\psi}{L+H}\left[v_1\left(V_\rho\right)_{11} + v_2\left(V_\rho\right)_{21}\right]\Bigg\},\end{aligned} \tag{E.6a}$$

$$\begin{aligned}\kappa_W = \sqrt{\frac{m_Z^2 - m_W^2}{2Em_Z^2m_W^2}}\Big\{&Gc_\xi^2 u_L\left(V_\rho\right)_{31} + Ls_\xi^2 u_R\left(V_\rho\right)_{41}\\ &+\left(Gc_\xi^2 + Ls_\xi^2\right)\left[v_1\left(V_\rho\right)_{11} + v_2\left(V_\rho\right)_{21}\right] + 2glc_\xi s_\xi\left[v_1\left(V_\rho\right)_{21} + v_2\left(V_\rho\right)_{11}\right]\Big\}.\end{aligned} \tag{E.6b}$$

In practice, we always input $\psi = 0$ in Eq. (E.6a) and, besides, the mixing angle ξ always turns out to be extremely small in our fits. When $\psi = \xi = 0$ one obtains, from Eqs. (10b), (11), (A.3), and (A.5a),

$$E = \frac{GLH}{GL+GH+LH}, \qquad M_W = \frac{GV_L^2}{2}, \qquad M_Z = \frac{(GL+GH+LH)\,V_L^2}{2}. \tag{E.7}$$

Then, from Eqs. (E.6),

$$\begin{aligned}\kappa_Z = \kappa_W &= \frac{M_W}{V_L^2}\sqrt{\frac{2\,(M_Z - M_W)}{EM_ZM_W}}\left[v_1\left(V_\rho\right)_{11} + v_2\left(V_\rho\right)_{21} + u_L\left(V_\rho\right)_{31}\right]\\ &= \frac{v_1c_1 + v_2s_1c_2 + u_Ls_1s_2c_3}{\sqrt{V_1+V_2+U_L}},\end{aligned} \tag{E.8}$$

where use was made of Eq. (33) in the last step. Thus, in our model, with $\psi = 0$ and in the limit $\xi = 0$, κ_Z and κ_W become equal and are necessarily smaller than one. In our fits ξ may deviate slightly from zero and therefore for some points κ_W is slightly larger than one, but never much.

κ_t and κ_b The Yukawa couplings of the top and bottom quarks to the scalars include, according to Eq. (60b),

$$\mathcal{L}_{\text{Yukawa}} = \cdots - \frac{y_1\rho_1 + y_2\rho_2}{\sqrt{2}}\left(\bar{t}_L t_R + \bar{t}_R t_L\right) - \frac{y_1\rho_2 + y_2\rho_1}{\sqrt{2}}\left(\bar{b}_L b_R + \bar{b}_R b_L\right). \tag{E.9}$$

Using then Eqs. (62),

$$\mathcal{L}_{\text{Yukawa}} = \cdots - \sum_{i=1}^{4} S_{i+4}^0 \left[\frac{(-v_1 m_t + v_2 m_b)\left(V_\rho\right)_{1i} + (v_2 m_t - v_1 m_b)\left(V_\rho\right)_{2i}}{\sqrt{2}\,(V_2 - V_1)} \left(\bar{t}_L t_R + \bar{t}_R t_L\right) \right.$$
$$\left. + \frac{(-v_1 m_t + v_2 m_b)\left(V_\rho\right)_{2i} + (v_2 m_t - v_1 m_b)\left(V_\rho\right)_{1i}}{\sqrt{2}\,(V_2 - V_1)} \left(\bar{b}_L b_R + \bar{b}_R b_L\right) \right]. \quad \text{(E.10)}$$

The Yukawa couplings of S_5^0 should be compared to the Yukawa couplings of H in the SM, which are given by

$$\mathcal{L}_{\text{SM}} = \cdots - \frac{e m_Z}{2 m_W \sqrt{m_Z^2 - m_W^2}} H \left[|m_t| \left(\bar{t}_L t_R + \bar{t}_R t_L\right) + |m_b| \left(\bar{b}_L b_R + \bar{b}_R b_L\right) \right]. \quad \text{(E.11)}$$

One thus has

$$\kappa_t = \sqrt{\frac{2 m_W^2 \left(m_Z^2 - m_W^2\right)}{E m_Z^2 m_t^2}} \, \frac{(v_2 m_t - v_1 m_b)\left(V_\rho\right)_{21} + (v_2 m_b - v_1 m_t)\left(V_\rho\right)_{11}}{(V_2 - V_1)}, \quad \text{(E.12a)}$$

$$\kappa_b = \sqrt{\frac{2 m_W^2 \left(m_Z^2 - m_W^2\right)}{E m_Z^2 m_b^2}} \, \frac{(v_2 m_b - v_1 m_t)\left(V_\rho\right)_{21} + (v_2 m_t - v_1 m_b)\left(V_\rho\right)_{11}}{(V_2 - V_1)}. \quad \text{(E.12b)}$$

Appendix F. Determination of the VEVs and of the gauge coupling constants

General case Part of our input is formed by M_l, M_h, $\bar{M}_l$, $\bar{M}_h$, ξ, ψ,[24] and E. Using this input we determine the VEVs and the gauge coupling constants in the following way. We firstly define

$$x \equiv \frac{E}{G}, \quad y \equiv \frac{E}{L}, \quad z \equiv \frac{E}{H}, \qquad a_1 \equiv E V_1, \quad a_2 \equiv E V_2, \quad a_3 \equiv E U_L, \quad a_4 \equiv E U_R. \quad \text{(F.1)}$$

Equation (11) is equivalent to

$$x + y + z = 1. \quad \text{(F.2)}$$

We use the input to compute

$$R = M_l c_\psi^2 + M_h s_\psi^2, \qquad S = M_l s_\psi^2 + M_h c_\psi^2, \qquad T^2 = (M_h - M_l)^2 \, c_\psi^2 s_\psi^2, \quad \text{(F.3)}$$

$$A = \bar{M}_l c_\xi^2 + \bar{M}_h s_\xi^2, \qquad B = \bar{M}_l s_\xi^2 + \bar{M}_h c_\xi^2, \qquad D^2 = \left(\bar{M}_h - \bar{M}_l\right)^2 c_\xi^2 s_\xi^2. \quad \text{(F.4)}$$

cf. Eqs. (A.27) and (A.9). The first Eq. (A.3) and Eq. (A.5a) imply

$$\begin{aligned} t \equiv \frac{A}{R} &= \frac{G\,(L + H)}{GL + GH + LH} \\ &= \left[\frac{1}{1 - y - z}\left(\frac{1}{y} + \frac{1}{z}\right)\right]\left[\frac{1}{1 - y - z}\left(\frac{1}{y} + \frac{1}{z}\right) + \frac{1}{yz}\right]^{-1} \\ &= \frac{z + y}{z + y + 1 - y - z} \\ &= z + y. \end{aligned} \quad \text{(F.5)}$$

[24] In actual practice we always input $\psi = 0$, but the method that we delineate here works for arbitrary ψ.

Therefore, x is computed from the input as

$$x = 1 - \frac{A}{R}. \tag{F.6}$$

Since $x = E/G$ is by definition positive, *we must enforce the condition*

$$R \geq A \tag{F.7}$$

on the input. We then define

$$a_s \equiv a_1 + a_2. \tag{F.8}$$

The first two Eqs. (A.3) and Eq. (A.5b) read, respectively,

$$2xA = a_s + a_3, \tag{F.9a}$$

$$2yB = a_s + a_4, \tag{F.9b}$$

$$2yz\,(y+z)\,S = a_s z^2 + a_3 y^2 + a_4\,(y+z)^2\,. \tag{F.9c}$$

Equations (F.9) are solved as

$$a_s = \frac{xy^2A + y\,(y+z)^2\,B - yz\,(y+z)\,S}{y\,(y+z)}, \tag{F.10a}$$

$$a_3 = \frac{xy\,(2z+y)\,A - y\,(y+z)^2\,B + yz\,(y+z)\,S}{y\,(y+z)}, \tag{F.10b}$$

$$a_4 = \frac{-xy^2A + y\left(y^2 - z^2\right)B + yz\,(y+z)\,S}{y\,(y+z)}. \tag{F.10c}$$

Equation (A.5c) yields

$$4T^2 = \frac{x+y+z}{xyz\,(y+z)^2}\,(ya_3 - za_s)^2\,. \tag{F.11}$$

Plugging Eqs. (F.10) into Eq. (F.11) one obtains

$$4\,(y+z)^2\,xyzT^2 = (x+y+z)\left[xyA - (y+z)^2\,B + z\,(y+z)\,S\right]^2. \tag{F.12}$$

Then, using $x = 1 - t$ and

$$y = t - z, \tag{F.13}$$

one obtains

$$4t^2\,(1-t)\,T^2\,(t-z)\,z = \left[t^2B + (t-1)\,(t-z)\,A - tzS\right]^2. \tag{F.14}$$

Equation (F.14) is a quadratic equation for z:

$$\begin{aligned} 0 = {} & z^2\left\{[(1-t)\,A - tS]^2 + 4t^2\,(1-t)\,T^2\right\} \\ & + 2z\left\{[(1-t)\,A - tS]\,[tB + (t-1)\,A] + 2t^2\,(t-1)\,T^2\right\}t \\ & + [tB + (t-1)\,A]^2\,t^2. \end{aligned} \tag{F.15}$$

One solves Eq. (F.15), enforcing on its solution the condition

$$0 \leq z \leq t. \tag{F.16}$$

Equation (F.13) then yields y. Equations (F.10) produce $a_1 + a_2$, a_3, and a_4; these must all turn out positive.

Case $\psi = 0$ In practice, we input $\psi = 0$. Then, according to Eqs. (F.3),

$$R = M_l, \qquad S = M_h, \qquad T = 0. \tag{F.17}$$

Equation (A.5c) then implies

$$HU_L = L\,(V_1 + V_2)\,, \tag{F.18}$$

which simplifies considerably the resolution of the system of equations. One obtains,

$$G = \frac{E\,M_l}{M_l - A}, \tag{F.19a}$$

$$L = \frac{E\,M_l\,(M_h - M_l + A)}{A\,(M_h - B)}, \tag{F.19b}$$

$$H = \frac{E\,M_l\,(M_h - M_l + A)}{A\,(A + B - M_l)}, \tag{F.19c}$$

$$V_1 + V_2 = \frac{2A\,(M_h - B)\,(M_l - A)}{E\,M_l\,(M_h - M_l + A)}, \tag{F.19d}$$

$$U_L = \frac{2A\,(M_l - A)\,(A + B - M_l)}{E\,M_l\,(M_h - M_l + A)}, \tag{F.19e}$$

$$U_R = \frac{2A\,(M_h - B)\,(A + B - M_l)}{E\,M_l\,(M_h - M_l + A)}. \tag{F.19f}$$

Note that one must input values of $\bar{M}_l$, $\bar{M}_h$, and ξ such that

$$A < M_l, \qquad M_l - A < B < M_h, \tag{F.20}$$

where A and B are given by the first two Eqs. (F.4).

V_1 *and* V_2 It remains to separate a_1 from a_2. This we do by having recourse to the third Eq. (A.3):

$$a_1 a_2 = xyD^2. \tag{F.21}$$

Therefore,

$$a_1 = \frac{1}{2}\left[a_s - \sqrt{(a_s)^2 - 4xyD^2}\right], \qquad a_2 = \frac{1}{2}\left[a_s + \sqrt{(a_s)^2 - 4xyD^2}\right]. \tag{F.22}$$

In Eqs. (F.22), $\sqrt{(a_s)^2 - 4xyD^2}$ is by definition positive, *viz.* we assume, without loss of generality, that $V_1 \leq V_2$.

Proof that $\bar{M}_h < M_h$ Because of Eqs. (A.3)–(A.5) and (F.18), when $\psi = 0$

$$A = \frac{G\,(L+H)}{2L}\,U_L, \tag{F.23a}$$

$$B = \frac{L}{2}\,U_R + \frac{H}{2}\,U_L, \tag{F.23b}$$

$$\begin{aligned} M_h &= \frac{L+H}{2}\,U_R + \frac{H}{2}\,U_L \\ &= B + \frac{H}{2}\,U_R. \end{aligned} \tag{F.23c}$$

Now,

$$\bar{M}_h = \frac{1}{2}\left[B + A + \sqrt{(B-A)^2 + 4D^2}\right]. \tag{F.24}$$

Therefore, using Eq. (F.23c),

$$\begin{aligned} M_h - \bar{M}_h &= \frac{1}{2}\left[B + HU_R - A - \sqrt{(B-A)^2 + 4D^2}\right] \\ &\approx \frac{1}{2}\left(HU_R - \frac{2D^2}{B-A}\right) \\ &> 0, \end{aligned} \tag{F.25}$$

because both A and D are of order the electroweak scale squared, *viz.* V_1, V_2, and U_L, while $B \sim U_R$ is much larger. One thus concludes that the heavy neutral gauge boson is always heavier than the heavy charged gauge boson, at least when $\psi = 0$.

Appendix G. Mass matrices of the scalars

Mass matrix of the scalars The mass terms of the scalars are contained in the mass matrix M_ρ, which is defined through

$$V = \cdots + \frac{1}{2}\begin{pmatrix} \rho_1, & \rho_2, & \rho_L, & \rho_R \end{pmatrix} M_\rho \begin{pmatrix} \rho_1 \\ \rho_2 \\ \rho_L \\ \rho_R \end{pmatrix}. \tag{G.1}$$

That matrix may be computed from the input observables as

$$M_\rho = V_\rho \times \mathrm{diag}\left(\mu_5^2,\ \mu_6^2,\ \mu_7^2,\ \mu_8^2\right) \times V_\rho^T, \tag{G.2}$$

where V_ρ is a function of the mixing angles θ_i ($i = 1, 2, \ldots, 6$) through Eq. (32). Using Eqs. (28), (59), and (D.3) one finds the matrix elements of M_ρ:

$$\begin{aligned} \left(M_\rho\right)_{11} = {} & \frac{m_1 v_2 - m_2 v_1}{V_1 - V_2}\,u_L u_R + \frac{V_2}{V_1 - V_2}\left[\left(\lambda_{3L} - \lambda_{4L}\right)U_L + \left(\lambda_{3R} - \lambda_{4R}\right)U_R\right] \\ & + 4\lambda_1 V_1 + \left(8\lambda_2 + 4\lambda_3\right)V_2 + 8\lambda_4 v_1 v_2, \end{aligned} \tag{G.3a}$$

$$\begin{aligned} \left(M_\rho\right)_{22} = {} & \frac{m_1 v_2 - m_2 v_1}{V_1 - V_2}\,u_L u_R + \frac{V_1}{V_1 - V_2}\left[\left(\lambda_{3L} - \lambda_{4L}\right)U_L + \left(\lambda_{3R} - \lambda_{4R}\right)U_R\right] \\ & + 4\lambda_1 V_2 + \left(8\lambda_2 + 4\lambda_3\right)V_1 + 8\lambda_4 v_1 v_2, \end{aligned} \tag{G.3b}$$

$$\begin{aligned}\left(M_\rho\right)_{12} &= \frac{m_1 v_1 - m_2 v_2}{V_2 - V_1} u_L u_R + \frac{v_1 v_2}{V_2 - V_1} \left[\left(\lambda_{3L} - \lambda_{4L}\right) U_L + \left(\lambda_{3R} - \lambda_{4R}\right) U_R\right] \\ &\quad + \left(4\lambda_1 + 8\lambda_2 + 4\lambda_3\right) v_1 v_2 + 4\lambda_4 \left(V_1 + V_2\right), \end{aligned} \tag{G.3c}$$

$$\left(M_\rho\right)_{13} = m_2 u_R + 2\left(\lambda_{4L} v_1 + \lambda_{5L} v_2\right) u_L, \tag{G.3d}$$

$$\left(M_\rho\right)_{14} = m_2 u_L + 2\left(\lambda_{4R} v_1 + \lambda_{5R} v_2\right) u_R, \tag{G.3e}$$

$$\left(M_\rho\right)_{23} = m_1 u_R + 2\left(\lambda_{3L} v_2 + \lambda_{5L} v_1\right) u_L, \tag{G.3f}$$

$$\left(M_\rho\right)_{24} = m_1 u_L + 2\left(\lambda_{3R} v_2 + \lambda_{5R} v_1\right) u_R, \tag{G.3g}$$

$$\left(M_\rho\right)_{33} = 4\lambda_L U_L - \left(m_1 v_2 + m_2 v_1\right) \frac{u_R}{u_L}, \tag{G.3h}$$

$$\left(M_\rho\right)_{44} = 4\lambda_R U_R - \left(m_1 v_2 + m_2 v_1\right) \frac{u_L}{u_R}, \tag{G.3i}$$

$$\left(M_\rho\right)_{34} = m_1 v_2 + m_2 v_1 + 2\lambda_{LR} u_L u_R. \tag{G.3j}$$

Mass matrix of the pseudoscalars The mass terms of the pseudoscalars are contained in the mass matrix M_η, which is defined through

$$V = \cdots + \frac{1}{2}\begin{pmatrix}\eta_a, & \eta_b\end{pmatrix} M_\eta \begin{pmatrix}\eta_a \\ \eta_b\end{pmatrix}, \tag{G.4}$$

cf. Eq. (42). The matrix M_η may be computed from the input observables as

$$M_\eta = \begin{pmatrix} c_\eta & s_\eta \\ -s_\eta & c_\eta \end{pmatrix} \begin{pmatrix} M_{\eta 1} & 0 \\ 0 & M_{\eta 2} \end{pmatrix} \begin{pmatrix} c_\eta & -s_\eta \\ s_\eta & c_\eta \end{pmatrix}, \tag{G.5}$$

cf. Eq. (43). Using Eqs. (28), (40), (59), and (D.3) one finds the matrix elements of M_η:

$$\begin{aligned}\left(M_\eta\right)_{11} &= u_L u_R \frac{V_1 + V_2}{V_1 - V_2}\left(\frac{m_1}{v_2} - \frac{m_2}{v_1}\right) - \frac{u_L u_R \left(m_1 v_1^3 + m_2 v_2^3\right)}{v_1 v_2 \left(V_1 + V_2\right)} \\ &\quad + \left(V_1 + V_2\right)\left[4\lambda_3 - 8\lambda_2 + \frac{\left(\lambda_{3L} - \lambda_{4L}\right) U_L + \left(\lambda_{3R} - \lambda_{4R}\right) U_R}{V_1 - V_2}\right], \end{aligned} \tag{G.6a}$$

$$\left(M_\eta\right)_{22} = -\frac{T_2}{T_1 u_L u_R}\left(m_1 v_2 + m_2 v_1\right), \tag{G.6b}$$

$$\left(M_\eta\right)_{12} = \frac{\sqrt{T_2}}{T_1}\left(m_1 v_1 - m_2 v_2\right), \tag{G.6c}$$

where T_1 and T_2 are defined in Eqs. (41).

Mass matrix of the charged scalars The mass terms of the charged scalars are contained in the mass matrix M_φ, which is defined through

$$V = \cdots + \begin{pmatrix}\varphi_a^-, & \varphi_b^-\end{pmatrix} M_\varphi \begin{pmatrix}\varphi_a^+ \\ \varphi_b^+\end{pmatrix}, \tag{G.7}$$

cf. Eq. (49). The matrix M_φ may be computed from the input observables as

$$M_\varphi = \begin{pmatrix} c_\varphi & s_\varphi \\ -s_\varphi & c_\varphi \end{pmatrix} \begin{pmatrix} M_{\varphi 1} & 0 \\ 0 & M_{\varphi 2} \end{pmatrix} \begin{pmatrix} c_\varphi & -s_\varphi \\ s_\varphi & c_\varphi \end{pmatrix}, \tag{G.8}$$

cf. Eq. (50). Using Eqs. (28), (47), (59), and (D.3) one finds the matrix elements of M_φ:

$$\begin{aligned}\left(M_\varphi\right)_{11} = {}& \frac{\lambda_{3L}-\lambda_{4L}}{V_1-V_2}\,K_1 + \frac{\lambda_{3R}-\lambda_{4R}}{V_1-V_2}\,\frac{4V_1V_2U_LU_R}{K_1} \\ & + \frac{m_1v_2+m_2v_1}{u_Lu_R\left(V_2-V_1\right)^2}\left(-U_RK_1 - U_L\,\frac{4V_1V_2U_LU_R}{K_1}\right) \\ & + \frac{4\left(m_1v_1+m_2v_2\right)v_1v_2u_Lu_R}{\left(V_2-V_1\right)^2},\end{aligned} \tag{G.9a}$$

$$\left(M_\varphi\right)_{22} = \frac{K_2}{K_1}\left[\left(\lambda_{3R}-\lambda_{4R}\right)\left(V_1-V_2\right) - \frac{\left(m_1v_2+m_2v_1\right)u_L}{u_R}\right], \tag{G.9b}$$

$$\begin{aligned}\left(M_\varphi\right)_{12} = {}& -2v_1v_2u_Lu_R\,\frac{\sqrt{K_2}}{K_1}\left[\lambda_{3R}-\lambda_{4R} - \frac{\left(m_1v_2+m_2v_1\right)u_L}{u_R\left(V_1-V_2\right)}\right] \\ & + \frac{m_1v_1+m_2v_2}{V_2-V_1}\sqrt{K_2},\end{aligned} \tag{G.9c}$$

where K_1 and K_2 are defined in Eqs. (48).

A constraint From Eqs. (G.6) and (G.9) one obtains

$$\begin{aligned}& T_2\left[2v_1v_2u_Lu_R\left(M_\varphi\right)_{22} + \sqrt{K_2}\left(V_1-V_2\right)\left(M_\varphi\right)_{12}\right] \\ & = K_2\left[2v_1v_2u_Lu_R\left(M_\eta\right)_{22} + \sqrt{T_2}\left(V_2-V_1\right)\left(M_\eta\right)_{12}\right].\end{aligned} \tag{G.10}$$

Equation (G.10) is a clear-cut prediction of our model for observable quantities (remember that the VEVs, and hence K_2 and T_2 too, are functions of the input observables, *cf.* appendix F). That prediction may be written

$$\begin{aligned}M_{\eta2} = {}& \left\{T_2\left[2v_1v_2u_Lu_R\left(M_\varphi\right)_{22} + \sqrt{K_2}\left(V_1-V_2\right)\left(M_\varphi\right)_{12}\right]\right. \\ & \left. + \left[K_2\sqrt{T_2}\left(V_2-V_1\right)c_\eta s_\eta - 2v_1v_2u_Lu_RK_2s_\eta^2\right]M_{\eta1}\right\} \\ & \times\left[2v_1v_2u_Lu_RK_2c_\eta^2 + K_2\sqrt{T_2}\left(V_2-V_1\right)c_\eta s_\eta\right]^{-1}.\end{aligned} \tag{G.11}$$

Thus, given $M_{\varphi1}$, $M_{\varphi2}$, $M_{\eta1}$, and the mixing angles φ and η, one may calculate $M_{\eta2}$.

Determination of the parameters of the potential Suppose that we already know the values of the VEVs u_L, u_R, v_1, and v_2 and that we input all the scalar masses and mixing angles. We may then

1. Use Eqs. (G.6b) and (G.6c) to determine m_1 and m_2.
2. Then use Eqs. (G.3h) to determine λ_L, (G.3i) to determine λ_R, and (G.3j) to determine λ_{LR}.
3. Next use either Eq. (G.9b) or Eq. (G.9c) to determine $\lambda_{3R}-\lambda_{4R}$, and then Eq. (G.9a) to determine $\lambda_{3L}-\lambda_{4L}$.
4. Equations (G.3d)–(G.3g) may now be employed to separately determine λ_{3R}, λ_{4R}, λ_{5R}, λ_{3L}, λ_{4L}, and λ_{5L}.
5. Equation (G.6a) pins down $\lambda_3-2\lambda_2$.
6. Equations (G.3a)–(G.3c) separately determine λ_1, λ_2, λ_3, and λ_4.

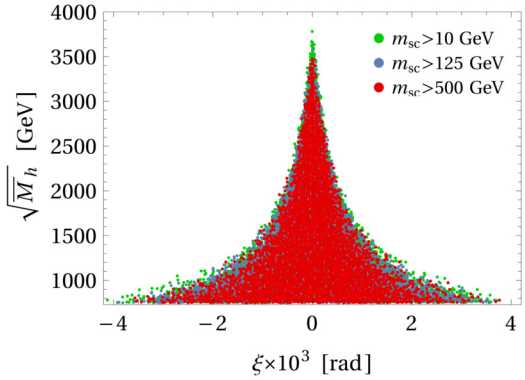

Fig. 4. Scatter plot of the mass of the heavy charged gauge boson ($\sqrt{\bar{M}_h}$) *versus* the mixing angle between the two charged gauge bosons (ξ), for the three cases where all the scalars have masses above 10 GeV (green points), 125 GeV (blue points), and 500 GeV (red points).

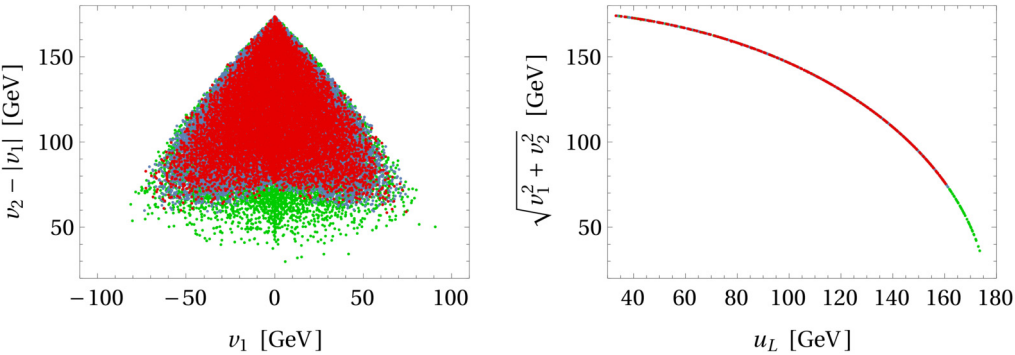

Fig. 5. Scatter plot of the relations among the vacuum expectation values v_1, v_2, and u_L that break $SU(2)_L$. The points, and the colour code for them, are the same as in Fig. 3. Left panel: $v_2 - |v_1|$ *versus* v_1. Right panel: $\sqrt{v_1^2 + v_2^2}$ *versus* u_L. Remember that in our conventions v_2 and u_L are always positive, and v_2 is always larger than $|v_1|$.

Appendix H. The ranges of the parameters of the LRM

In this appendix we provide more information on the fits mentioned in section 7. We present scatter plots with green, blue, and red points following the code introduced in that section. However, the scatter plots in this appendix do not dwell on the fitting of the $Zb\bar{b}$ vertex, rather on the parameters of the LRM itself. Moreover, in the scatter plots of this appendix we only display the points of Fig. 3 that satisfy the 2σ bounds on both R_b and A_b, *viz.* the points that are both in between the dashed orange lines and in between the magenta dashed lines in the left panel of that figure.

In Fig. 4 we plot the mass $\sqrt{\bar{M}_h}$ of the heavy charged gauge boson *versus* the mixing angle ξ between the two charged gauge bosons. One sees that the mixing angle lies within a narrow range $[-0.004,\ +0.004]$. This happens because of the lower bound 750 GeV that we have imposed on $\sqrt{\bar{M}_h}$ and $\sqrt{M_h}$; if we had opted for a more stringent and realistic lower bound [39–50], say 2 or 3 TeV, then ξ would have to lie in an even narrower range. The various lower bounds on the masses of the scalars have no effect on this scatter plot, which results almost exclusively from

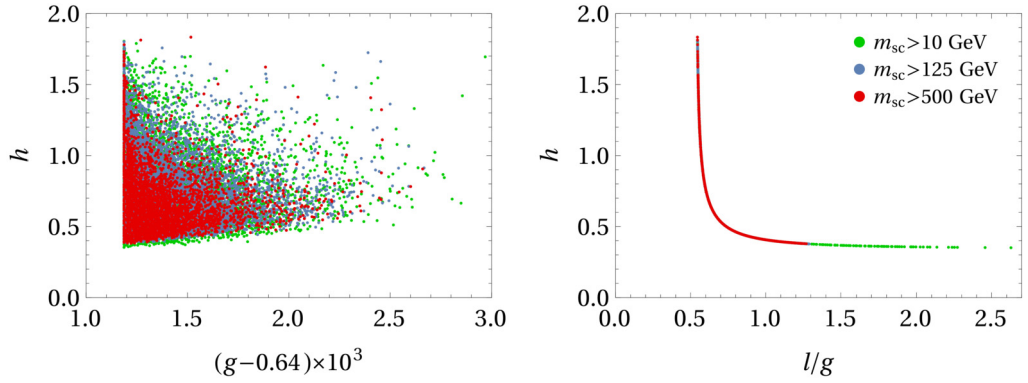

Fig. 6. Scatter plot of the gauge coupling constants g of $SU(2)_L$, l of $SU(2)_R$, and h of $U(1)_X$. Both the points and the colour code used to mark them are the same as in Fig. 3. Left panel: h *versus* g. Right panel: h *versus* l/g.

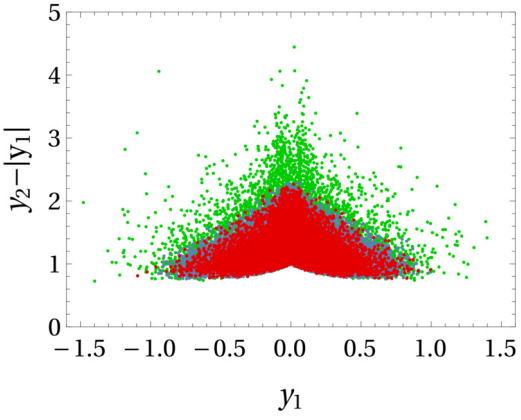

Fig. 7. Scatter plot of the Yukawa coupling y_2 and y_1. Remember that in our convention y_2 is always positive and larger than $|y_1|$. The points and the colour code are the same as in Fig. 3.

the procedure in Appendix F. Namely, if one chooses larger values for ξ, then either one violates the first inequality (F.20) or one ends up with negative values for either G, V_1, or U_L—which must all be positive, because they are the squares of real quantities. Therefore, ξ must always be very small.

In Fig. 5 we display the correlations among the vacuum expectation values. In the left panel one sees that $|v_1|$ is always at least 30 GeV smaller than v_2. Furthermore, $\sqrt{v_1^2+v_2^2} \lesssim 174$ GeV provides an upper bound both on $|v_1|$ and on v_2. In the right panel one observes the almost exact curve $\sqrt{v_1^2+v_2^2+u_L^2} \approx 174$ GeV that arises from the masses of the gauge bosons W_l and Z_l being fixed to their observed values.

Fig. 6 displays the gauge constants g of $SU(2)_L$, l of $SU(2)_R$, and h of $U(1)_X$. One sees in the horizontal scale of the left panel that g hardly deviates from it s SM value. On the other hand, h may vary from $2g/3$ to $3g$, approximately.

In the right panel of Fig. 6 one sees the counterpart, for the gauge coupling constants, of the relation observed in the right panel of Fig. 5 for the VEVs. Indeed, because we set $\psi = 0$,

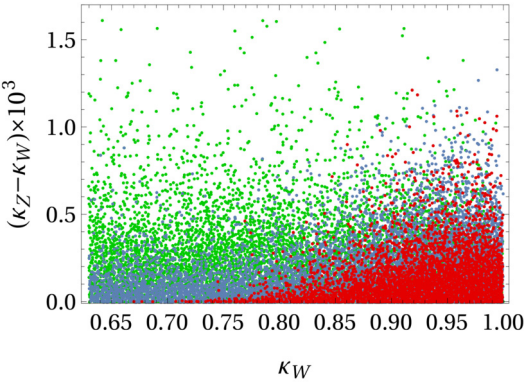

Fig. 8. Scatter plot of the coupling modifiers κ_W and κ_Z, for the three cases where all the scalars have masses above 10 GeV (green points), 125 GeV (blue points), and 500 GeV (red points).

Table 4
Approximate ranges of the parameters of the scalar potential.

Parameter	Range
m_1 [GeV]	-300 to 3
m_2 [GeV]	-140 to 130
λ_1	0 to 3.6
λ_2	-1 to 0.9
λ_3	-3 to 3
λ_4	-1.1 to 1.1
λ_L	0 to 4.2
λ_R	0 to 0.2
λ_{LR}	-1.0 to 0.6
λ_{3L}	-6 to 11
λ_{3R}	-0.7 to 0.6
λ_{4L}	-3.8 to 9.5
λ_{4R}	-0.7 to 0.6
λ_{5L}	-6 to 6
λ_{5R}	-0.8 to 0.8

Eq. (F.18) forces $h/l = \sqrt{v_1^2+v_2^2}\Big/u_L$. One sees that l/g saturates the bound in Eq. (13), but may also be much higher: in a separate dedicated search we have found points with $l/g \sim 6$ that satisfy (at the price of very low-mass scalars) the 1σ bounds on R_b and A_b.

In Fig. 7 we illustrate the Yukawa couplings y_1 and y_2. One sees that in most cases $|y_1|$ and y_2 are below $\sqrt{4\pi} \approx 3.5$; only a few points have them larger than 3.5, but always quite below our relaxed perturbativity bound 4π. One sees that $y_2 - |y_1|$ is always larger than 0.8, that y_1 is either positive or negative with the same likelihood, and that $|y_1| \lesssim 1.5$.

In Fig. 8 we depict the correlation between the coupling modifiers κ_W and κ_Z. One observes that in the LRM they are equal for all practical purposes and they are always smaller than 1. We have also examined the parameters κ_t and κ_b; they do not correlate with each other and they fully cover their full ranges in conditions [52].

In Table 4 we show the approximate ranges of some parameters of the scalar potential. Note that in a left–right-symmetric model one must have $\lambda_L = \lambda_R$, $\lambda_{3L} = \lambda_{3R}$, $\lambda_{4L} = \lambda_{4R}$, and $\lambda_{5L} = \lambda_{5R}$; these relations of course lead to restrictions on the masses and mixing of the scalars. It should be noted that the various lower bounds on the scalar masses that we have imposed do not greatly impact the ranges of the parameters of the potential.

References

[1] Particle Data Group Collaboration, R.L. Workman, Review of particle physics, PTEP 2022 (2022), 083C01.
[2] J.H. Field, Indications for an anomalous right-handed coupling of the b quark from a model independent analysis of LEP and SLD data on Z decays, Mod. Phys. Lett. A 13 (1998) 1937–1954, arXiv:hep-ph/9801355.
[3] H.E. Haber, H.E. Logan, Radiative corrections to the Z b anti-b vertex and constraints on extended Higgs sectors, Phys. Rev. D 62 (2000) 015011, arXiv:hep-ph/9909335.
[4] J. Erler, A. Freitas, Electroweak model and constraints on new physics, in: Ref. [1], 177 ff.
[5] D. Jurčiukonis, L. Lavoura, Fitting the $Zb\bar{b}$ vertex in the two-Higgs-doublet model and in the three-Higgs-doublet model, J. High Energy Phys. 07 (2021) 195, arXiv:2103.16635.
[6] D. Choudhury, T.M.P. Tait, C.E.M. Wagner, Beautiful mirrors and precision electroweak data, Phys. Rev. D 65 (2002) 053002, arXiv:hep-ph/0109097.
[7] D. Fontes, L. Lavoura, J.C. Romão, J.a.P. Silva, One-loop corrections to the $Zb\bar{b}$ vertex in models with scalar doublets and singlets, Nucl. Phys. B 958 (2020) 115131, arXiv:1910.11886.
[8] K.Y. Lee, Probing anomalous right-handed current in Z b anti-b vertex, Phys. Lett. B 472 (2000) 366–372, arXiv:hep-ph/9904435.
[9] X.-G. He, G. Valencia, The $Z \to b\bar{b}$ decay asymmetry and left-right models, Phys. Rev. D 66 (2002) 013004, arXiv:hep-ph/0203036; Erratum: Phys. Rev. D 66 (2002) 079901.
[10] X.-G. He, G. Valencia, A**b(FB) and R(b) at LEP and new right-handed gauge bosons, Phys. Rev. D 68 (2003) 033011, arXiv:hep-ph/0304215.
[11] D. Liu, J. Liu, C.E.M. Wagner, X.-P. Wang, Bottom-quark forward-backward asymmetry, dark matter and the LHC, Phys. Rev. D 97 (5) (2018) 055021, arXiv:1712.05802.
[12] R. Dermisek, S.-G. Kim, A. Raval, New vector boson near the Z-pole and the puzzle in precision electroweak data, Phys. Rev. D 84 (2011) 035006, arXiv:1105.0773.
[13] R. Dermisek, S.-G. Kim, A. Raval, Z' near the Z-pole, Phys. Rev. D 85 (2012) 075022, arXiv:1201.0315.
[14] K. Agashe, R. Contino, L. Da Rold, A. Pomarol, A custodial symmetry for $Zb\bar{b}$, Phys. Lett. B 641 (2006) 62–66, arXiv:hep-ph/0605341.
[15] L. Da Rold, Solving the A_{FB}^b anomaly in natural composite models, J. High Energy Phys. 02 (2011) 034, arXiv:1009.2392.
[16] J. Papavassiliou, A. Santamaria, Extra dimensions at the one loop level: Z → b anti-b and B anti-B mixing, Phys. Rev. D 63 (2001) 016002, arXiv:hep-ph/0008151.
[17] J.F. Oliver, J. Papavassiliou, A. Santamaria, Universal extra dimensions and Z → b anti-b, Phys. Rev. D 67 (2003) 056002, arXiv:hep-ph/0212391.
[18] T. Jha, A. Datta, $Z \to b\bar{b}$ in non-minimal universal extra dimensional model, J. High Energy Phys. 03 (2015) 012, arXiv:1410.5098.
[19] D. Choudhury, A. Kundu, P. Saha, Z-pole observables in an effective theory, Phys. Rev. D 89 (1) (2014) 013002, arXiv:1305.7199.
[20] D. d'Enterria, C. Yan, Revised QCD effects on the $Z \to b\bar{b}$ forward-backward asymmetry, arXiv:2011.00530.
[21] A. Crivellin, C.A. Manzari, M. Alguero, J. Matias, Combined explanation of the $Z \to b\bar{b}$ forward-backward asymmetry, the Cabibbo angle anomaly, and $\tau \to \mu\nu\nu$ and $b \to s\ell^+\ell^-$ data, Phys. Rev. Lett. 127 (1) (2021) 011801, arXiv:2010.14504.
[22] C.W. Murphy, Bottom-quark forward-backward and charge asymmetries at hadron colliders, Phys. Rev. D 92 (5) (2015) 054003, arXiv:1504.02493.
[23] S. Gori, J. Gu, L.-T. Wang, The $Zb\bar{b}$ couplings at future e^+ e^- colliders, J. High Energy Phys. 04 (2016) 062, arXiv:1508.07010.
[24] B. Yan, C.P. Yuan, Anomalous $Zb\bar{b}$ couplings: from LEP to LHC, Phys. Rev. Lett. 127 (5) (2021) 051801, arXiv:2101.06261.
[25] H. Dong, P. Sun, B. Yan, C.P. Yuan, Probing the $Zb\bar{b}$ anomalous couplings via exclusive Z boson decay, Phys. Lett. B 829 (2022) 137076, arXiv:2201.11635.

[26] B. Yan, Z. Yu, C.P. Yuan, The anomalous $Zb\bar{b}$ couplings at the HERA and EIC, Phys. Lett. B 822 (2021) 136697, arXiv:2107.02134.
[27] H.T. Li, B. Yan, C.P. Yuan, Jet charge: a new tool to probe the anomalous $Zb\bar{b}$ couplings at the EIC, Phys. Lett. B 833 (2022) 137300, arXiv:2112.07747.
[28] J.C. Pati, A. Salam, Lepton number as the fourth color, Phys. Rev. D 10 (1974) 275–289; Erratum: Phys. Rev. D 11 (1975) 703.
[29] R.N. Mohapatra, J.C. Pati, A natural left-right symmetry, Phys. Rev. D 11 (1975) 2558.
[30] R.N. Mohapatra, J.C. Pati, Left-right gauge symmetry and an isoconjugate model of CP violation, Phys. Rev. D 11 (1975) 566–571.
[31] G. Senjanovic, R.N. Mohapatra, Exact left-right symmetry and spontaneous violation of parity, Phys. Rev. D 12 (1975) 1502.
[32] G. Senjanovic, Spontaneous breakdown of parity in a class of gauge theories, Nucl. Phys. B 153 (1979) 334–364.
[33] D. Chang, R.N. Mohapatra, M.K. Parida, Decoupling of parity- and $SU(2)_R$-breaking scales: a new approach to left-right symmetric models, Phys. Rev. Lett. 52 (1984) 1072.
[34] V. Bernard, S. Descotes-Genon, L. Vale Silva, Constraining the gauge and scalar sectors of the doublet left-right symmetric model, J. High Energy Phys. 09 (2020) 088, arXiv:2001.00886.
[35] S. Karmakar, J. More, A.K. Pradhan, S.U. Sankar, Constraints on the doublet left-right symmetric model from Higgs data, arXiv:2211.08445.
[36] J. Erler, P. Langacker, S. Munir, E. Rojas, Improved constraints on Z-prime bosons from electroweak precision data, J. High Energy Phys. 08 (2009) 017, arXiv:0906.2435.
[37] I.D. Bobovnikov, P. Osland, A.A. Pankov, Improved constraints on the mixing and mass of Z' bosons from resonant diboson searches at the LHC at $\sqrt{s} = 13$ TeV and predictions for Run II, Phys. Rev. D 98 (9) (2018) 095029, arXiv:1809.08933.
[38] P. Osland, A.A. Pankov, I.A. Serenkova, Updated constraints on Z' and W' bosons decaying into bosonic and leptonic final states using the run 2 ATLAS data, Phys. Rev. D 103 (5) (2021) 053009, arXiv:2012.13930.
[39] P. Osland, A.A. Pankov, I.A. Serenkova, Bounds on the mass and mixing of Z' and W' bosons decaying into different pairings of W, Z, or Higgs bosons using CMS data at the LHC, arXiv:2206.01438.
[40] TWIST Collaboration, R. Bayes, et al., Experimental constraints on left-right symmetric models from muon decay, Phys. Rev. Lett. 106 (2011) 041804.
[41] O. Civitarese, J. Suhonen, K. Zuber, Combining data from high-energy pp-reactions and neutrinoless double-beta decay: limits on the mass of the right-handed boson, Int. J. Mod. Phys. E 25 (10) (2016) 1650081.
[42] K.S. Babu, K. Fujikawa, A. Yamada, Constraints on left-right symmetric models from the process $b \to s\gamma$, Phys. Lett. B 333 (1994) 196–201, arXiv:hep-ph/9312315.
[43] W. Dekens, D. Boer, Viability of minimal left-right models with discrete symmetries, Nucl. Phys. B 889 (2014) 727–756, arXiv:1409.4052.
[44] S. Bertolini, A. Maiezza, F. Nesti, Present and future K and B meson mixing constraints on TeV scale left-right symmetry, Phys. Rev. D 89 (9) (2014) 095028, arXiv:1403.7112.
[45] L. Vale Silva, Phenomenology of left-right models in the quark sector, PhD thesis, Saclay, 2016, arXiv:1611.08187.
[46] M. Blanke, A.J. Buras, K. Gemmler, T. Heidsieck, Delta F = 2 observables and $B \to X_q\gamma$ decays in the left-right model: Higgs particles striking back, J. High Energy Phys. 03 (2012) 024, arXiv:1111.5014.
[47] K.S. Babu, A. Thapa, Left-right symmetric model without Higgs triplets, arXiv:2012.13420.
[48] CMS Collaboration, A.M. Sirunyan, et al., Search for high mass dijet resonances with a new background prediction method in proton-proton collisions at $\sqrt{s} = 13$ TeV, J. High Energy Phys. 05 (2020) 033, arXiv:1911.03947.
[49] M. Thomas Arun, T. Mandal, S. Mitra, A. Mukherjee, L. Priya, A. Sampath, Testing left-right symmetry with an inverse seesaw mechanism at the LHC, Phys. Rev. D 105 (11) (2022) 115007, arXiv:2109.09585.
[50] CMS Collaboration, A.M. Sirunyan, et al., Search for W' bosons decaying to a top and a bottom quark at $s = 13$ TeV in the hadronic final state, Phys. Lett. B 820 (2021) 136535, arXiv:2104.04831.
[51] ATLAS Collaboration, A combination of measurements of Higgs boson production and decay using up to 139 fb^{-1} of proton–proton collision data at $\sqrt{s} = 13$ TeV collected with the ATLAS experiment.
[52] CMS Collaboration, A.M. Sirunyan, et al., Combined measurements of Higgs boson couplings in proton–proton collisions at $\sqrt{s} = 13$ TeV, Eur. Phys. J. C 79 (5) (2019) 421, arXiv:1809.10733.
[53] D. Fontes, J.C. Romão, FeynMaster: a plethora of Feynman tools, Comput. Phys. Commun. 256 (2020) 107311, arXiv:1909.05876.
[54] D. Fontes, J.C. Romão, Renormalization of the C2HDM with FeynMaster 2, J. High Energy Phys. 06 (2021) 016, arXiv:2103.06281.
[55] N.D. Christensen, C. Duhr, FeynRules – Feynman rules made easy, Comput. Phys. Commun. 180 (2009) 1614–1641, arXiv:0806.4194.

[56] A. Alloul, N.D. Christensen, C. Degrande, C. Duhr, B. Fuks, FeynRules 2.0 – a complete toolbox for tree-level phenomenology, Comput. Phys. Commun. 185 (2014) 2250–2300, arXiv:1310.1921.
[57] P. Nogueira, Automatic Feynman graph generation, J. Comput. Phys. 105 (1993) 279–289.
[58] R. Mertig, M. Bohm, A. Denner, FEYN CALC: computer algebraic calculation of Feynman amplitudes, Comput. Phys. Commun. 64 (1991) 345–359.
[59] V. Shtabovenko, R. Mertig, F. Orellana, New developments in FeynCalc 9.0, Comput. Phys. Commun. 207 (2016) 432–444, arXiv:1601.01167.
[60] V. Shtabovenko, R. Mertig, F. Orellana, FeynCalc 9.3: new features and improvements, Comput. Phys. Commun. 256 (2020) 107478, arXiv:2001.04407.
[61] D. Fontes, Multi-Higgs models: model building, phenomenology and renormalization, PhD thesis, U. Lisbon (main), 2021, arXiv:2109.08394.
[62] D. Fontes, M. Löschner, J.C. Romão, J.a.P. Silva, Leaks of CP violation in the real two-Higgs-doublet model, Eur. Phys. J. C 81 (6) (2021) 541, arXiv:2103.05002.
[63] A. Denner, Techniques for calculation of electroweak radiative corrections at the one loop level and results for W physics at LEP-200, Fortschr. Phys. 41 (1993) 307–420, arXiv:0709.1075.
[64] A. Denner, S. Dittmaier, Electroweak radiative corrections for collider physics, Phys. Rep. 864 (2020) 1–163, arXiv:1912.06823.
[65] CMS Collaboration, V. Khachatryan, et al., Search for a charged Higgs boson in pp collisions at $\sqrt{s} = 8$ TeV, J. High Energy Phys. 11 (2015) 018, arXiv:1508.07774.
[66] A. Arbey, F. Mahmoudi, O. Stal, T. Stefaniak, Status of the charged Higgs boson in two Higgs doublet models, Eur. Phys. J. C 78 (3) (2018) 182, arXiv:1706.07414.
[67] K. Kannike, Vacuum stability conditions and potential minima for a matrix representation in lightcone orbit space, Eur. Phys. J. C 81 (10) (2021) 940, arXiv:2109.01671; Addendum: Eur. Phys. J. C 82 (2022) 247.
[68] K. Kannike, Vacuum stability conditions from copositivity criteria, Eur. Phys. J. C 72 (2012) 2093, arXiv:1205.3781.
[69] G. Chauhan, Vacuum stability and symmetry breaking in left-right symmetric model, J. High Energy Phys. 12 (2019) 137, arXiv:1907.07153.